NSG-N2-61

COLUMBIA UNIVERSITY

IN THE CITY OF NEW YORK

SCHOOL OF ENGINEERING AND APPLIED SCIENCE

ELECTRONICS RESEARCH LABORATORIES

BIOMEDICAL ENGINEERING LABORATORY

METHODS FOR DETERMINING BLOOD FLOW THROUGH INTACT VESSELS OF EXPERIMENTAL ANIMALS UNDER CONDITIONS OF GRAVITATIONAL STRESS AND IN EXTRA-TERRESTRIAL SPACE CAPSULES

STATUS REPORT P-3/168

AUGUST 1, 1962 TO JULY 31, 1963

COLUMBIA UNIVERSITY
IN THE CITY OF NEW YORK
SCHOOL OF ENGINEERING AND APPLIED SCIENCE
ELECTRONICS RESEARCH LABORATORIES
BIOMEDICAL ENGINEERING LABORATORY

METHODS FOR DETERMINING BLOOD FLOW THROUGH INTACT VESSELS OF EXPERIMENTAL ANIMALS UNDER CONDITIONS OF GRAVITATIONAL STRESS AND IN EXTRA-TERRESTRIAL SPACE CAPSULES

STATUS REPORT P-3/168

AUGUST 1, 1962 TO JULY 31, 1963

Prepared for
National Aeronautics and Space Administration
Washington 25, D.C.
(NASA Research Grant NsG 112-61)

NASA CR-53302;
CU-3-63-NASA-112-ERL;

1 August 1, 1963

632 West 125th Street
New York 27, New York

ABSTRACT

A thirty- to ninety-day orbital study of the effects of sustained space flight upon physiologic performance has been designed utilizing experimental animals (primates) as the subjects. The study emphasizes complete assessment of the performance of the cardiovascular and respiratory systems. Three techniques are utilized: continuous measurement and telemetry of physiologic performance of critical organ systems; an inflight sensory-motor study making use of an operant conditioning schedule; a complete inflight metabolic-balance study and preflight-postflight organ function tests.

Systems analysis of alternative orbital systems has been performed and weight, power and similar requirements are presented for recoverable vs nonrecoverable systems, battery power vs solar power, for Rhesus monkeys and chimpanzees of various numbers, and for missions of various durations.

Key biosensors suitable for this orbital program are under development in this laboratory. A flight model implantable electromagnetic blood flowmeter for continuous measurement of cardiac output and regional bloodflow has been designed and tested. A laboratory model of this same device has been fabricated for use in simulation chambers, laboratories, and hospitals. A prototype implantable oximeter has been designed and fabricated for measurement of blood oxygen saturation within various blood vessels of the body. An implantable hematocrit sensor has been fabricated and implantable blood pressure transducers have been evaluated.

Author

AUTHORIZATION

The research summarized in this report was performed in the Biomedical Engineering Laboratory of the Electronics Research Laboratories, School of Engineering and Applied Science, Columbia University.

This report was prepared by Robert Feldstein, James M. Kennedy, Louis B. Lambert, Albert F. Sciorra and Robert F. Shaw.

This project is sponsored by the National Aeronautics and Space Administration under Research Grant NsG-112-61.

Submitted by:

R. F. Shaw, M.D.
Assistant Professor of
Biomedical Engineering
Director, Biomedical
Engineering Laboratory,
Electronics Research
Laboratories

Approved by:

for L. H. O'Neill
Associate Dean and
Professor of
Electrical Engineering
Director, Electronics
Research Laboratories

PROFESSIONAL STAFF

Robert F. Shaw, M. D. Director, Biomedical Engineering Laboratory Electronics Research Laboratories Assistant Professor Biomedical Engineering	Project Director
Louis B. Lambert Senior Staff Scientist and Laboratory Supervisor	Project Supervisor
Albert F. Sciorra Senior Staff Scientist and Laboratory Supervisor	Project Supervisor
James M. Kennedy Senior Research Engineer	Participant
Robert Feldstein Senior Research Physicist	Participant
Irving Weintraub Senior Research Engineer	Participant
Milton Rabinowitz Senior Research Engineer	Participant
Alan Katz Research Assistant	Participant
Steven Kanor Laboratory Assistant	Participant

TABLE OF CONTENTS

TABLE OF CONTENTS (CONT'D.)

TABLE OF CONTENTS (CONT'D.)

LIST OF FIGURES

LIST OF FIGURES (CONT'D.)

LIST OF FIGURES (CONT'D.)

I. STATUS OF THIS PROGRAM

This report summarizes the progress on Research Grant NsG-112-61 from August 1, 1962 through July 31, 1963. This program has been devoted to a study of the "Development of Physiological Biotechnology Suitable for Sustained Satellite Studies."

At the request of the program's monitor, the Director of Biotechnology, Division of Biotechnology and Human Research, Office of Advanced Research and Technology, and orbital experiment was designed for an "Experimental Assessment of the Effects of Sustained Space Flight on Physiological Performance." An experimental design for a 30- to 90-day orbital experiment utilizing primates was prepared. This program makes use of three techniques: (1) continuous measurement and telemetry of the physiological performance of critical organ systems; (2) an inflight motor study on an operant condition in the schedule; and (3) a series of preflight and postflight organ tests and an inflight complete metabolic balance study. By far the most important of these techniques is the continuous measurement and telemetry of physiological performance of critical organ systems, and is accomplished by means of advanced electronic biosensors surgically implanted in the subject primates prior to flight. The most important biosensors are under development by NASA in this laboratory. By means of these biosensors, a quantitative assessment of the performance of the two most critical organ systems (cardiovascular and respiratory) in relation to the demands placed upon them by the stresses of sustained space

flight can be precisely obtained. The experimental design for the sustained orbital study constitutes Sec. II of this report.

A systems analysis of alternative orbital systems to support sustained orbital studies was performed. Calculations of weight, power requirements, etc., of such systems and possible trade-offs were made for alternative systems such as recovery versus non-recovery, battery power versus solar cell power, Rhesus monkey subjects versus chimpanzees, various numbers of experimental animals and various mission durations. Section III of this report presents this analysis.

Several biosensors suitable for physiological studies in space are under development in this laboratory.

Section IV of this report describes progress in electromagnetic blood flowmeter research during the report period. Accurate, reliable and stable instruments for the measurement of cardiac output have been designed, constructed and tested. A model suitable for space flight studies has been designed, fabricated and tested. Two problems which interfere with ideal flowmeter performance on blood vessels other than the aorta and pulmonary artery remain incompletely solved. Experimentation has continued directed toward the solution of these two problems: the establishment of an absolute electronic zero and the elimination of the so-called "proximity effect." These phenomena do not pose a problem in flowmeter instrumentation of the aorta or pulmonary artery, as, for example, in the orbital experiment design. A general purpose laboratory-type flowmeter suitable for use in any experimental laboratory has been designed and fabricated during the current report period. This

unit is entirely self contained and has many ancillary components that make it especially easy to use in laboratories without engineering expertise.

A second biosensor, important not only for space studies but for general medical investigation, is an implantable transducer for continuously measuring blood oxygen saturation within various vessels of the body. This device has been under development during the current report period. Prototype models which have been constructed and evaluated have proved quite satisfactory. Research activities in this area are described in Sec. V of this report.

Section VI describes the prototype chronic implantable hematocrit sensor developed during this report period.

Section VII covers evaluation studies of commercially available pressure transducers suitable for chronic implantation for blood pressure measurements.

Section VIII of this report describes initial feasibility studies of the "Pulsed Doppler" flowmeter by means of which blood flow in various blood vessels within the body would be measured from a transducer wholly external to the body.

II. THE ASSESSMENT OF THE EFFECTS OF SUSTAINED SPACE FLIGHT ON PHYSIOLOGIC PERFORMANCE: AN EXPERIMENTAL DESIGN

A. RATIONALE FOR ASSESSING THE PHYSIOLOGIC EFFECTS OF SUSTAINED SPACE FLIGHT ON EXPERIMENTAL ANIMALS

Man will play a primary and central role in future space flight and exploration. Consequently, the success or failure of these missions will depend upon man's ability to maintain a high level of physiologic performance under the stresses imposed during sustained periods in space. Little, however, is actually known about the effects upon human physiology of sustained periods in space. Nor can such information be gleaned from experiments performed on earth, since the space ambient is neither completely defined nor can it be satisfactorily simulated upon earth (the absence of gravity, remoteness of magnetic fields, heavy primary cosmic ray flux, etc.).

As part of its mission, the Division of Biotechnology and Human Research of the Office of Advanced Research and Technology, National Aeronautics and Space Administration, has been concerned with the effect of sustained space flight upon human physiology. Since man is a critical component of space systems even now being planned, it is important to assess the effects of sustained periods in space upon physiologic performance as soon as possible. Then, if degradations of physiologic processes are found to occur, studies to eliminate or compensate for these disabilities can be instituted at once rather than at some later critical time when giant programs may have to be delayed or halted to await the results of biological investigation.

Valuable and interesting information in this general area has already been acquired from the Mercury flight program. The mere fact of survival carries with it gross physiological implications. The additional fact that the few physiological parameters monitored deviated little from normal is of interest, as is the information that the astronaut pilots felt good and were themselves unaware of any physiologic degradation.

Unfortunately, the Mercury flights were of brief duration in contrast to the sustained periods that have relevance to future programs. The physiologic parameters monitored were rather incidental to critical organ and system function. And it is quite possible to suffer considerable impairment of physiologic processes without subjective awareness.

Since man will be a critical component and perhaps the critical component of space systems of the future, it is important that physiologic performance and reliability be assessed with the same sensitivity, precision and objectivity with which performance and reliability of other components of space systems are assessed. At this state-of-the-art of both biomedical instrumentation and space flight, such studies are most aptly performed with experimental animals.

There are a number of reasons why experimental animals rather than men are the appropriate subjects in which to study the effects of sustained periods in space upon physiologic performance. One of these is the rather considerable risk inherent in a sustained orbital mission at this time. From the point of view of experimental design, it would be highly desirable to have the experiment continue well beyond the earliest indications of physiologic impairment of the subject and well into physiological destruction, should that occur.

A second and practical consideration has to do with payload capacities of available booster vehicles. Present vehicles can orbit quantities of life support materials capable of supporting only animals considerably smaller than man for the 30 to 90 days specified for this experiment.

Perhaps the most important consideration, however, has to do with the differences in physiologic information that can be acquired from experimental animals versus human subjects. At the present state-of-the-art of biotechnology, biosensors capable of acquiring meaningful measures of critical organ and system physiologic performance from human subjects during space flight simply do not exist. With experimental animals, on the other hand, since it is possible to perform surgical operations and strategically place biosensors within the bodies of the animals, advanced biosensors do exist that will monitor critical measures of physiologic performance for weeks, months or even years.

Information acquired in this manner from experimental animals will be directly applicable to human astronauts. This is, in fact, the fundamental modus operandi of medical science. Questions of human physiology are most often answered in the experimental animal laboratory. In actuality, the overwhelming predominance of information found in textbooks of human physiology is based on data from animal experiments. For while dogs and monkeys are not men, hearts are hearts, livers are livers, lungs are lungs, and so forth; and within certain well recognized constraints the physiological systems of the various higher mammals, including man, function according to the same principles and follow the same laws. Not only is the overwhelming predominance of that body of knowledge comprising human physiology acquired from experimental animals, but even such matters as the technical details of complex surgical op-

erations such as for heart disease, peptic ulcer, etc., are worked out upon experimental animals and applied directly to patients. There is no question that conclusions concerning the effect of sustained periods in space upon physiologic performance acquired from experimental animals will be directly applicable to astronauts.

The biological experiment designed to study the effects of sustained periods in space upon physiologic performance, the rationale of its concepts and the methods of implementation are presented in the following sections. With a view toward obtaining data applicable to manned missions of the future, the Office of Advanced Research and Technology chose thirty-to-ninety days of earth orbit as the mission profile for this study.

In general, attention was focused upon the most important organ systems. Only methods furnishing meaningful measures of organ and system function were selected, and methods furnishing data either not readily interpretable or simply "interesting" were rejected. Reliability of the experimental method and safety of the experimental animals were given high priority. Thus techniques such as electrocardiograms and electroencephalograms were not included because of the uncertainty of interpretation and uncertainty regarding the significance of deviations of wave patterns from normal; methods of requiring puncture of blood vessels or insertion of catheters or other instruments into the blood stream were not included because of the high probability of bleeding or blood clots. Biosensor transducers requiring or permitting surgical implantation inside the experimental subjects's body were uniformly selected in order that interference with instrumentation by the experimental animal, a very real hazard, could be avoided.

B. CHOICE OF EXPERIMENTAL ANIMALS

Because of their postural resemblances to man and their ability to learn fairly complex pre-flight psychological training programs, small monkeys or chimpanzees were chosen as the experimental subjects.

Consultation with the primate laboratories of the National Institute of Neurological Diseases and Blindness, the Holloman Air Force Base, and with individual investigators having extensive experience with both monkeys and chimpanzees, resulted in a uniform consensus of opinion strongly in favor of chimpanzees for the type of program considered. The marked preference for chimpanzees in favor of small monkeys was based primarily on the superior intelligence of the chimpanzees and their markedly greater tractability. It was felt that not only more meaningful psychological programs could be taught to the chimps, but that their superior intelligence would be a decided advantage in helping them to survive an extended orbital period.

The distinct advantage of animal tractability should not be minimized. In a program such as the one envisaged, it will be necessary to work with animals for periods well over a year. After a period of gentling, young chimpanzees can be readily handled, related to and communicated with. Their general deportment often resembles that of a mischievous pre-teenage youngster. In contrast, young rhesus and related monkeys remain persistently hostile and must be cautiously handled and overpowered whenever used. There is a marked and decided advantage to using tractable animals in a program where animals must be worked with almost daily for an extended period of time.

Chimpanzees for an orbital program should be in the thirty-to-thirty-five-pound weight range. Rhesus monkeys and related

monkeys may be as small as eight pounds, but monkeys approaching twelve-to-fifteen-pound range would be more desirable.

Because of the questionable significance of any positive experimental findings in a study in which only one experimental subject is used, it is most important that more than one animal be used in each flight. Orbital systems for chimpanzees or rhesus monkeys, or combinations thereof, are considered in the Sec. III of this report.

C. PHYSIOLOGIC PRINCIPLES

The experiment is designed with special attention focused on the body's most vital physiologic systems. For the benefit of readers for whom mammalian physiology may be a bit remote, a brief review of fundamentals follows.

In the early paleontological eras that witnessed the dawn of life on this planet, the earliest animal forms were unicellular organisms that lived in the sea. They acquired from the sea around them the oxygen and other nutriments to sustain life and they excreted into their immediate environs the waste products of cellular metabolism. (Fig. 1A)

With the evolution of multicellular forms, and especially with the evolution from sea to land forms, each cell was no longer in contact with the organism's environment. There evolved, as a consequence, an "internal sea" of body fluids that bathed each cell. From this "internal sea" each cell obtained the oxygen and other nutriments necessary to support life processes and into this "sea" the waste products of cellular metabolism were excreted. (Fig. 1B)

The circulatory system developed as a highly specialized transport and distribution system to carry oxygen and other nutriments to the "internal sea" that bathed each cell and to

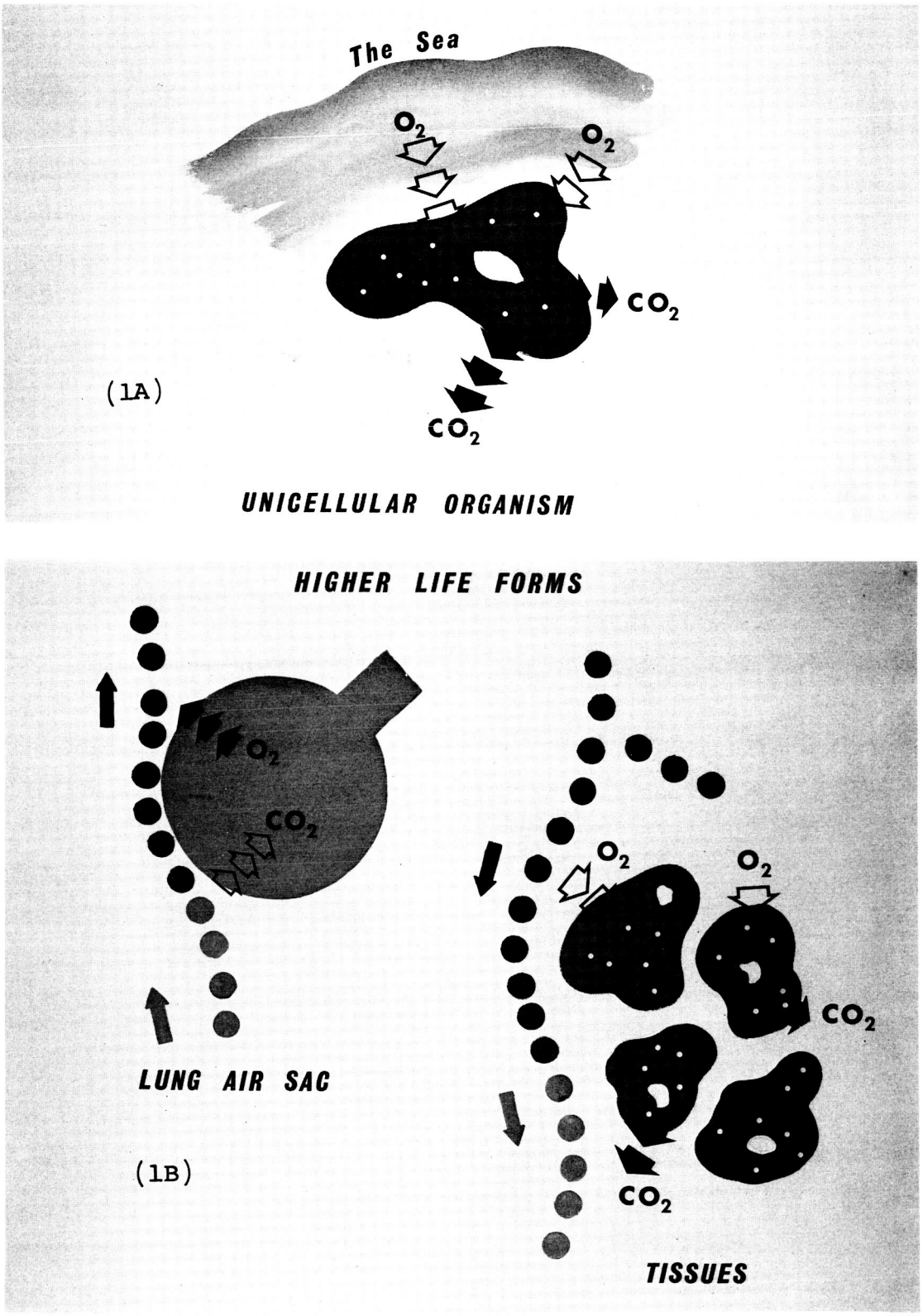

Fig. 1 Relation of Living Cells to Their Environment

carry away the carbon dioxide and other products of cellular metabolism. The red blood cells suspended in the fluid portion of the blood and transported around the body by the circulatory system evolved as packets of complex organic molecules particularly adapted to carrying large amounts of oxygen and carbon dioxide.

The respiratory system developed into a specialized mechanism for transferring oxygen from the breath atmosphere into the blood and for transferring the carboned dioxide from the blood out into the atmosphere. The lungs are made of millions of tiny thin-walled air sacs called alveoli. The thin alveolar walls, or membranes, combined have a huge surface area which is in intimate contact with the blood stream. The transfer of gases across the alveolar membrane takes place by simple diffusion. Blood entering the lungs comes from the tissues and is rich in carbon dioxide and poor in oxygen. Consequently, in the lungs there is a transfer of carbon dioxide from the blood into the air sacs and a transfer of oxygen from the air sacs into the blood. Because of the hemoglobin molecules of the red blood cells, very large quantities of gases can be carried by the blood. In the tissues the opposite transfer takes place: Oxygen diffuses from the blood into the "internal sea"; carbon dioxide diffuses from the tissues into the "internal sea" and then into the blood. The diffusion gradient that determines the level of oxygen and carbon dioxide in the blood is determined by the rate at which oxygen is utilized and carbon dioxide produced by the tissues and the rate at which the alveoli are ventilated with fresh gas. Thus, for the system to perform satisfactorily, the level of metabolic activity by the tissues must be parallelled by changes in the ventilation of gases into and out of the lungs.

Ventilation must be sufficient to meet demand, but not excessive, for carbon dioxide is the most important buffer material in body chemistry and variations in the amount of carbon dioxide that are out of the range of normal cause disturbances in the body's acid-base chemistry.

The biochemical pathways of cellular metabolism are oxygen dependent and the more sensitive tissues of the body, such as the brain and heart, can survive only a few minutes if deprived of oxygen. This is the reason why the cardiovascular and respiratory systems are the two most critical systems in the body.

The energy to transport blood throughout the circulation comes from the periodic contraction of the heart (Fig. 2). Figure 2 is a diagramatic representation of the cardiovascular system. It will be noted that the heart functions as two pumps. The right heart receives from the tissues blood low in oxygen concentration and high in carbon dioxide concentration. The right heart pumps blood to the lungs where carbon dioxide leaves the blood and oxygen enters, and the oxygenated blood continues to the left heart.

The left heart, like the right heart, is a pump which operates with variable stroke rate and stroke volume. The left heart pumps blood into the large arterial tree which operates as a pressurized reservoir or surge tank, kept at a suitable pressure head by the variable stroke output and stroke rate of the heart. Baro receptors positioned in the walls of the arterial tree operate as pressure sensors and through feedback circuits via nerve pathways, send signals that adjust heart rate and stroke volume in order that the arterial reservoir might be kept within a physiologic range of pressures.

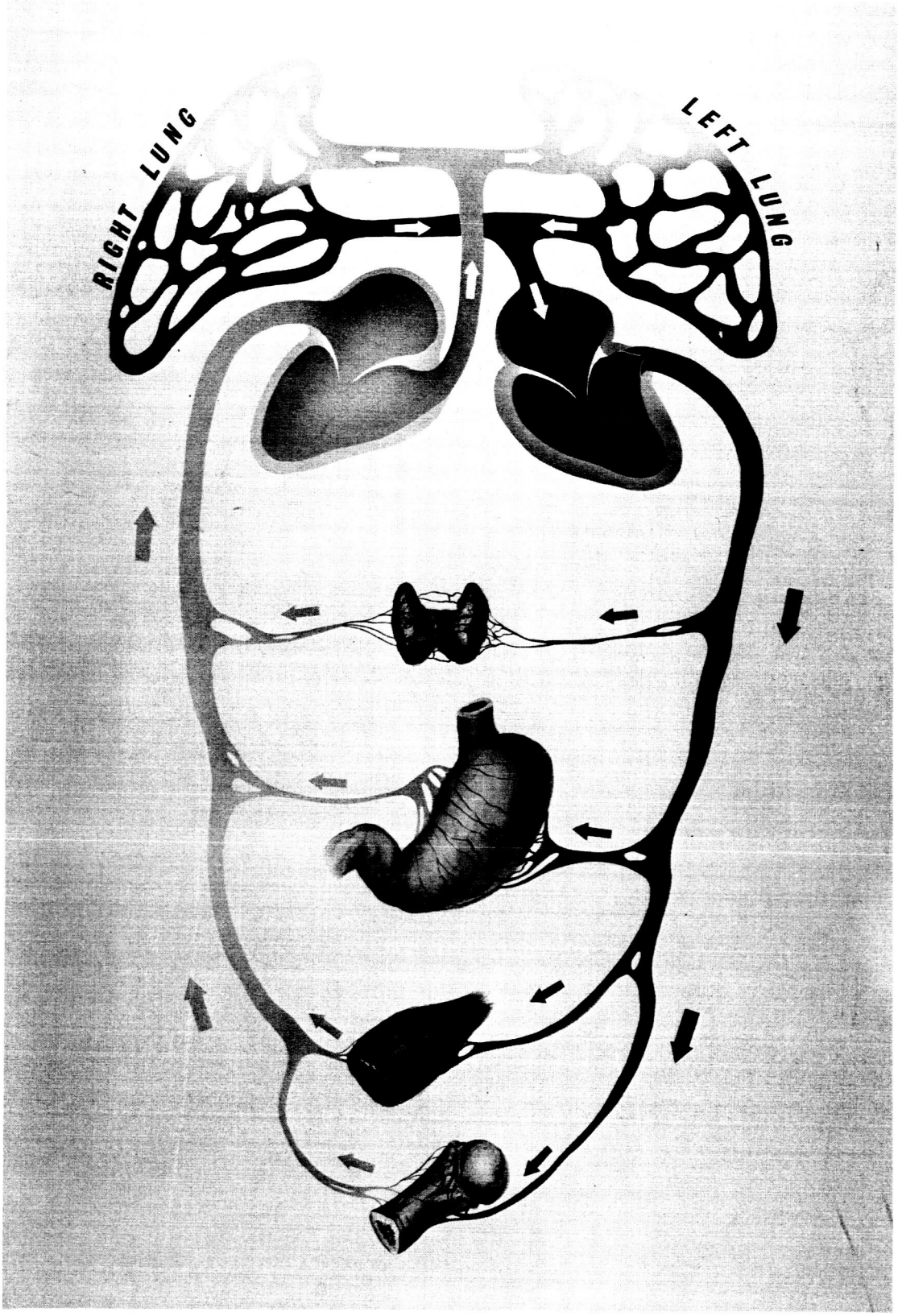

Fig. 2 Diagramatic Representation of the Cardiovascular Circulatory System

The organs and tissues of the body receive blood from the multiple branching arterial system. These organs and tissues are aligned in parallel and tap-off the pressurized arterial reservoir. In general, by variations of the smallest branches of the arterial tree contained within the organs and tissues, blood flow is divided among the various organs and regulated in each individual organ at a level consistent with that organ's metabolic needs.

D. THE INTEGRATED PERFORMANCE OF THE CRITICAL LIFE SYSTEMS: CARDIOVASCULAR AND RESPIRATORY

Figure 3 depicts the integrated performance of these two most critical systems.

The performance of life processes by cells, tissues and organs required a certain level of metabolic activity which is oxygen dependent (A). It is consequently necessary that adequate oxygen be delivered to the tissue (B) and this requires the combined satisfactory performance of both cardiovascular (C) and respiratory (D) systems. The heart and circulation must deliver a satisfactory total volumetric blood flow rate to the tissues and organs (E). The respiratory system is responsible for maintaining an adequate concentration of oxygen and carbon dioxide in the blood that is delivered (F).

To accomplish its task of maintaining an adequate total volumetric blood flow rate, the heart must perform a particular level of external mechanical work (G). This is accomplished by variable dynamics of cardiac contraction and relaxation (H) and through variations in stroke volumes (I) and stroke rates (J) against varying peripheral resistances (K).

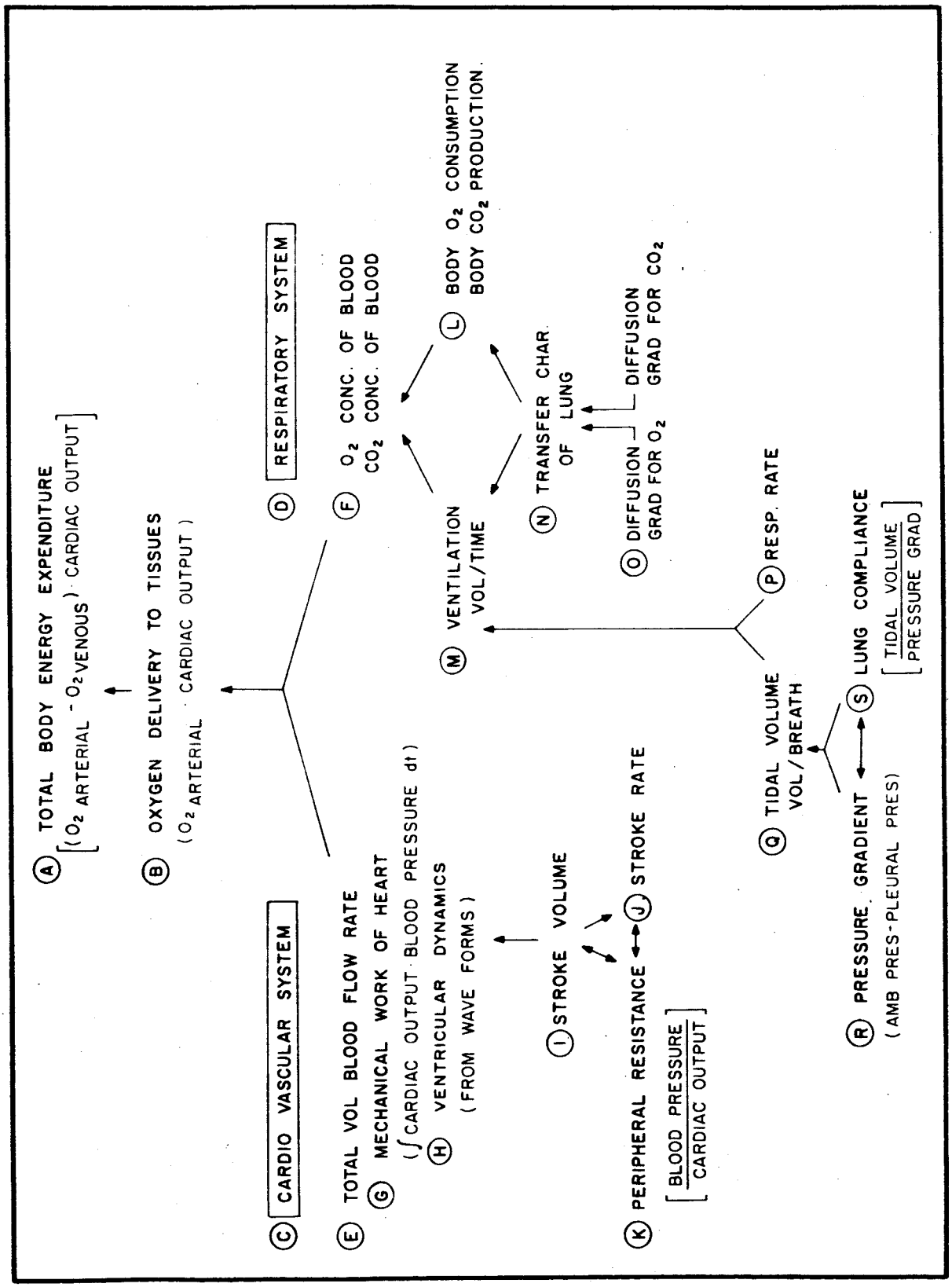

Fig. 3 Integrated Performance of Cardiovascular-Respiratory Systems

The task of the respiratory system is to effect a suitable concentration of oxygen and carbon dioxide in the blood that passes through the lungs (F). This is accomplished by transferring suitable quantities of oxygen and carbon dioxide between the blood and the ambient atmosphere. These gases are transferred by simple diffusion and consequently the quantities transferred are determined by the amounts of oxygen used and carbon dioxide produced by the tissues (L), the volume of ambient gas ventilated into and out of the lungs (M) and the diffusion characteristics (N) of the lung. This last item can be characterized by the diffusion gradients for oxygen and carbon dioxide. Lung ventilation (m) (volume of gas per unit time) is a function of the interplay respiratory rate (P) and the tidal volume (Q) (volume per breath). The tidal volume (Q) in turn, is dependent upon the pressure gradient that forces ambient gas into the lungs (R) (not partial pressure, but total pressure) and the compliance of the lungs (S) (the ease or difficulty with which the air sacs will fill). The pressure gradient responsible for moving the air into and out of the lungs is the pressure between the ambient pressure and the pressure within the chest cavity. The pressure within the chest cavity goes negative with respect to ambient pressure when the chest wall expands and diaphragm contracts (inspiration); it goes positive with respect to ambient pressure when the chest wall and diaphragm relax and return by elastic forces to their former state (expiration).

The integrated interplay of all of these factors results in satisfactory performance of the respiratory system. The overall performance of the respiratory system is geared to meet the needs of body energy metabolism. A great number of combinations and permutations of the various factors that interplay with each other can satisfactorily furnish oxygen and eliminate carbon dioxide to meet bodily needs.

E. NATURE OF INFORMATION AVAILABLE FROM A PHYSIOLOGICAL EXPERIMENT IN SPACE

What information concerning the performance of the body's two most critical physiological systems can be acquired from an orbital mission? Since the Mercury program represents the state-of-the-art, let us review briefly what has been obtainable from the Mercury program.

In the nine Mercury flights it has been possible to measure heart rate, respiratory rate and occasional arterial blood pressures. As can be seen from the somewhat simplified diagram of cardiovascular-respiratory system performance of Fig. 3, these particular physiologic phenomena are highly dependent and incidental parameters of cardio-respiratory function. They are not particularly revealing in indicating whether or not the cardiovascular and respiratory system are functioning adequately or inadequately. As a matter of fact, values for each of these parameters may be within certainly "normal" limits at a time that the physiological systems are not meeting the demands being placed upon them. Or alternatively, quite "abnormal" values may be indicators of the response the physiologic systems are making to (adequately) perform their function. Unfortunately the physiological sensors available and used did not permit an assessment of how adequately or inadequately these two most critical physiologic systems are doing their job.

The Program set forth in this report frankly emphasizes performance of the cardio-vascular and respiratory system, since they are the body's two most critical systems. If maximum use is made of surgical implantation of biosensors in experimental animals, EACH AND EVERY ONE OF THE CARDIO-VASCULAR AND RESPIRATORY PHENOMENA LISTED IN FIG. 3 CAN BE CONTINUOUSLY MEASURED AND/OR COMPUTED (see Sec. IV). The adequacy with

which any of the systems is meeting the demands placed upon them, and the demands themselves, can be quantitated, AND each and every one of these phenomena can be monitored and/or computed continuously during lift-off, sustained earth orbit, reentry and landing with the information telemetered.

Items one through seven of Fig. 4 list those cardio-respiratory physiological phenomena to be directly measured and the technique by which the measurement will be made. Figure 4 also contains information concerning power requirements, signal bandwidth and weight of flight equipment. These seven biosensors listed in Fig. 4 are either used individually to monitor each of the physiologic phenomena depicted in Fig. 3 or are used in combination to compute the phenomena from the equations shown.

F. IMPLEMENTATION OF CARDIOVASCULAR AND RESPIRATORY STUDIES BY IMPLANTABLE BIOSENSORS

In the experiment designed, the cardiovascular and respiratory phenomena depicted in Fig. 3 will be continuously monitored and/or computed by means of a surgically implanted, composite electronic biosensor consisting of the first seven instruments listed in Fig. 4.

The volumetric output of the left heart will be measured stroke by stroke by means of a miniaturized, transistorized electromagnetic flowmeter (Fig. 4, Item #3) the transducer probe of which encircles the base of the aorta (the blood vessel carrying blood from the left heart to the tissues). Incorporated in the same transducer probe will be a pair of miniaturized spectrophotometric backscatter devices (Items 1 & 2) employing injection lasers and solid state photodetectors. By means of these spectrophotometric devices arterial oxygen saturation will be continuously measured through the wall of

MEASUREMENTS (PER ANIMAL)	AVERAGE POWER Watts	SIGNAL BANDWIDTH Cps	EQUIPMENT WEIGHT Pounds	CONTINUOUSLY RECORDED INTERMITTENTLY TELEMETERED MEASUREMENT TECHNIQUE
1. Arterial Oxygen Saturation	1.0	10	1.0	Spectrophotometric
2. Venous Oxygen Saturation	1.0	10	1.0	Spectrophotometric
3. Cardiac Stroke Output	3.0	40	2.0	Electromagnetic Flowmeter
4. Left Ventricular/Arterial Blood Pressure	0.1	40	0.2	Solid State Piezoresistive
5. Respiration Rate and Volume	0.1	20	0.2	Impedance Pneumograph or Integrated Diaphragmatic EMG
6. Tissue Carbon Dioxide Tension	0.2	<1	0.5	Polarographic
7. Pleural Pressure	0.1	20	0.2	Solid State Piezoresistive
8. Body Temperature	0.1	<1	0.2	Thermistor
9. Eye Motion Nystagmus Sleep-Wakefulness	0.2	10	0.2	Implanted Temporal Electrode
10. Perceptual - Motor Studies	10.0	20	20.0	Performance Test Panel and Physical Exercise Apparatus with On-Board Task Programmer and Response Encoder
11. Television (2 Sec./Frame)	2.0	--	21	
Total	17.8		46.5	

Fig. 4 Characteristics of Systems for Acquisition of Recorded Intermittently Telemetered Physiological Data

the aorta and venous oxygen saturation measured through the wall of the adjacent pulmonary artery (which carries the venous blood that has come from the tissues from the right heart to the lungs) (Fig. 2).

Phasic blood pressure within the left ventricle or arterial blood pressure will be measured by means of a miniaturized solid-state piezoresistive element situated between the endocardium of the left ventricular chamber or outside the aorta. (#4) Pleural pressure will be measured by a similar transducer (#5) located in the pleural space, the space between the chest wall and the lungs. Carbon dioxide partial pressure will be measured by a mico-miniaturized polarographic (#6) electrode incorporated in the composited sensor. And respiratory rate and volume will be measured either by means of the impedance pneumograph or integrate diaphragmatic electro myogram (#5): the first of these devices senses the electrical impedance between two electrodes placed on either side of the chest cavity; the second of these quantitates the mean electrical signals that accompany contraction of the muscle fibers that make up the diaphragm.

The surgically implanted transducer probe portions of these instruments will be physically incorporated into a single biosensor strategically located in the animal's mediastinums. None of these sensors will be inserted into blood vessels or will come into contact with blood, for the likelihood of hemorrhage and/or blood clotting under such circumstances is prohibitive. An appropriately placed electrical connector situated beneath the skin will be used to deliver power to the composite probe and will conduct the electrical output signals to the signal processing modules located elsewhere in the space capsule

Returning to Fig. 3, oxygen saturation of arterial blood (in A, B, F) and mixed venous blood will thus be directly measured. Similarly the volumetric output of the left heart (A, B, G) will be directly measured. The difference between arterial and venous oxygen saturation multiplied by the cardiac output will continuously reveal the moment-by-moment oxygen utilization of the animal (A) which is the single, most critical measure of total body energy expenditure. At programmed intervals during orbit, the animal will perform graded and measured muscular exercise tasks in which it has previously been trained. The manner and extent to which a sustained period in space alters total body energy expenditures and requirements at rest and during work (the demands which the physiologic systems must meet) will thereby be assessed.

Arterial oxygen saturation multiplied by cardiac output will continuously measure the amount of oxygen being delivered to the tissues (B). This parameter, as noted previously, is a measure of the integrated performance of the cardio-vascular and respiratory systems.

Total volumetric blood flow (cardiac output) (C) (#1) will be directly measured. Ventricular blood pressure and/or arterial blood pressure (G, H, K) (#4) will be directly measured and the mechanical work being performed by the heart (G) is the integral of the product of cardiac output times blood pressure, with respect to time. The mechanical work performed by the heart (G) will be continuously computed and the effect of the various phases of the flight profile, the sustained orbital state and variable work loads under these conditions on cardiac work will be assessable.

Comparison of cardiac work, as so computed, and total body energy expenditure, as computed above, will reveal the adequacy of cardiac performance to meet metabolic needs. POSSIBLE DECRE-

MENTS IN CARDIAC WORK THAT APPEAR DURING FLIGHT WILL THUS BE ASSESSABLE AS DETERIORATION IN THE ABILITY OF THE HEART TO MEET BODILY NEEDS, OR ALTERNATIVELY AS ADAPTIVE ADJUSTMENTS IN CARDIAC WORK PARALLELING A REDUCTION IN THE LEVEL OF BODY REQUIREMENTS.

The dynamics of ventricular contraction and relaxation (H) will be directly monitored by the intraventricular pressure signals and cardiac output wave forms. Stroke volume (1) and stroke rate (J) are similarly directly measured by the electromagnetic flowmeter. From the ventricular/arterial pressure signal and the cardiac output signal, peripheral vascular resistance (K) will be continuously computed. There has been considerable discussion regarding the maintenance of peripheral vascular resistance or "tone" during extended periods in the nongravitational state. By these means the effect of the prolonged weightlessness on vascular tone and the added stress of reentry following weightlessness will be directly quantitated.

As mentioned earlier, the role of the respiratory system is two-fold: (1) adequate oxygenation of the circulating blood, and (2) adequate but not excessive elimination of carbon dioxide (F). These two functions will be directly and continuously monitored. The first, by the arterial oxygen saturation biosensor; (#1) the second, by the miniaturized implanted carbon dioxide polarographic electrode (#6). Measurement of oxygen and carbon dioxide levels within the body and knowledge of the levels of these two gases in the spacecraft atmosphere define the diffusion gradients for these two substances (O), thereby characterizing the transfer characteristics of the lung (N)

Minute ventilation (M), respiratory rate (P) and tidal volume will all be directly measured by the impedance pneumograph and/or the integrated diaphragmatic electro myogram (#5).

Direct measurement of the pressure within the pleural space (#7) and knowledge of atmospheric pressure permits continuous computation of the pressure gradient (R) inflating the lungs. Computation of the ratio of tidal volume (Q) to this last pressure gradient defines the compliance of the lungs (S) and lung compliance is of considerable functional and diagnostic importance since it is the single most sensitive index of the physical state of the lungs. Arterial oxygen saturation, measured directly as described above (#1), is the most sensitive indicator of perfusion-ventilation characteristics of the lungs. And these two characteristics, compliance and perfusion-ventilation characteristics are the most sensitive, meaningful and accurate methods known to modern sciences for assessing the state of the lungs and evaluating any possible lung pathology that might occur during flight.

G. ADDITIONAL IMPLANTABLE BIOSENSORS

Two additional biosensors, not directly measuring cardiovascular nor respiratory phenomena, will be surgically implanted in the experimental animal and will furnish data for telemetry (Figs. 4 & 5).

One of these is a pair of miniature electrodes implanted beneath the skin on the temporal regions of the skull, either side of the eyes (9). Since the eye is an electrical dipole by virtue of its metabolic activity, eye movements can readily be detected by sensing the potential difference between the two implanted as electrodes and eye position can be determined to 1.5 degrees.

Nystagmus, a jerky oscillatory movement of the eyes with a rapid component in the opposite direction, can be readily detected and quantitated by this technique. Nystagmus is intimately associated with malfunction of the vestibular apparatus, that portion of the inner ear that functions as three

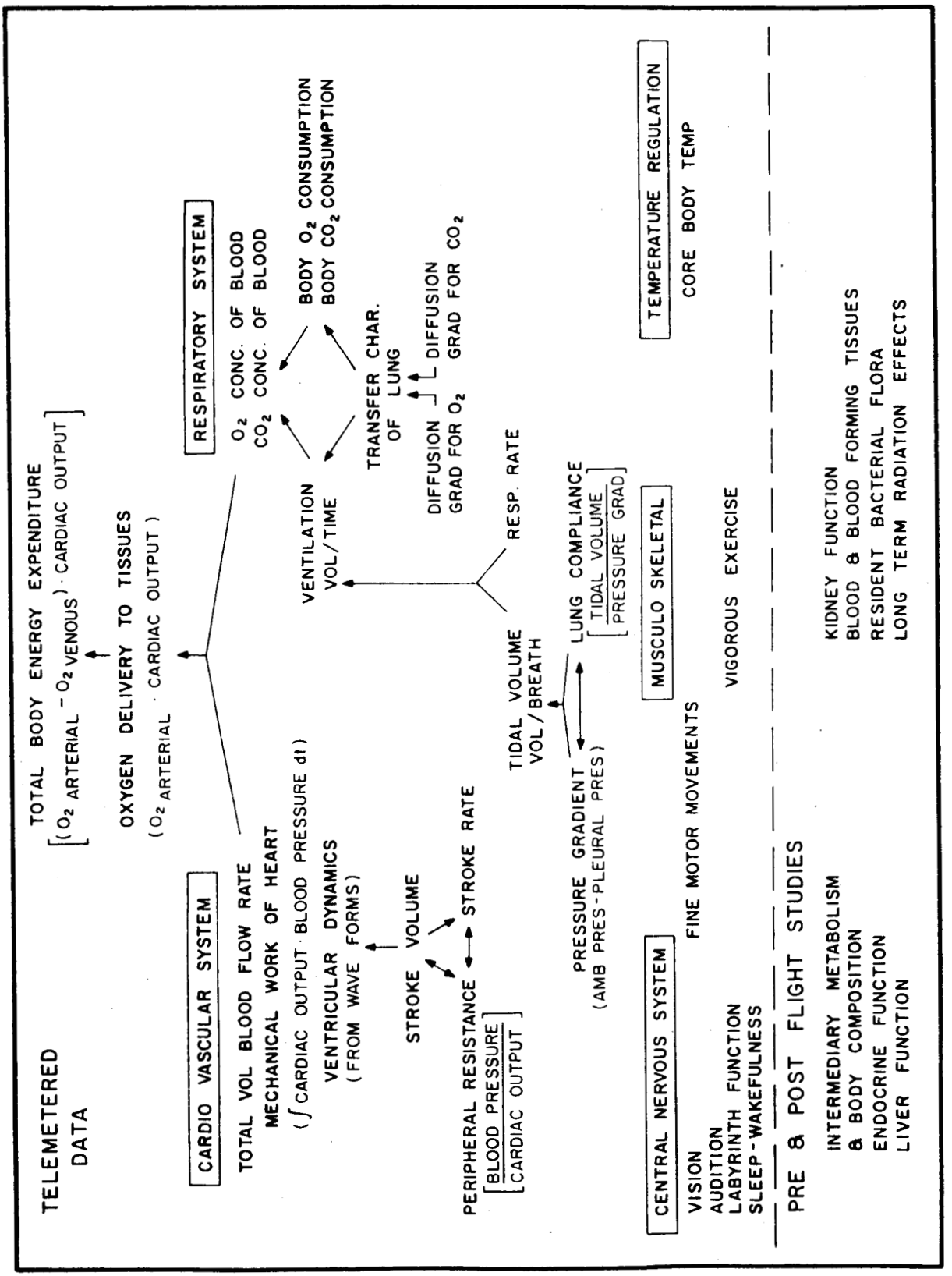

Fig. 5 Physiological Studies of Sustained Orbital Program

mutually perpendicular accelerometers. Abnormalities in vestibular function, manifest by dizziness and motion sickness, have been experienced by both American and Russian astronauts and have been a cause of some concern during space flight.

Through the use of flashing lights of various intensity, the visual threshold can be objectively determined. This same technique permits rather crude assessment of the limits of the visual fields. And, in addition, the temporal electrodes will also permit differentiation between periods of wakefulness and sleep, thereby permitting the evaluation of sleep-wakefulness cycles during sustained orbit in space.

The other biosensor chosen for implantation is the thermistor (8) which will measure core body temperature. This sensor will furnish information concerning the body's temperature regulating mechanism and will be of significant assistance in operational evaluation of the state of well-being of the primates and in evaluating the performance of the life support system.

H. USEFULNESS OF DATA TELEMETERED FROM IMPLANTED BIOSENSORS IN DIAGNOSIS AND THERAPY OF SUBJECTS IN SPACE, MANAGEMENT OF SPACE MISSION AND CONTROL OF ENVIRONMENTAL CONTROL SYSTEM

Telemetry of information from the surgically implanted biosensor transducers will be of value in following the status of the subjects during the course of the mission and will permit diagnostic assessment of the cause of abnormalities as they develop. On the basis of physiologic measurements telemetered to the ground, operational decisions regarding specific corrective measures or the introduction of therapeutic medical regimens can be remotely signaled to the capsule or decisions regarding terminating the mission can be made. Alternatively, "sets" of physiologic abnormalities can be programmed to automatically intro-

duce corrective therapeutic measures by means of a logic contained within the capsule.

As an example, body temperature elevation, decreased lung compliance and minimal oxygen desaturation represent a "set" indicative of lung pathology, such as atelectasis or broncho-pneumonia, both of which might be feared during a sustained mission. An on-board computer could be programmed to introduce particular therapeutic measures whenever the "set" existed and certain parameters set exceeded pre-set limits. Thus an antibotic could be introduced into the animal's drinking water if temperature exceeds 102°F during any four-hour period; an expectorant could be introduced and the increased concentrations of cabin oxygen regulated on a schedule programmed with changes in lung compliance and arterial oxygen saturation.

Similarly, telemetry from the surgically implanted biosensor transducer will furnish valuable supplementary assessment regarding operation of the life support system. Because implanted transducers will probably have greater stability and reliability than the cabin transducers, especially regarding partial pressures of oxygen and carbon dioxide, it may prove wise to fit the physiologic biosensors into the environmental control system feedback loop or, with an appropriate logic, program these sensors into an override on the environmental control system.

For example, progressive decrease in arterial oxygen saturation accompanied by decreased carbon dioxide tension, hyperventilation, elevation of blood pressure and increased heart rate form a"set" indicative of oxygen deficiency. Regardless of the indications of the cabin oxygen partial-pressure sensor, a switch to a back-up oxygen supply is indicated.

On the other hand, all of these parameters may be identical with the preceding "set" except that carbon dioxide tension may be up -- indicating airway problems. Should the decreased arterial oxygen saturation be caused by heart failure, all of above parameters may be identical except that carbon dioxide tension would be UP and blood pressure probably DOWN. Cardiac output would definitely distinguish between these last two "sets."

Or, once again, body temperatures above some particular value would appropriately shut down the heating system and start up the cooling system, regardless of whether the cause of the hyperthermia be malfunction of the Environmental Control System or infection within the animal.

Because the surgically implanted biosensor transducers will continuously monitor and frequently telemeter (once per orbit, see Sec. B) meaningful measures of organ and system physiologic performance, a detailed account of the effect of sustained periods in space upon the critical body systems will be obtained, even if the recovery phase of the mission is unsuccessful.

I. PERCEPTUAL-MOTOR STUDIES

A simple programed schedule of perceptual-motor tasks, for which the primates have been previously trained, will be performed during the flight. This program will include a visual discrimination task, an auditory discrimination task, a temporal discrimination task, a fine motor-movement task and a task requiring the performance of considerable muscular work. Both reinforcement and avoidance operant conditioning schedules will be used.

This portion of the experiment is designed to assess the effects of sustained orbital conditions upon fundamental

sensory thresholds and to evaluate possible degradation in temporal discrimination and fine motor abilities, all of which are important during space flight. Perhaps equally important, the programed activities will furnish necessary physical exercise for the restrained animal and will introduce attention occupying activities to dispel boredom.

Exercise for both arms and legs will be performed on a bicycle wheel type apparatus (the torso will be restrained in a webbed suit affixed to the flight contour couch) and the exercise will be sufficiently demanding to constitute a challenge to the cardio-vascular, respiratory and other physiological systems. By introducing periods of muscular stress, physiologic degradations, which may not be apparent during rest, will become discernible.

J. PRE- AND POST-FLIGHT METABOLIC AND ORGAN FUNCTION STUDIES

In order to accomplish an over-all survey of the various organ and system functions and to assess intermediary metabolism, a series of pre-flight and post-flight tests is planned and a complete in-flight metabolic balance study will be performed (Fig. 5). These studies neither complicate nor add jeopardy to the flight program for they entail only fractional collection or sampling of urine and stool and monitoring of water and food intake. Fractional collection or sampling should not complicate management of the animal's waste for stools, and urinary wastes will probably be frozen and urinary water may be reclaimed and re-cycled. By means of the pre- and post-flight tests and the post-flight analyses of waste collections, intermediary metabolism, endocrine system function, kidney, liver, and gastro-intestinal function, and the status of the hematopoietic system will be evaluated.

1. Intermediary Metabolism

Body composition will be thoroughly assessed prior to and immediately following flight; a complete metabolic balance study will be performed for the flight period. In this manner, alteration in body composition will be determined, and the particular metabolic pathways by which the body met its metabolic needs determined. The elucidation of preferential dietary pathways by which metabolic needs are met in the space ambient will furnish a rational basis for planning diets during manned missions. Thirst and appetite will be assessed on a daily basis, as will the metabolic aspects of caloric, water, electrolyte, nitrogen, calcium, phosphorus, and magnesium metabolism. (Even the brief Mercury manned missions have suggested some abnormality in calcium metabolism as a consequence of the space ambient.)

a. Pre-Flight and Post-Flight Tests of Body Composition

Weight, total body water, K_{40} content (lean body mass), exchangeable Na, bromide space, plasma volume, sodium, chloride, potassium, calcium, magnesium, phosphorus, plasma, proteins.

b. Water and Diet Intake Measurements

c. Daily Urine Fractions

Analysed for volume, specific gravity, electrolytes, nitrogen, calcium, phosphorus.

d. Four-Day Stool Fractions

Analysed for fat and nitrogen.

2. Endocrine System Function

Pituitary, adreno-cortical, adreno-medullary, thyroid, and gonadal function will be evaluated pre-flight and post-flight. Because the pituitary-adrenal axis and the sympathetico-adrenal medullary system are intimately involved in the

body's response to stress, they will be evaluated on a daily basis. Specifically, the following pre-flight and post-flight tests will be performed:

a. Pre-Flight and Post-Flight Studies

Adreno-Cortical Status

serum and urine oxysteroids, aldosterone, and 17 ketosteroids, baseline and in response to test doses of ACTH.

Sympathetico-Adrenal Medullary System

serum and urine catecholamines.

Thyroid Status

protein bound iodine, radioactive iodine uptake.

Gonadal Status

urinary estrogens and androgens.

b. Daily Urinary Fractions

Analyzed for hydroxycorticoids, 17 ketosteroids, catecholamines, and electrolytes.

3. Renal Function

Renal function tests will evaluate kidney status pre-flight and post-flight. Indications of daily function will be assessable from the aforementioned analyses of fractional daily urine samples.

Renal Function Tests

BUN, inulin clearance, PAH clearance.

4. Hepatic Function

Will be evaluated pre-flight and post-flight.

Liver Profile Tests

Flocculation tests, bilirubin, alkaline phosphatase, BSP excretion, serum proteins.

5. Gastro-Intestinal Function

Will be evaluated from the balance data regarding dietary intake and from daily fractional stools. Microscopic examination of blood and bacteriological studies of stool flora will be performed.

6. Hematopoietic System

Pre-flight and post-flight RBC mass and bone marrow biopsis will indicate whether any abnormalities in blood production or RBC destruction mechanisms are caused by the space ambient. Because of the sensitivity of the hematopoietic system to irradiation and the propensity of irradiation to cause late leukemias, it will be important to follow those animals for extended periods post-flight.

K. CONCLUSIONS

This three-part program of (1) continuous measurement and telemetry of critical physiological performance, (2) the in-flight perceptual motor studies on the operant conditioning schedule, and (3) the series of pre-flight and post-flight organ function tests and in-flight metabolic balance, constitutes a thorough and definitive evaluation of the effects of sustained space flight in body physiology. Any degradations detected in physiological performance will furnish a rational basis for programs designed to eliminate or compensate for these degradations in support of the space programs being planned.

If degradations are observed as a consequence of this mission, NASA should have as definitive a reliability check on man as a component in the space systems of the future as medical science can now offer.

III. AN ANALYSIS OF ORBITING SYSTEMS FOR SUSTAINED (30-90 DAY) ORBITAL STUDIES

A. INTRODUCTION AND DISCUSSION OF ASSUMPTIONS

A preliminary analysis was performed of the orbiting systems which would be required to support a sustained orbital program of the type described in the preceding section of this report. The discussion that follows represents a "first cut" at estimating the weights, power requirements and so forth of such systems and examines the trade-offs presented by such alternatives as recovery versus non-recovery, battery power versus solar cell power, Rhesus monkeys versus chimpanzees, various numbers of experimental animals and various mission durations. The discussion that follows is not the result of a detailed design study. The estimates are based to a large extent on data obtained during May 1963, through discussions with personnel of Lockheed Aircraft Corporation, North American Aviation Corporation, AiResearch Division of the Garrett Corporation, Douglas Aircraft Corporation, MRD Division of the General American Transportation Corporation, McDonnell Aircraft Company, Holloman Air Force Base, the Applied Physics Laboratories of Johns Hopkins University and the Office of Advanced Research and Technology of the National Aeronautics and Space Administration.

Specifically, system requirements are estimated for systems accommodating one, two and four chimpanzees or two, four or eight Rhesus monkeys (or any combination thereof)

for mission durations of 30, 60 and 90 days. Recoverable and nonrecoverable systems and battery powered and solar cell powered systems are examined.

A most important assumption in these estimates is that launch will occur in the last quarter of 1964 (18 months from analysis to lift-off). This very short time scale dictates that the selected systems possess the greatest simplicity consistent with achievement of the mission objectives, that it involve the minimum possible development and the maximum use of readily-available flight-proven techniques and hardware.

If recovery is desirable, the choice of re-entry vehicles subject to the minimum development constraint is a narrow one. Only the Mercury space craft and the Discoverer vehicle have flight-proven re-entry capability. Discussion with personnel at the Lockheed Aircraft Corporation demonstrated that the Discoverer vehicle could accommodate only one small monkey. Because the significance of findings in one experimental animal would always be subject to doubt, and because the chimpanzee was felt to be a far more desirable experimental subject than a small Rhesus or related monkey, the Mercury space craft was felt to be a vastly preferable choice. It appears possible to fit into the Mercury space craft most of the equipment necessary for the chimpanzee on these extended missions. In addition, there was reason to believe that one of three completed and surplus Mercury Spacecrafts might be made available for this project.

Therefore the calculations in the exercise that follows are based on the Mercury Spacecraft, both for recoverable and nonrecoverable systems. It should be recognized, however, that in the latter case, it might be feasible to employ a different vehicle since flight proven re-entry capability would

not be required. The Mercury numbers are used in this exercise both for simplicity and to gain a notion of the weight penalty imposed by the recoverability requirement. A further assumption is a low inclination angle orbit of approximately 220 miles altitude which is consistent with the maximum mission duration.

B. ESTIMATES AND COMPARISON OF FOUR SYSTEMS (RECOVERABLE, NONRECOVERABLE, SOLAR CELL POWERED AND BATTERY POWERED) TO SUPPORT TWO CHIMPANZEES OR FOUR RHESUS MONKEYS IN ORBITAL PROGRAM FOR 90 DAYS

Approximate volume calculations for the Mercury Spacecraft, the experimental animals and associated equipment indicated that everything required for the missions with the exception of batteries and atmospheric gases could probably be fitted into the Mercury spacecraft. The batteries and gases would have to be located external to the capsule. A matching section to mate the Mercury spacecraft to the Saturn-IV would be a necessary development item in any case. This section would be made large enough to contain these items. An approximate notion of the configuration can be gotten from Fig. 6 which shows the Mercury spacecraft, the matching section, the Saturn-IV, an auxiliary umbilical assembly and an overall view of the launch assembly. This arrangement was suggested by the Douglas Aircraft Company.

Figure 7 shows the weight computations for two 30-lb chimpanzees or four Rhesus monkeys, or a combination thereof, orbiting 90 days in each of the four systems considered. Three of the systems are recoverable and one is not. Of the recoverable systems, one is battery-powered and two are not. These latter differ in that one tracks the sun continuously when it is in view while the other employs the

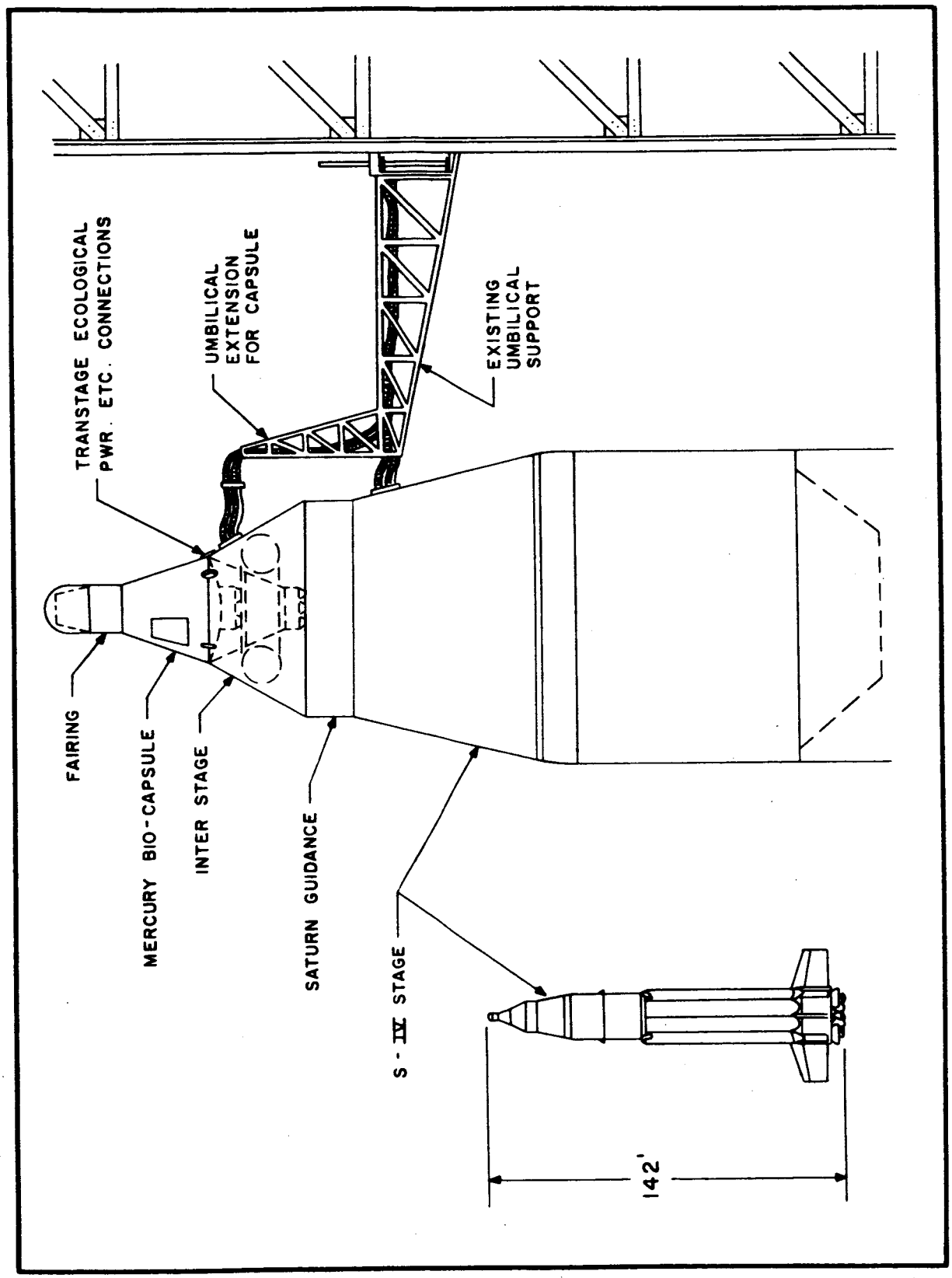

Fig. 6 Saturn IV Mated with the Mercury Spacecraft

ITEM	RECOVERABLE SYSTEMS			NON-RECOVERABLE SYSTEM
	BATTERY POWERED	SOLAR CELL POWERED		SOLAR CELL POWERED
	LIMITED-g ACS	LIMITED-g ACS	SUNSEEKER ACS	LIMITED-g ACS
	WEIGHT pounds	WEIGHT pounds	WEIGHT pounds	WEIGHT pounds
SPACECRAFT (Including ACS)	2530	2530	2890	1560
STORAGE AND MATCHING SECTION	704	220	193	213
PRIME POWER SOURCE	5330	496	237	389
LIFE SUPPORT SYSTEM AND EXPERIMENTAL SUBJECTS	1181	1181	1181	1181
COMMUNICATIONS AND T/M (includes TV)	244	244	244	224
EXPERIMENTAL APPARATUS	50	50	50	50
TOTAL	10039	4721	4795	3617

ALTERNATIVELY, AND PERHAPS OPTIMALLY, ONE CHIMPANZEE AND TWO RHESUS MONKEYS.

Fig. 7 Estimated Weights of Orbiting Systems

automatic control system (ACS) during the main portion of the flight merely to maintain tumbling at a low enough rate to keep an essentially weightless condition in the capsule. The ACS is similarly employed in the other two cases. The system components have been divided into six parts, several of which will be discussed in detail hereafter. The first is the spacecraft itself which includes the Mercury structure, automatic control system and fuel, the Mercury electrical system, some cabin equipment and miscellaneous items, together with heat shield and recovery equipment where applicable. These figures indicate a weight penalty of about 1000 lb for recovery. The sunseeker system is heavier than the random oriented systems by virtue of the additional fuel required for solar tracking. Fuel estimates[2] are one pound each day for the low-G ACS and five pounds a day for the sunseeker. The second item is the service module or storage and matching section which contains batteries and gases and which would be jetisoned prior to re-entry. The weight estimates are based on 150 lb plus 10 per cent of stored weight (batteries, gas and tankage). The third item, prime power source, includes batteries (both in-flight and recovery) solar cells, inverters, regulators and the like. For this case (two chimps - 90 days) a 5000-lb penalty for battery operation is imposed. Solar cell weights are based on 1.5 lb/ft^2 for cells and frames, 10 $watts/ft^2$ at normal solar incidence, a 50 per cent to 50 per cent light-dark cycle (which is quite conservative), a 50 per cent battery charging efficiency, and a 4:1 area penalty in the tumbling mode for the nonrecoverable system. This was increased to 5:1 for the recoverable system on the grounds that there might be geometrical constraints in

[2] From Lockheed.

this system which would lead either to shading of the cells by the spacecraft or to additional weight for deployment apparatus. Battery weights are estimated on a 65 watt-hr/lb basis. The fourth item is the life support system for the animals (discussed in Sec. C below). The fifth item, communications and telemetry, includes command and control equipment for the capsule, communications and telemetry equipment for the experiment, beacons and the like. The experimental apparatus (25 lb/animal) includes the sensors, electronics and psychomotor equipment discussed in the previous section (Fig. 4) of the experimental subjects, the chimpanzees would be of the 30-lb weight range and the rhesus monkeys would each weigh approximately 15 lb (rhesus monkeys down to weights of 8 lb, each would be acceptable).

For the mission chosen for illustration, there is little weight difference between the two recoverable systems employing solar cells; the randomly oriented system is to be preferred for reasons of reliability. The recovery penalty is about 1000 lb, as noted earlier, and the penalty for battery operation is about 5000 lb. Payload weight would have to be very cheap, indeed, to justify this added reliability and simplicity.

C. LIFE SUPPORT SYSTEM

Figure 8 shows a breakdown of weights in the life support system for two chimpanzees orbiting 90 days. The animals each weigh 30 lb and they lie on 12-lb couches. Sixty pounds of food are allowed for each animal (based on tests conducted at Holloman AFB where 30-lb chimpanzees were sustained on an ad-lib normal residue diet for 30 days). Water requirements (again from Holloman AFB) were estimated at 380 lb for 90 days but 50 per cent recovery by reprocessing atmospheric water

ITEM	WEIGHT pounds	POWER watts	COMMENTS
Chimpanzees*	60	0	
Couches, Restraints, Supports	50	0	
Food, Water, Feeders, Waste Collectors	610	0	Assumes Recovery of Atmospheric Water (50% of Animal Intake)
Atmospheric Control System	381	20 (Fan)	Non-Regenerative Stored Gas System CO_2 Removal By LiOH Bed; Assumes 0.5 lb/Day Leak Rate
Thermal Control System	80	25 (Pump) 15 (Water Recovery)	Includes Water Recovery System
Total	1181	60	

* Two to four small Rhesus monkeys may replace each chimpanzee.

Fig. 8 Characteristics of Life Support System Two 30 lb Chimpanzees for 90 Days

is assumed; this figure is probably slightly conservative. The atmospheric control system weight is mostly gases and LiOH. Oxygen requirements were based on calculations by Charles Swet of the Johns Hopkins Applied Physics Laboratory; the oxygen is cryogenically tanked as is the nitrogen in the two-gas system considered. Nitrogen calculations assume a 0.5 lb/day leak rate. At 7-psi cabin pressure, this is a factor of about six better than the current Mercury leak rate of 2.1 lb/day at 5 psi. Engineers at both AiResearch Corporation and McDonnell Aircraft Corporation seem to feel that this improvement is feasible at pressures even higher than 7 psi. CO_2 removal is effected by a LiOH bed with no oxygen regeneration. The thermal control system includes a centrifugal water separator after the heat exchanger. Radiative cooling is employed as evaporative cooling would require approximately 1500 lb of expendable coolant. If the radiator could not be located at the recovery end of the Mercury capsule, it would presumably go on the service module and a water connection would have to be broken there when the module is jettisoned. Evapaorative cooling is used on re-entry.[3]

D. COMMUNICATIONS AND TELEMETRY SYSTEM

A second item common to the four orbiting systems is the communications and T/M equipment (cf. Fig. 9). Approximately 70 lb and 7 watts average power are required for the capsule and the remainder for the primates. Calculations indicate that telemetry both from the primates and the capsule can be performed on standard IRIG channels using either PCM or FM/FM encoding.[4]

---

[3] Details of the calculations are given in Appendix III-A.
[4] Details are given in Appendix III-B.

ITEM	WEIGHT Pounds	AVG. POWER Watts
CAPSULE SYSTEM		
TRANSPONDER	14	3
2 COMMAND RECEIVER AND DECODER	24	4
RECOVERY BEACON	20	-
ANTENNA SYSTEM	4	-
WIRING, JUNCTION BOXES, ETC.	10	-
TWO SYSTEMS FOR TWO PRIMATES		
COMMUTATORS, A/D CONVERTER, SUBMULTIPLEXERS	24	8
RECORDER	50	40
TELEMETRY MIXER AND TRANSMITTER	28	-
ANTENNA SYSTEM	8	-
WIRING, JUNCTION BOXES, ETC.	20	-
TELEVISION	42	6
	244	61

Fig. 9 Characteristics of Communications and T/M Systems

E. POWER REQUIREMENTS

Power requirements for the several systems are shown in Fig. 10. Life support and T/M requirements are about equal and the experiment requires 16 watts per animal. The automatic control system requires 35 extra watts when the sun is tracked continuously.[5]

F. SPACECRAFT, SERVICE MODULE AND POWER SOURCES

Figure 11 compares those items which differ from system to system. Weight costs for recovery and sunseeking ACS appear in the Mercury spacecraft breakdown.[6] The service module structure weight was estimated on the basis of 150 lb plus 10 per cent of stored weight as noted above.[7] Battery, power conditioning and solar cell weights are shown under "Power Sources." In-flight battery requirements for the solar-cell cases are based on peak power requirements and imply a discharging of only about 5 per cent of stored energy on the dark side of the orbit. As mentioned before a storage density of 65 WH/lb is assumed.[8]

G. VARIATION OF WEIGHTS WITH MISSION REQUIREMENTS (Fig.12)

Using the assumptions detailed above for the two chimpanzees' 90-day mission, weights were also computed for each of the four systems for various mission profiles. These estimates are intended to give a notion of the weight requirements on a per animal and a per-unit-time basis. One, two and four 30-pound chimpanzees were considered on 30-, 60- and 90-day missions. Insofar as overall weights are concerned,

---

[5] Details are given in Appendix III-C.
[6] Details are given in Appendix III-D.
[7] Details are given in Appendix III-E.
[8] Details are given in Appendix III-F.

IN-FLIGHT REQUIREMENTS	BATTERY-Limited g ACS SOLAR CELL-Limited g ACS			SOLAR CELL-Oriented			SOLAR CELL-Limited "g" ACS Non Recovered		
	1	2	4	1	2	4	1	2	4
LIFE SUPPORT SYSTEM	40	60	100	40	60	100	40	60	100
COMMUNICATION AND T/M	34	61	115	34	61	115	34	61	115
EXPERIMENT	16	32	64	16	32	64	16	32	64
ACS	5	5	5	40	40	40	5	5	5
TOTAL	95	158	284	130	193	319	95	158	284
RECOVERY REQUIREMENTS	130	190	310	130	190	310	0	0	0

Fig. 10 Power Requirements - Average Power - Watts

ITEM	RECOVERABLE SYSTEM			NON-RECOVERABLE SYSTEM
	BATTERY POWERED	SOLAR CELL POWERED		SOLAR CELL POWERED
	Lo-g ACS	Lo-g ACS	Sunseeker ACS	Lo-g ACS
	WEIGHT Pounds	WEIGHT Pounds	WEIGHT Pounds	WEIGHT Pounds
MERCURY SPACECRAFT				
STRUCTURE, CABIN, Elec., etc.	1270	1270	1270	1270
RECOVERY SYSTEM (ACS, Heatshield, Chutes)	1170	1170	1170	200
ADDITIONAL ACS FUEL FOR 90 Days OPERATION	90	90	450	90
	2530	2530	2890	1560
STORAGE AND MATCHING SECTION				
STRUCTURE	704	220	193	213
POWER SOURCES				
BATTERIES, and POWER CONDITIONING	5330	140	150	105
SOLAR CELLS	0	356	87	284
	5330	496	237	389
TOTAL	8564	3246	3320	2162

Fig. 11 Characteristics of Spacecraft and Power Sources

SYSTEM	No. OF CHIMPANZEES *	1			2			4		
	DURATION (Days)	30	60	90	30	60	90	30	60	90
RECOVERABLE										
I BATTERY-POWERED		4320	5690	7060	5460	7750	10040	7750	11880	16010
II SOLAR-POWERED	Random Orientation	3430	3650	3860	3990	4360	4720	5130	5790	6450
III SOLAR-POWERED	Solar Orientation	3390	3720	4060	3830	4310	4800	4710	5490	6280
COMBINATION OF I AND II					4080	4790	5500	6070	8300	10540
NON-RECOVERABLE										
IV SOLAR-POWERED		2370	2580	2780	2890	3250	3620	3930	4600	5260

* ALTERNATIVELY, TWO TO FOUR RHESUS MONKEYS MAY BE USED IN PLACE OF EACH CHIMPANZEE.

Fig. 12 Variation of Overall Weight with Mission Requirements

two to four Rhesus monkeys may be substituted for each chimpanzee. The figures in Fig. 12 are overall weights (spacecraft, service module, communications and T/M, life support, power weight and experimental weight - in short, payload) for the several cases. The four-chimpanzee (eight Rhesus monkeys) numbers are somewhat academic since it would be impossible to fit the four animals into the Mercury spacecraft.

In the battery-powered case it appears that a 6000-lb payload could support one chimpanzee or two Rhesus for between 60 and 90 days or, alternatively, two chimps or four Rhesus for between 30 and 60 days. A 5000-lb payload should suffice for two chimpanzees or four Rhesus for 90 days on a recoverable mission employing solar cells. A 4000-lb pay load suffices for the same mission without recovery.[9]

Also included in Fig. 12 are estimated weights for a system which combines solar cells and batteries. The numbers are approximate and are based on calculations given in Appendix III-G. For this last system it is assumed that the service module is an 8-ft diameter 3-ft long cylinder which is covered with solar cells. The orientation of the spacecraft is random and the average power developed by the solar cells is calculated for a 50 to 50 dark-light cycle and 50 per cent efficiency of storage in the batteries when more power is developed than is necessary for the demand at the time. Storage batteries are included for power requirements exceeding the power developed by the solar cells. The calculations show that all power requirements are met by the solar cells for the one-chimp case, about 80 per cent for the two-chimp case and about 50 per cent for the four-chimp case. This system

[9] Details are given in Appendix III-G.

brings the two-chimp, 90-day mission under the 6000-lb payload figure.

Two additional points should be made in connection with this system. The first is that no attempt has been made to estimate the weight or reliability consequences of hydridizing the power source. Appropriate logical and protective equipment would have to be developed at the juncture of the battery and solar cell power sources before the regulators. The second is that the hybrid system offers a reliability advantage in that (for the two chimp case) about 20 per cent of the electrical energy requirement for the mission is stored in batteries. This means that should the solar cell system fail at any stage of the mission it would be possible with appropriate circuitry to fly 20 per cent of the remainder of the mission on battery power. Thus for a planned 90-day mission, should solar cells become inoperative by some mishap at launch, approximately 18 days of the mission could still be flown.

H. FINAL REMARKS

The numbers developed in this exercise are "first cut" estimates and are not based on detailed system design. They should, however, be representative and give an indication both of the actual payload which this experiment would require and of its variation with type of system, number of experimental animals and mission duration.

APPENDIX III-A

LIFE SUPPORT SYSTEM

Weight and power estimates for the life support system are detailed in Table A-1. Weights are grouped in three categories: those which depend only on the number of experimental animals; those which depend only on the mission duration; and those which depend on both. The total weight of the life support system is thus

$$103\ N + 99\ \frac{T}{90} + 438\ N\ \frac{T}{90} \text{ pounds}$$

where

N is the number of chimpanzees (or 2 × the number of Rhesus monkeys)

T is the mission duration in days.

Parenthetical numbers preceding each item refer to the life support system breakdown in Fig. 3 , viz.,

1. Experimental animals
2. Couches, restraints, supports
3. Food, water, feeders, waste collection
4. Atmospheric control system
5. Thermal control system.

Several items in Table A-1 deserve comment. " Couches, restraints, supports" include a 12-lb couch (Lockheed

TABLE A-1

WEIGHT AND POWER BREAKDOWN - LIFE SUPPORT SYSTEM

	Weight Per Chimp	Weight Per 90 days	Weight Per Chimp Per 90 days	Power	Power Per Chimp
	Pounds	Pounds	Pounds	Watts	Watts
(1) Chimpanzees	30	--	--	--	--
(2) Couches, restraints, supports	25	--	--	--	--
(3) Food, feeder	--	--	70	--	--
(3) Water, tank, feeder	--	--	210	--	--
(3) Waste collection apparatus	--	--	25	--	--
(4) Oxygen, tank	--	--	92	--	--
(4) LiOH, container	--	--	41	--	--
(4) Nitrogen, tank	--	99	--	--	--
(4) Fan and plumbing	8	--	--	10	5
(5) Thermal control pump	3	--	--	5	10
(5) Water separator	3	--	--	5	5
(5) Heat exchanger, valves, plumbing	14	--	--	--	--
(5) Water filter	10	--	--	--	--
(5) Radiator	10	--	--	--	--
	103	99	438	20	20

estimate) or a 10-lb support and a 3-lb harness. "Food, feeder" includes 60 lb of food and a 10-lb feeder and is based on the experience at Holloman AFB. A 30-lb chimp on a normal residue, ad lib diet consumed 22 lb of food in 30 days. "Water, tank, feeder" includes 190 pounds of water and a 20-lb feeder and tank. (A water intake of 126 lb in 30 days was measured at Holloman AFB.) If 50 per cent of this intake can be recovered from the atmosphere, then the 90-day requirement is

$$3 \times \frac{1}{2}\ 126 = 189 \text{ pounds.}$$

This is probably conservative since Holloman AFB measured a 30-day urine output of 52 lb and a 30-day fecal output of 9 lb.

"Oxygen tank" includes 42 lb of O_2 and a cryogenic tank weight of 1.2 times this figure. The 42-lb requirement is an extrapolation to 30-lb primates of calculations by APL for primates up to 20 lb. "LiOH, container" is calculated from the O_2 requirement using

$$0.8 \text{ pound } CO_2 / \text{ pound } O_2$$

$$1.09 \text{ pound LiOH/pound } CO_2$$

and 10 per cent for the container. "Nitrogen, tank" includes all leakage from the capsule at the 0.5 lb/day assumed rate and 1.2 lb cryogenic tankage/lb gas. The N_2 weight could be reduced somewhat and the O_2 weight correspondingly increased since both gases leak from the capsule in proportion to their abundance in the capsule atmospheric constitution, but the total weight of leakage gas will remain unchanged. As noted in the main body of this report,

the 0.5-lb/day leak rate at 7 psi cabin pressure represents a factor of 6 improvement over Mercury's present 2.1 lb/day at 5 psi. Should this prove unattainable, it should still be possible to avoid some of the weight penalty due to storage of additional gas to make up for leakage by enclosing the primates in well-scaled life cells operating at pressure determined on physiological grounds and operating the remainder of the cabin at lower pressures determined by cooling requirements for the electrical systems in the cabin.

The remaining numbers in Table A-1 are "guesstimates" in the absence of a detailed life support system design. Since more than 90 per cent of the life support equipment weight is included in the items already discussed this is serious in only one respect. This is that inaccuracies in estimating power requirements could lead to significant errors in overall system weight. For the battery-power system and a 90-day, two-chimpanzee mission the power penalty is about 37 lb/watt. Thus a 25 per cent error in the estimated 60-watt life support power requirement would result in a 500-lb overall weight error. For the randomly oriented solar cell system, the power penalty is less than 5 lb/watt and the seriousness of an error in estimating power requirements is correspondingly reduced.

Using the estimates in Table A-1, Table A-2 was prepared and gives powers and weights for life support systems for one, two and four chimpanzees (or two, four or eight Rhesus monkeys, or combinations thereof) for 30, 60 and 90 days.

TABLE A-2

LIFE SUPPORT SYSTEM POWERS AND WEIGHTS FOR SEVERAL MISSIONS

Number of Chimpanzees*	1			2			4		
Mission Duration, (days)	30	60	90	30	60	90	30	60	90
Weights									
103 pound/chimpanzee	103	103	103	206	206	206	412	412	412
99 pound/90 days	33	66	99	33	66	99	33	66	99
438 pound/chimpanzee/90 day	146	292	438	292	584	876	584	1168	1752
TOTAL	282	461	640	531	856	1181	1029	1646	2263
Powers									
20 watt	20	20	20	20	20	20	20	20	20
20 watt/chimpanzee	20	20	20	40	40	40	80	80	80
TOTAL	40	40	40	60	60	60	100	100	100

* Two to four Rhesus monkeys may replace each chimpanzee

APPENDIX III-B

COMMUNICATIONS AND TELEMETRY

The communications and telemetry equipment used for the experiment will be compatible with the ground support equipment presently employed by the Mercury and Minitrack systems. Estimated in-flight weight and average power requirements are given in Fig. 9 for a two-chimpanzee experiment. One communications system is common to the capsule while one recording and telemetry subsystem is required for each animal.

Communications devices include a beacon transponder for tracking purposes, two command receivers and decoders (for redundancy), a recovery beacon (if needed) requiring 50 watts and powered by storage batteries, and the associated antennas and wiring.

Experimental and flight support data are recorded and transmitted once per orbit over a tracking station. Included in the power and weight estimates are the recorders, commutators, analog/digital converters, submultiplexers, mixers and transmitters, and associated antennas and wiring. Since the telemetry transmitter operates only once per orbit, its average power needs are negligible. The television estimates include both the camera and a transmitter for a one-half frame per second system.

A summary of weight vs number of primates and mission duration is given in Table B-1.

TABLE B-1

COMMUNICATIONS AND TELEMETRY

Number of Chimpanzees*	1			2			4		
Mission Duration	30	60	90	30	60	90	30	60	90
Transponder	14	14	14	14	14	14	14	14	14
Two Command Receiver and Decoders	24	24	24	24	24	24	24	24	24
Recovery Beacon	20	20	20	20	20	20	20	20	20
Antenna System	4	4	4	4	4	4	4	4	4
Wiring, Junction Boxes, etc.	10	10	10	10	10	10	10	10	10
Commutators, A/D Converter, Submultiplexers	12	12	12	24	24	24	48	48	48
Recorder	25	25	25	50	50	50	100	100	100
Telemetry Mixer and Transmitter	14	14	14	28	28	28	56	56	56
Antenna System	4	4	4	8	8	8	16	16	16
Wiring, Junction Boxes, etc.	10	10	10	20	20	20	40	40	40
Television and Transmitter	21	21	21	42	42	42	84	84	84
	158			244			416		

* Two to four Rhesus monkeys may replace each chimpanzee.

APPENDIX III-C

POWER REQUIREMENTS

A summary of the power requirements for the four systems is given in Fig. 6. The data are self explanatory with the exception of the recovery requirements. These are summarized in Table C-1.

TABLE C-1

POWER REQUIREMENTS - RECOVERY
(12 HOUR RECOVERY PERIOD ASSUMED)

No. of Chimpanzees*	1	2	4
Life support	40	60	100
Experiment	16	32	64
Convert and record	24	48	96
Beacons	50	50	50
Total Power watts	130	190	310
Watt-hours	1560	2280	3720

* Two to four Rhesus monkeys may replace each chimpanzee.

APPENDIX III-D

SPACECRAFT

Mercury spacecraft weights are detailed in Table D-1. The first column contains "present mercury data" obtained from Douglas Aircraft Corporation.* Column II contains Douglas estimates for a 4-rhesus, 90-day mission. Column III contains CUERL estimates for a low G ACS mission, Column IV CUERL estimates for a solar oriented ACS mission, and Column V CUERL estimates for a non-recoverable mission. Fuel estimates for the ACS are based on information from Lockheed Aircraft Corporation. The item "Equipment Reduction (Redundant)" is not clear. It is assumed that evaporative coolant for re-entry (Del Duca: about 150 #) is included in this table, probably in the 319-# "Landing and Recovery" item.

* Ref: A2-260 - S/WT-62-91, 3-15-62, Project Mercury Actual Weight Report, McDonnell Report #8586.

TABLE D-1

SPACECRAFT WEIGHT BREAKDOWN

Item	Column I Present	Column II Douglas	Column III CUERL Low G ACS	Column IV CUERL Sunseeker	Column V CUERL Non-Rec.
Structure, Cabin, Elec, etc.					
Structure	610	610	610	610	610
Cabin and equipment	113	113	113	113	113
Electrical system	332	332	332	332	332
Manufacturing variations	24	24	24	24	24
Equipment reduction (redundant)	150	150	150	150	150
Ballast	39	39	39	39	39
TOTAL	1268	1268	1268	1268	1268
Recovery System					
Heat shield	304	304	304	304	0
Stabilization and control	281	200	200	200	200
Retro system	295	295	295	295	0
Landing and recovery	319	319	319	319	0
Crew and survival equipment	244	20	20	20	0
Recovery gear	35	35	35	35	0
TOTAL	1478	1173	1173	1173	200
Additional ACS Fuel					
for 30 days operation	-	-	30	150	30
for 60 days operation	-	-	60	300	60
for 90 days operation	-	-	90	450	90
Additional Mercury Items not included					
Communications	249	249	Cf. Appendix II		
Environmental control	137	60	Cf. Appendix I		
Escape tower	1022	0	0	0	0
Totals: Present and Douglas	4214	2750	-	-	-
CUERL 30 days	-	-	2470	2591	1498
CUERL 60 days	-	-	2501	2741	1528
CUERL 90 days	-	-	2531	2891	1558

APPENDIX III-E

SERVICE MODULE

A cylindrical service module, 8 ft in diameter and 3 ft long, can be provided to mount those items which can not be fitted into the Mercury Capsule. Accordingly, the module would house the expendable oxygen and nitrogen supplies, and either solar arrays or primary batteries depending upon which power source is utilized. Secondary batteries, regulators and inverters are mounted in the capsule.

The module would consist of a framework structure covered with a 1/16 in. skin of aluminum. Skin weight is approximately 150 pounds and the structure weight is estimated to be 10 per cent of the weight of its contents. Table E-1 gives the weight of the module contents for the various systems as a function of number of chimpanzees and mission duration. A summary of total weights including 150 pounds for the shell is given in Table E-2.

TABLE E-1

WEIGHTS OF ITEMS MOUNTED IN SERVICE MODULE

Number of Chimpanzees*	1			2			4		
Mission Duration (days)	30	60	90	30	60	90	30	60	90
Oxygen and container	31	62	93	62	124	186	124	248	372
Nitrogen and container	33	66	99	33	66	99	33	66	99
Primary Batteries	1050	2100	3150	1750	3500	5250	3150	6300	9450
Solar Cells - oriented	88	88	88	147	147	147	264	264	264
Solar Cells - random	244	244	244	416	416	416	760	760	760
Solar Cells - random non-recoverable	201	201	201	344	344	344	630	630	630

* Two to four Rhesus monkeys may replace each chimpanzee.

TABLE E-2

TOTAL WEIGHT OF SERVICE MODULE

Number of Chimpanzees*	1			2			4		
Mission Duration (days)	30	60	90	30	60	90	30	60	90
Battery powered recoverable	261	373	484	335	519	704	480	810	1142
Solar Cell - oriented recoverable	165	172	178	174	184	193	192	208	224
Solar Cell - random recoverable	181	187	194	201	211	220	242	257	273
Solar Cell - random non-recoverable	177	183	189	194	203	213	229	244	260

* Two to four Rhesus monkeys may replace each chimpanzee.

APPENDIX III-F

POWER SOURCES

Weight requirements for the various power systems were calculated as follows:

A. BATTERIES - A figure of 65 watt-hours of energy per pound of battery was used. Thus,

$$\text{lbs} = .37\ PT$$

where P = power in watts
T = time in days.

B. SOLAR CELLS - ORIENTED

A figure of 10 watts per square foot of cell array was used. The weight per square foot of array including support frames was estimated at 1.5 lb. A light-dark ratio of one was assumed; during the light portion of the cycle the cells must supply all equipment and charge the batteries at 50 per cent efficiency. Thus,

$$\text{lbs} = \frac{P}{10} \times 1.5 \times (1 + 2)$$

$$\text{lbs} = .45\ P$$

where

P = power in watts.

C. SOLAR CELLS - TUMBLING

The same procedures were followed as in the oriented mode except that the weights were multiplexed by 5 for the

recoverable case and 4 for the non-recoverable case. These factors take into account the ratio of total array area to average effective array area. It is expected that the array configuration can be more optimally designed in the non-recovery case and therefore the multiplier is less (4 vs 5) than in the recovery case.

A summary of weights as a function of number of chimpanzees and mission duration is given in Table F-1. These figures include the chargeable batteries, regulators, inverters, and recovery batteries. Secondary battery discharge during the dark cycle is approximately 5 per cent of capacity.

TABLE F-1

VARIATION IN POWER SOURCE WEIGHTS WITH MISSION REQUIREMENTS

Number of Chimpanzees	1			2			4		
Mission Duration (day)	30	60	90	30	60	90	30	60	90
Batteries									
Batteries	1050	2100	3150	1750	3500	5250	3150	6300	9450
Regulators, Inverters, Misc.	45	45	45	45	45	45	45	45	45
Recovery Batteries	25	25	25	35	35	35	60	60	60
	1120	2170	3220	1830	3580	5330	3255	6405	9555
Solar Cells - Oriented									
Solar Cells and Frames	58	58	58	87	87	87	144	144	144
Regulators, Inverters, Misc.	55	55	55	55	55	55	55	55	55
Batteries	30	30	30	36	60	60	120	120	120
Recovery Batteries	25	25	25	35	35	35	60	60	60
	168			237			379		
Solar Cells - Random									
Solar Cells and Frames	214	214	214	356	356	356	640	640	640
Regulators, Inverters, Misc.	45	45	45	45	45	45	45	45	45
Batteries	30	30	30	60	60	60	120	120	120
Recovery Batteries	25	25	25	35	35	35	60	60	60
	314			496			865		
Solar Cells - Non-Rec.									
Cells and Frames	171	171	171	284	284	284	510	510	510
Regulators, Inverters, Misc.	45	45	45	45	45	45	45	45	45
Batteries	30	30	30	60	60	60	120	120	120
	246			389			675		

APPENDIX III-G

VARIATION OF OVERALL WEIGHT WITH MISSION REQUIREMENTS

Table G-1 is a summary of the weights of the individual subsystems as listed in Tables A-2, B-1, D-1, E-2, F-1 and I-1.

TABLE G-1

VARIATION IN OVERALL WEIGHT WITH MISSION REQUIREMENTS

Number of Chimpanzees	1			2			4		
Mission Duration (days)	30	60	90	30	60	90	30	60	90
Recoverable Systems									
Battery-Powered									
Spacecraft	2470	2500	2530	2470	2500	2530	2470	2500	2530
Service Module	261	373	484	335	519	704	480	810	1142
Power Sources	1120	2170	3220	1030	3580	5330	3255	6405	9555
Life Support System	282	461	640	531	856	1181	1029	1646	2263
Communications and T/M	158	158	158	244	244	244	416	416	416
Experiment	26	26	26	52	52	52	104	104	104
Total	4317	5688	7058	5462	7749	10041	7754	11881	16010
Solar Powered (Random)									
Spacecraft	2470	2500	2530	2470	2500	2530	2470	2500	2530
Service Module	181	187	194	201	211	220	242	257	273
Power Sources	314	314	314	496	496	496	865	865	865
Life Support System	282	461	640	531	856	1181	1029	1646	2263
Communications and T/M	158	158	158	244	244	244	416	416	416
Experiment	26	26	26	52	52	52	104	104	104
Total	3431	3646	3862	3994	4359	4723	5126	5788	6451
Solar-Powered (Oriented)									
Spacecraft	2590	2740	2890	2590	2740	2890	2590	2740	2890
Service Module	165	172	178	174	184	193	192	208	224
Power Sources	168	168	168	237	237	237	379	379	379
Life Support System	282	461	640	531	856	1181	1029	1646	2263
Communications and T/M	158	158	158	244	244	244	416	416	416
Experiment	26	26	26	52	52	52	104	104	104
Total	3389	3725	4060	3828	4313	4797	4710	5493	6276
Non-Recoverable System									
Solar-Powered (random)									
Spacecraft	1500	1530	1560	1500	1530	1560	1500	1530	1560
Service Module	177	183	189	194	203	213	229	244	260
Power Sources	246	246	246	389	389	389	675	675	675
Life Support System	282	461	640	531	856	1181	1029	1646	2263
Communications and T/M	138	138	138	224	224	224	396	396	396
Experiment	26	26	26	52	52	52	104	104	104
Total	2369	2584	2799	2890	3254	3619	3933	4595	5258

APPENDIX III-H

COMBINED BATTERY AND SOLAR CELL SYSTEM

In these calculations the service module is taken to be a cylinder 8 ft in diameter and 3 ft in length. It is attached to the Mercury capsule as shown in upper figure and its sides and exposed circular face are covered with solar cells. When the sun's rays strike the module at an angle ϕ from its axis, as shown in lower figure, the projected area of solar cells as sun is

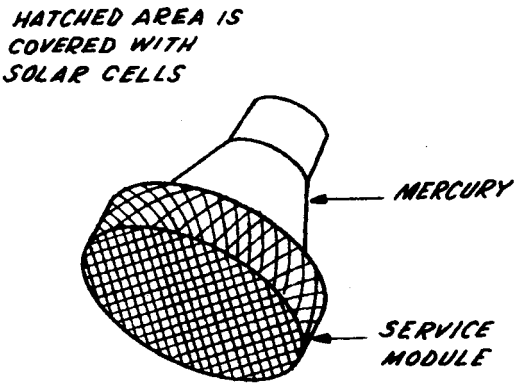

FIG. 13 MERCURY CAPSULE AND SPACE MODULE

$$A(\phi) = \frac{\pi D^2}{4} \cos \phi + DL \sin \phi \ ,$$

$$0 < \phi < \frac{\pi}{2}$$

$$= DL \sin \phi \ , \ \frac{\pi}{2} < \phi < \pi \ .$$

At this orientation the cells are capable

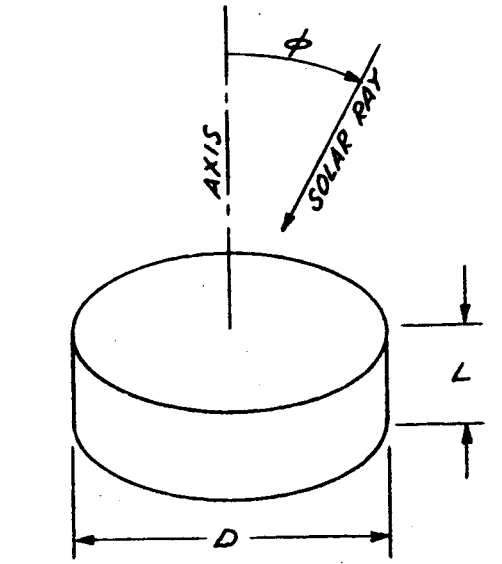

FIG. 14 GEOMETRY OF SOLAR INCIDENCE.

of producing

$$10\ A(\phi)\ \text{watts}$$

of electric power (since a 10-watt/ft^2 capability at normal incidence is assumed). If $10\ A(\phi)$ is less than the power requirements P_o of the system, then the additional power

$$P_o - 10\ A(\phi)$$

will be drawn from storage batteries. If $10\ A(\phi)$ exceeds the power requirements of the system, then the excess power

$$10\ A(\phi) - P_o$$

is fed to storage batteries which are charged with an assumed 50 per cent efficiency. Thus the net power developed by the cells in this case is

$$P_o + \frac{1}{2}\ (10\ A(\phi) - P_o) = \frac{1}{2}\ (P_o + 10\ A(\phi))\ .$$

In general the net power developed by the cells is

$$P_{eff}(\phi) = 10\ A(\phi)\quad ,\ 10\ A(\phi) < P_o$$

$$= \frac{1}{2}\ (P_o + 10\ A(\phi)),\quad P_o < 10\ A(\phi)\quad .$$

The probability density function for ϕ is

$$f(\phi) = \frac{1}{2} \sin \phi$$

Hence, the average net power developed by the solar cells while the spacecraft is on the sunny side of the earth is

$$\overline{P} = \int_o^\pi d\phi f(\phi) P_{eff}(\phi)$$

$$= \int_o^\pi d\phi \, \frac{1}{2} \sin \phi \, \frac{1}{2} \, (P_o + 10 \, A(\phi))$$

where P_o is taken to be the average power required by the system. For randomly oriented spacecraft P_o is given in Appendix III as

P_o	Number of Chimps	or Rhesus
95	1	2
158	2	4
284	4	8

For the module dimensions given above

$$D = 8 \text{ ft}$$

$$L = 3 \text{ ft}$$

$$A(\phi) = 50.3 \cos \phi + 24 \sin \phi \text{ ft}^2 \quad , \quad 0 < \phi < \frac{\pi}{2}$$

$$= 24 \sin \phi \text{ ft}^2 \quad , \quad \frac{\pi}{2} < \phi < \pi \quad .$$

Integrating numerically for $\overline{P}$ yields

$\overline{P}$	Number of Chimps	or Rhesus
220 w	1	2
260 w	2	4
310 w	4	8

Since the spacecraft is assumed to be in sunlight during only half of its orbit, these numbers should be halved to yield the average power developed by the solar cells, viz.,

Number of Chimps	or Rhesus Monkeys	$\frac{1}{2}\bar{P}$	P_o	$\frac{1}{2}\bar{P}/P_o$
1	2-4	110 w	95 w	> 1
2	4-8	130 w	158 w	82%
4	8-12	155 w	284 w	55%

Thus for one chimp, more than enough power is developed by the solar cells and their number can be reduced so that this system reduces to System II of Fig. 12. For two chimps 82 per cent of system power requirements are met and for four chimps 55 per cent. The weight savings effected in these cases are calculated in Table H-1.

IV. ELECTROMAGNETIC BLOOD FLOWMETER RESEARCH

A. GENERAL

Research on the electromagnetic blood flowmeter was continued during the current report period. It will be recalled that during previous years flowmeter research has concentrated on the fundamental phenomena basic to the measurement of blood flow by the Faraday effect and on the fundamental problems intrinsic to implementing this phenomena. Experimental blood flowmeter systems for both sine-wave (Fig. 15) and square-wave systems (Fig. 16) were constructed and a first model lightweight, low-power flight model blood flowmeter (Fig. 17) was designed and constructed. This latter was accomplished during a nine-week period, in order that it might be made available for a NASA balloon experiment. Each of these systems has been reported in preceding Status Reports.*

The flight model flowmeter system shown in Fig. 17, while not ideal, would be satisfactory for the orbital experiment described in Sec. II of this report (Item 3, Fig. 4). It is a highly stable and accurate device. When used to measure blood flow either in the aorta or pulmonary artery, as called for in the orbital experiment, a base-line reference is present during the diastolic interval (the resting phase) of each heart cycle: during the diastole, pulmonary artery blood flow is zero and aortic blood flow minus two per cent. However, this convenient reference is not present in other blood vessels of the body for

* "Methods for Determining Blood Flow Through Intact Vessels of Experimental Animals under Conditions of Gravitational Stress and in Extraterrestrial Space Capsules," Status Reports P-1/168 and P-2/168 covering period from November 1, 1960 to July 30, 1962, Electronics Research Laboratories, School of Engineering and Applied Science, Columbia University, New York, N. Y.

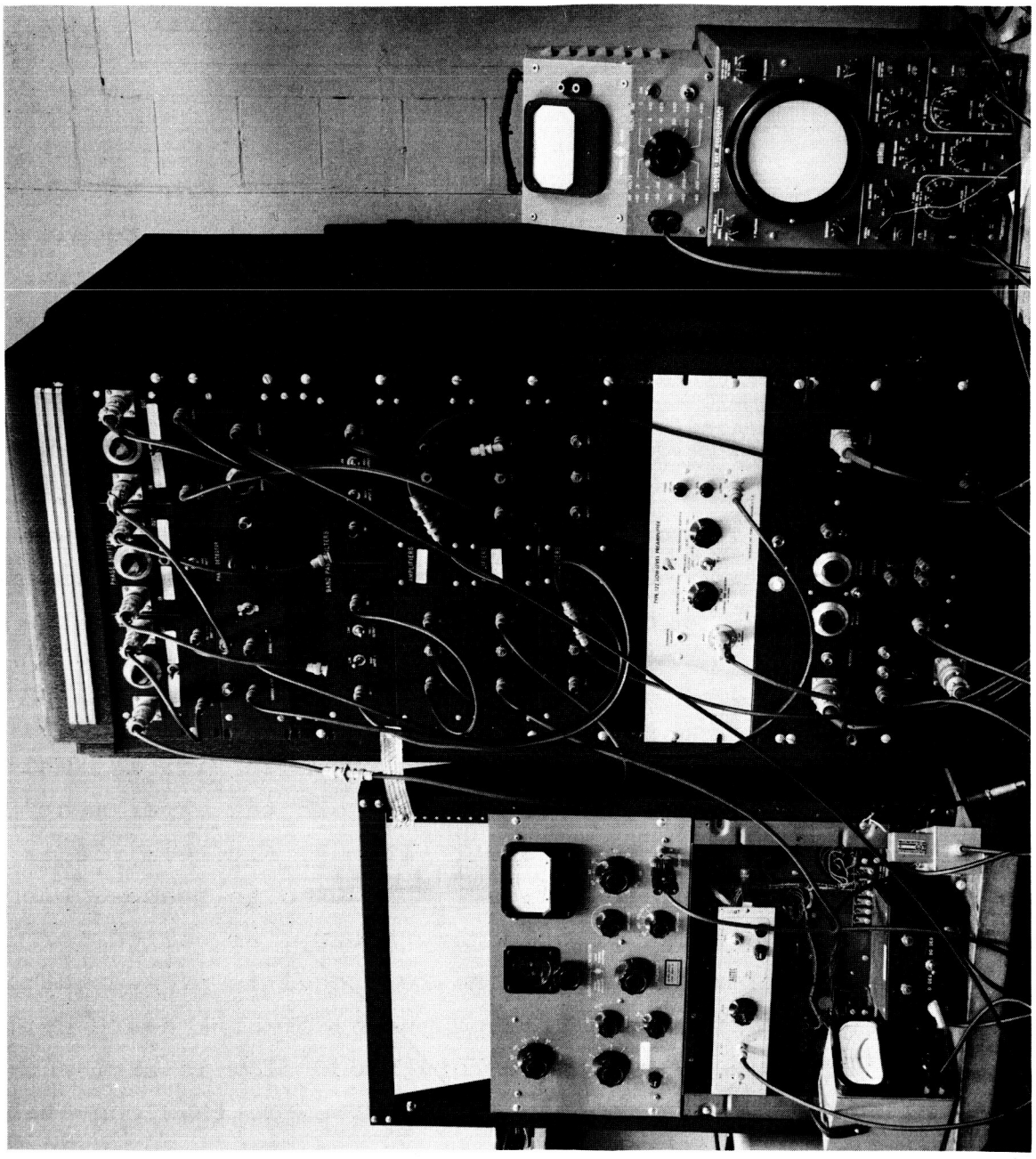

Fig. 15 Experimental Sine-Wave Blood Flowmeter System

810H-169-A-0057

APPENDIX III-I

PHYSIOLOGICAL EXPERIMENT

Weight and power estimates given in Fig. 4 for the experiment associated apparatus are self explanatory. On a per animal basis, exclusive of the television camera and transmitter which are included in the section on telemetry, these amount to 16 watts and 25 lb.

TABLE I-1

WEIGHT OF EXPERIMENTAL APPARATUS

Number of Animals from which Data being Recorded and Telemetered	1			2			4		
Mission Duration (days)	30	60	90	30	60	90	30	60	90
Experimental Apparatus	25	25	25	50	50	50	100	100	100

TABLE H-1

WEIGHTS SAVINGS EFFECTED IN COMBINED SOLAR CELL - BATTERY SYSTEM

Number of Chimpanzees*	2			4		
Mission duration T days	30	60	90	30	60	90
$\frac{1}{2}\overline{P}$	130	130	130	155	155	155
Battery weight saved ($.37 \frac{1}{2} \overline{P}$ T , Cf. Appendix VI)	1440	2880	4320	1720	3440	5160
Weight of solar cells and frames ($[\frac{\pi D^2}{4} + \pi DL] \times 1.5 \frac{H}{ft^2}$, Cf. Appendix VI)	189	189	189	189	189	189
Difference of above	1251	2691	4131	1531	3251	4991
Savings in service module structure (10% of above, Cf. Appendix V)	125	269	413	153	325	497
Net saving (sum of above)	1376	2960	4544	1684	3576	5468
Total Weight of battery powered system	5460	7750	10040	7750	11880	16010
Total weight of combined system (difference of above)	4084	4790	5496	6066	8304	10542
Rounded total weight	4080	4790	5500	6070	8300	10540

* Two Rhesus Monkeys

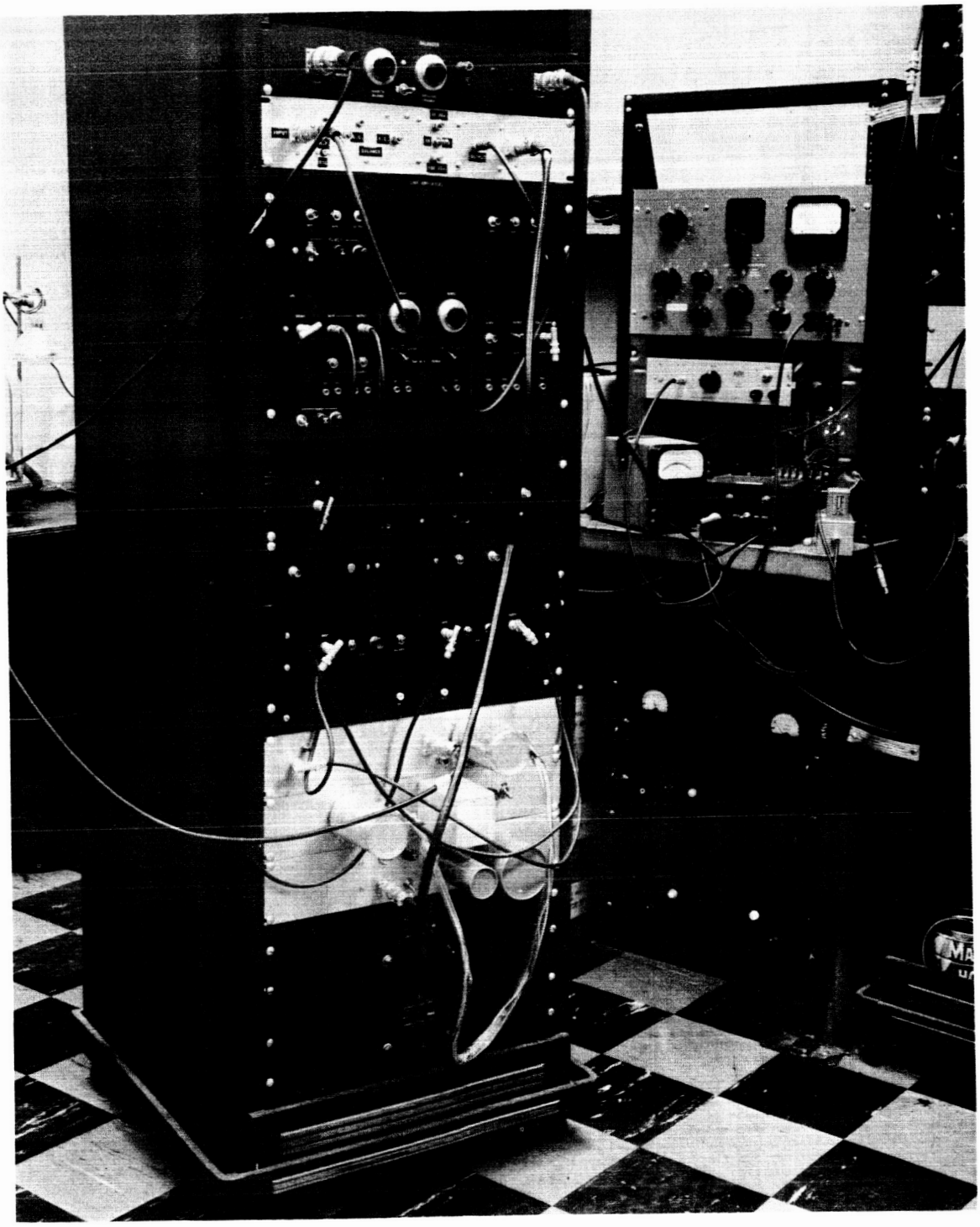

810H-169-A-0056

Fig. 16 Experimental Square-Wave Blood Flowmeter System

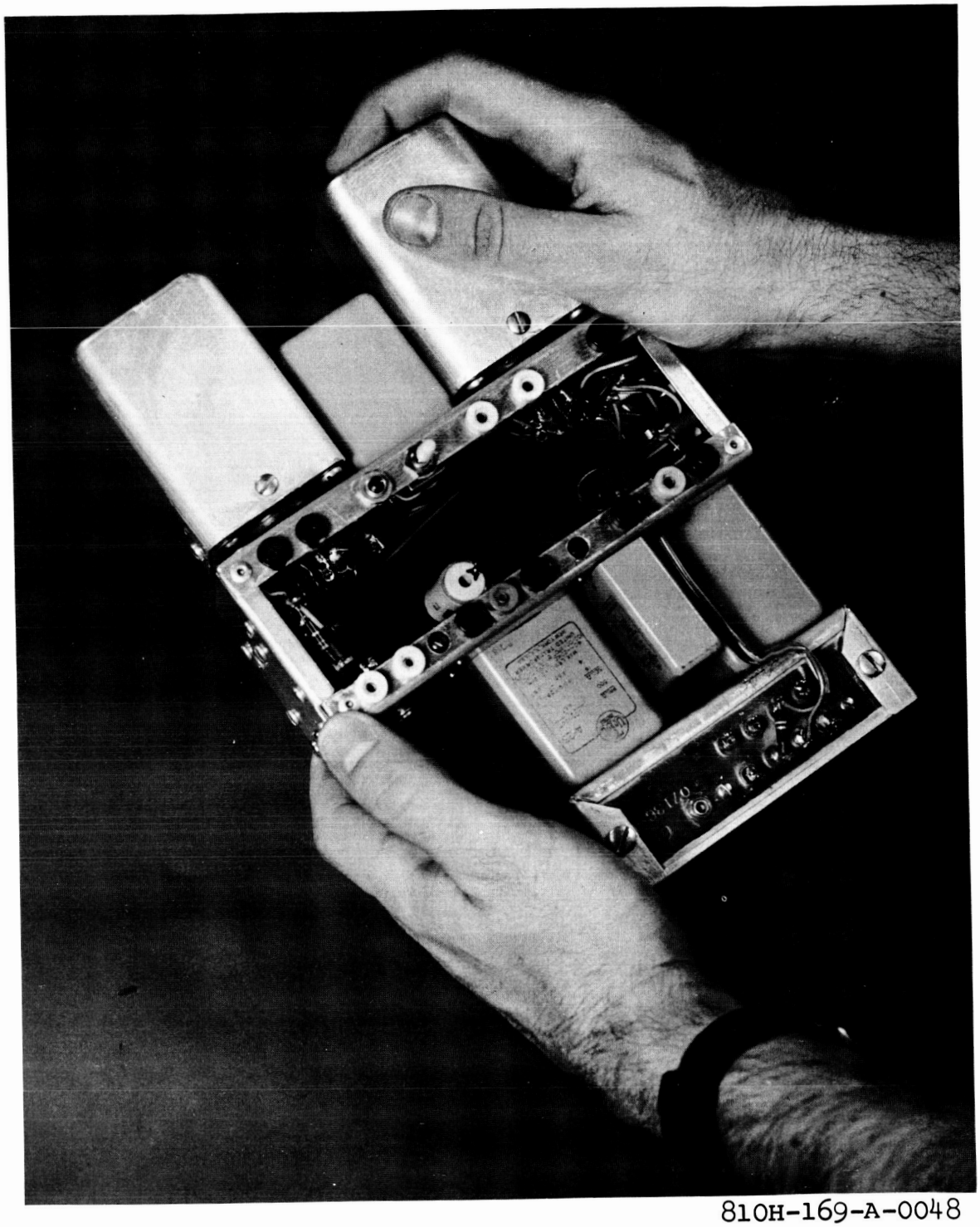

810H-169-A-0048

Fig. 17 Flight Model Blood Flowmeter, Model 1

forward flow occurs during diastole. If the electromagnetic blood flowmeter is to be equally useful for measurement of blood flow in these other blood vessels, an accurate and reliable electronic zero should be routinely obtainable.

We will consider blood flowmeter development complete when instruments with the accuracy, reliability and stability of the instruments shown in Figs. 15,16,17 designed and tested by this laboratory, have the further advantages of an absolute electronic zero, absence of all "proximity effects" and are suitably packaged. Effort on blood flowmeter during the current report period has concentrated on the development of an instrument suitable for use in any laboratory and on continued investigation of the phenomena interfering with the routine attainment of an absolute electronic zero and creating "proximity effects."

B. GENERAL PURPOSE LABORATORY FLOWMETER, MODEL A

1. General Description

Figure 18 is a photograph of the general-purpose laboratory blood flowmeter that has been designed and fabricated during the current report period. It has been designed with a particular view towards its convenient use by laboratories having little or no engineering expertise. It is solid state and has been designed in a modular fashion. The flowmeter has been designed as a complete self-contained unit. As such it has a number of ancillary components that give it considerable flexibility and convenience. For example, a small oscilloscope is contained within the unit and appropriately connected to various points within the circuitry so that flowmeter probes can be readily balanced and various waveforms internal to flowmeter operation can be examined.

A precision attenuator with controls on the face of the flowmeter operates on the output of the preamplifier so that

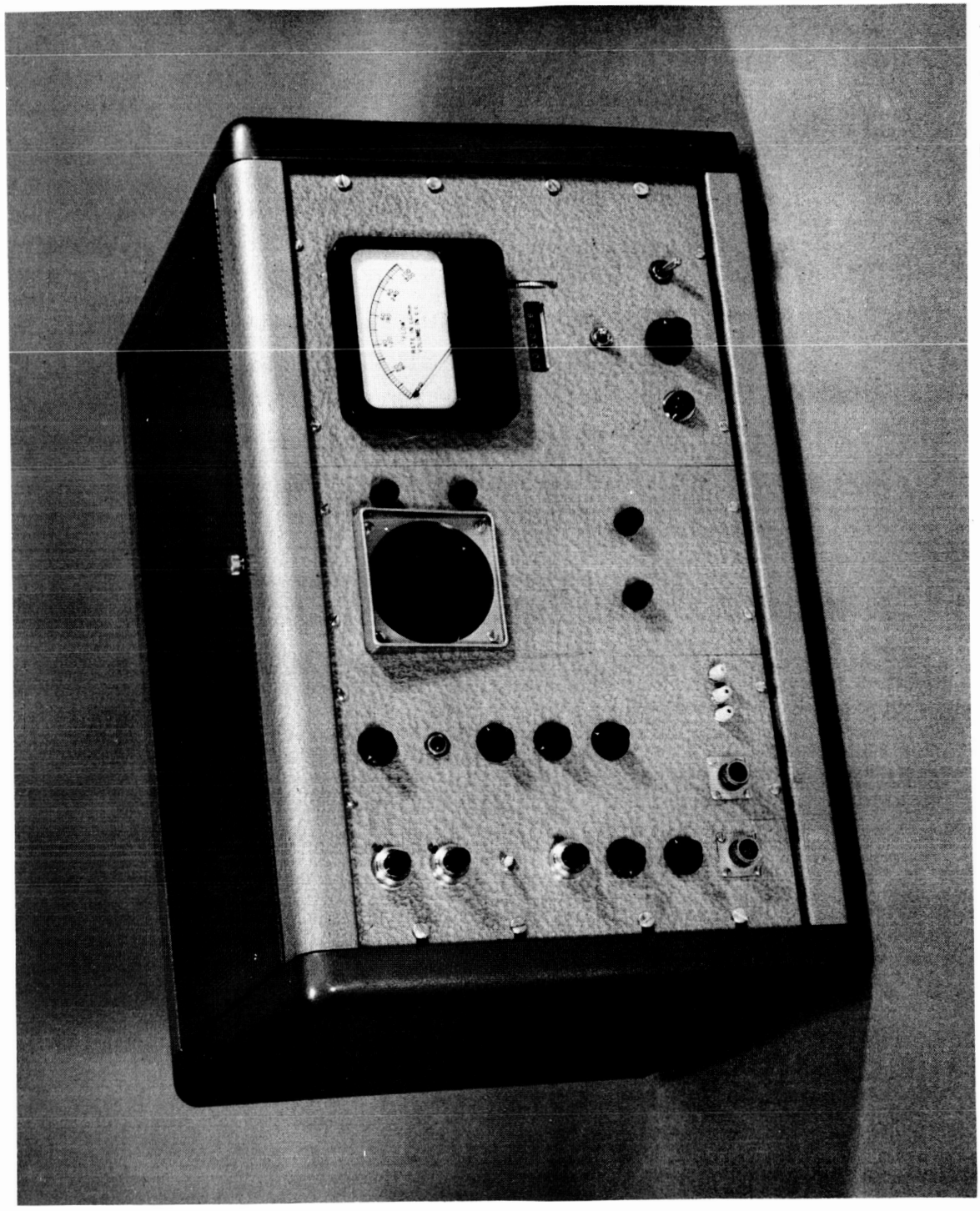

810H-169-A-0054

Fig. 18 General Purpose Laboratory Flowmeter

probes of various sensitivity can be readily adjusted to provide output indications in standard units. A "leak tester" is included so that by simple switching any electrical leakage between drive circuits and signal circuits might be readily detected. Such leakage may develop through wear and tear of the probes creating small breaks that permit the seepage of tissue fluids into the probe body. An electronic integrator is included in the instrument so that flow rates can be integrated into flow volumes. This integrator has the considerable advantage that at the end of any particular experiment the entire probe-electronic-flowmeter system can be absolutely calibrated with the probe situated on the blood vessel exactly as it has been used. This is accomplished by blood collection distal to the probe and comparing the collection of blood so obtained with the indications of the integrator. Other conveniences of the laboratory model are described in following sections.

2. Overall Operation

The structure of the laboratory model flowmeter may be divided into a few basic sections as illustrated in the block diagram of Fig. 19. These are: (1) a probe which fits around the intact blood vessel generates a time-varying magnetic field across the blood vessel and provides the flow signal by sensing the voltage developed as the stream of moving blood passes through the magnetic field; (2) a pre-amplifier to amplify the flow signal from the probe; and (3) a drive and timing system to provide excitation of the probe magnet and to sample and filter the pre-amp output, in order to recover the flow information. Additional equipment provided to extend the usefulness of the basic flowmeter as a laboratory instrument includes the following: a variable low-pass filter to convert the phasic flow signal into a mean flow signal; an integrator to accumulate flow volume: an oscilloscope to permit viewing of several internal

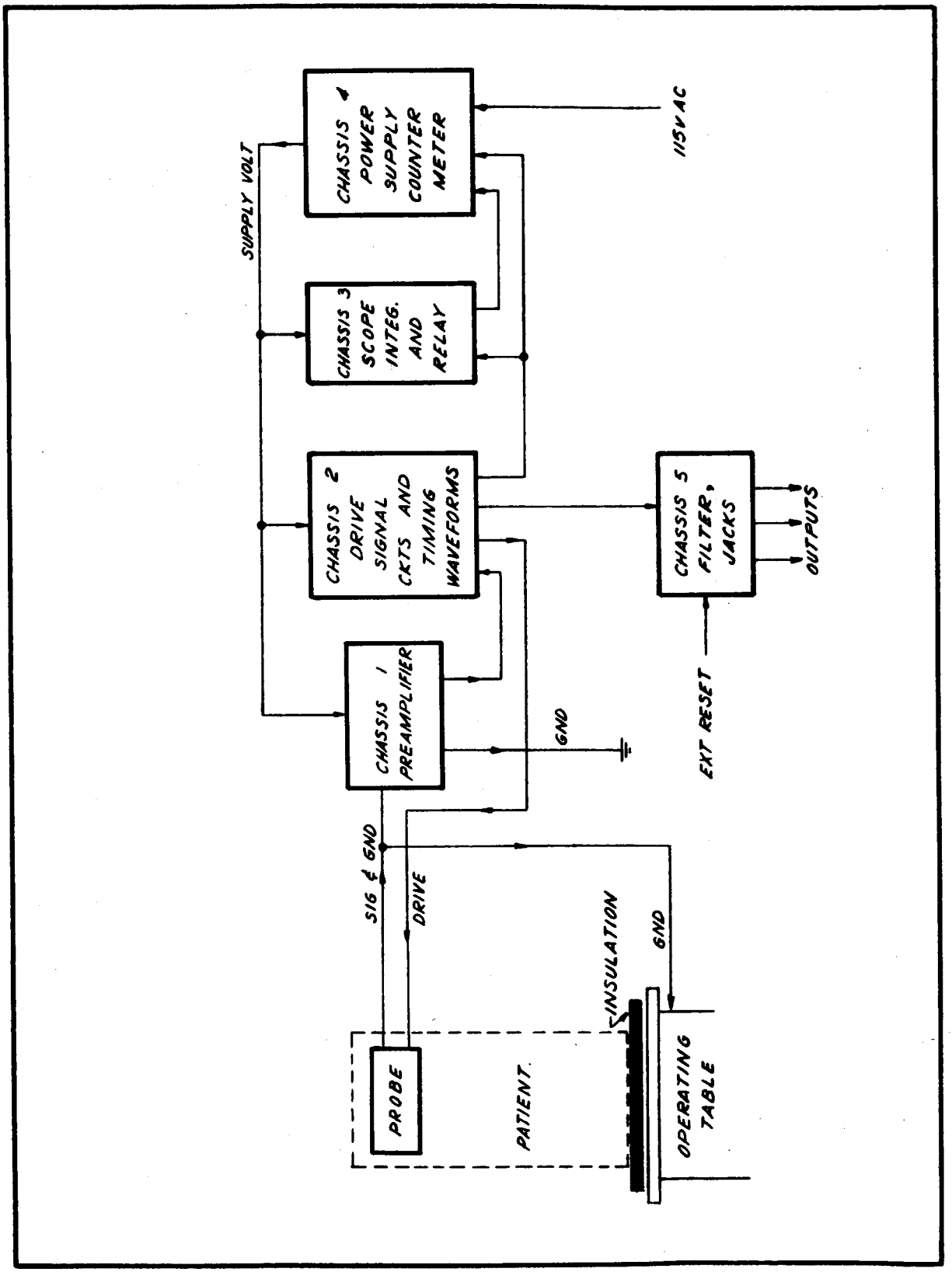

Fig. 19 Block Diagram of General Purpose Laboratory Flowmeter, Model 1

waveforms; a meter to display either flow rate or accumulated flow volume; a mechanical counter to extend the integrator range and permit the accumulation of large total flow volumes. A regulated power supply is provided to operate the various circuits.

In operation the magnet coil of the flowmeter probe is excited by a 200-cps square wave current and a 200-cps square wave field of magnetic flux is produced across the blood vessel. The flow of blood in the intact blood vessel induces a voltage as it flows through this field of the magnetic flux (Faraday phenomenon). This flow signal is sensed by a pair of electrodes on the outer surface of the blood vessel wall. A split lead is provided in order to buck out voltages induced by flux linkages between the electrodes and their connecting wires and the magnetic field. The output of the probe and the split-lead balancer is amplified by a pre-amplifier.

A calibration signal is available to permit precise adjustment of the pre-amplifier gain. And a precision attenuator at the output of the pre-amplifier is adjustable to a value provided by calibrating each probe individually. This allows a single, fixed set of electronic components to provide output indications in standard units for a variety of probes.

The output of the pre-amplifier is further amplified and a phase inverter is used to provide two indentical outputs 180 deg out of phase. Each output is sampled on alternate half cycles for a short time near the end of the half cycle.

The outputs of the two sample gates are combined at the input of a 75-cps low-pass filter. This "invert and add" detection technique considerably reduces the sensitivity of the system to low frequency noise. The 75-cps filter removes most of the high frequency noise with the exception of noise which is synchronous

with the sampling frequency. Noise in the region around 200 cps (±75 cps), the frequency which carries the blood flow information, or noise in the region around any odd harmonic of the sampling frequency such as 600 cps, 1000 cps, etc., will pass through the output filter. No long term offset can be generated by the high frequency noise since the phase relationship between the noise and the sampling frequency is random. However, short term variations in the output will occur. Therefore high frequency noise in the signal before the detector (sample gates) will cause low frequency noise at the output of the 75-cps filter. To minimize this effect the frequency response of the amplifier is deliberately limited to about 1000 cps.

The output of the filter is the phasic bloodflow signal. A second filter with a selectable time constant provides a separate front panel output with sharply reduced high frequency content, the mean or average flow rate. The flow output can also be integrated to provide an accumulating volumetric indication. When integrating, should the integrator reach full scale output it is automatically reset and the event recorded on an electromechanical counter which provides a long term record of total accumulated flow.

Phasic flow rate, mean flow rate or integrated flow (flow volume) are displayed on a meter, (subject to the frequency limitation of the meter itself in the case of the pulsatile flow signal) or may be separately recorded.

3. Probe and Input Balancer

The flowmeter probe contains a magnetic structure consisting of a coil of wire wound over a magnetic core, plus a flow section containing four electrodes which contact the external surface of the vessel under study. A simplified representation is shown in Fig. 20.

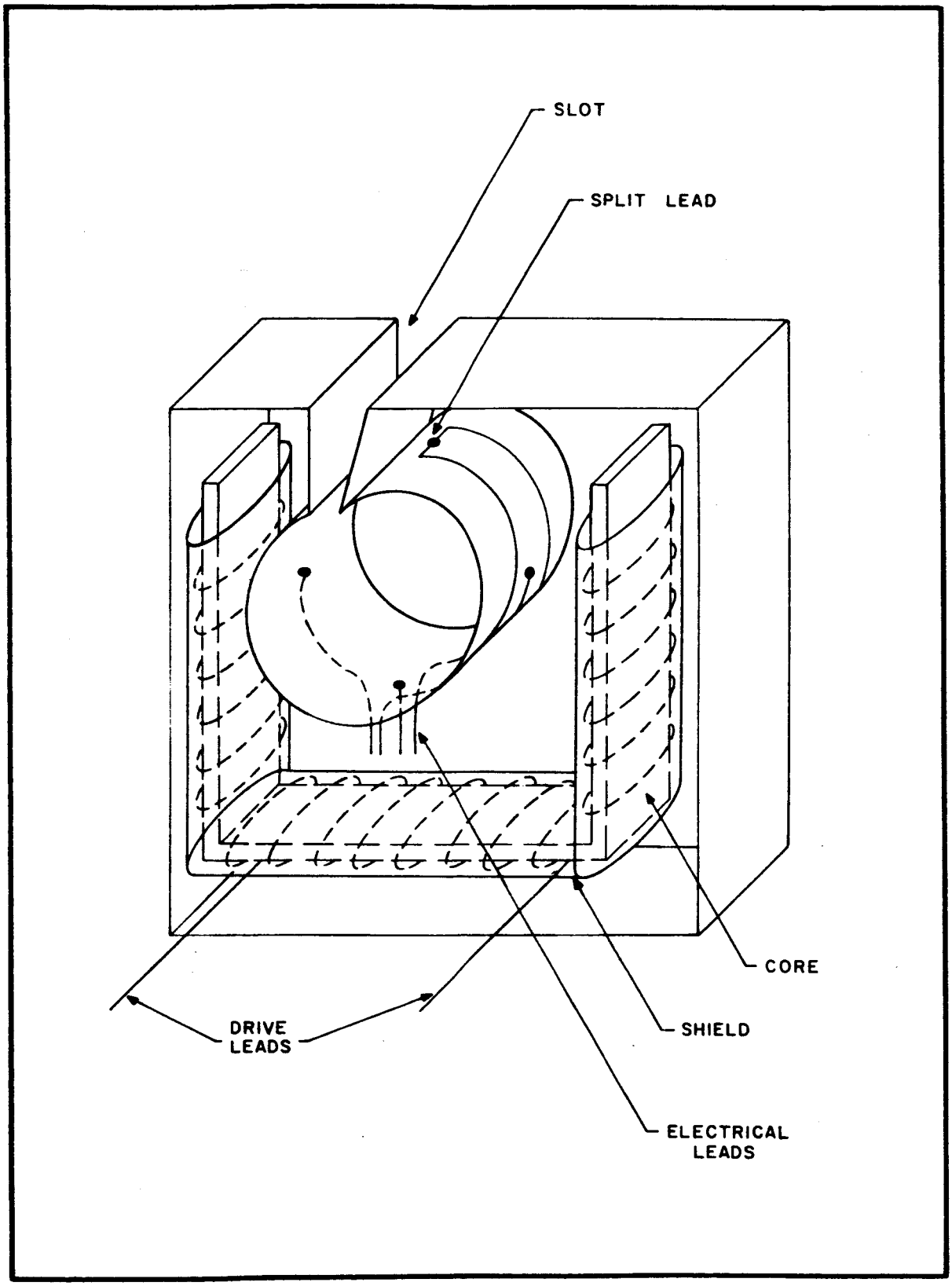

Fig. 20 Diagramatic Drawing of Flowmeter Probe

The u-shaped magnetic core is fabricated from high permeability ferrite. The use of a ferrite core provides saturation flux densities approaching those attainable in iron alloy core materials combined with high bulk resistivity which sharply curtails eddy currents. In ordinary iron alloy core materials, eddy currents in the pole faces not only distort the field in the region through which the blood flows, but also persist for a considerable period of time after the drive current has reached a stable value. Therefore $d\phi/dt$ does not fall to zero promptly at the beginning of each half cycle, but persists. While it is theoretically possible to balance out any $d\phi/dt$ induced signal, any residual signal or any error in balancing will provide an output not related to flow.

The magnet coil consists of several hundred turns of fine wire wound over the center of the u-core and insulated from it. In addition to magnetic coupling between the coil and electrodes, spurious signals can be induced either by resistive leakage currents flowing through the potting compound used to encase the body of the probe, or through capacitive coupling due to the finite dielectric constant of the potting compound. Both these effects are minimized by surrounding the coil with a conductive shield which is grounded. The shield is wrapped completely around the coil but the overlap is insulated to prevent the formation of a shorted turn in the field of the magnet.

Within the jaws of the magnet, a pipe or flow section is mounted which is an integral part of the probe body and flared smoothly at the ends to minimize abrasion where the probe contacts a blood vessel. The flow section contains four electrodes which contact the walls of the blood vessel when the probe is in place. Two electrodes, mounted close to the magnet jaws, are grounded. The other two electrodes, located on the centerline

of the probe perpendicular to the magnetic field, are connected to the input of a low noise differential preamplifier. The electrode nearest the magnet coil is directly connected to the preamplifier, while the electrode between the tips of the jaws is connected by means of two wires (split lead) to the ends of a potentiometer. The arm of the potentiometer is then connected to the other pre-amp input.

In practice the signal electrodes and their lead wires can never be placed precisely in the central plane of the probe (in the plane of the magnetic field). Therefore the electrodes, the blood vessel between the electrodes and the lead wires from the electrodes form a single turn transformer secondary within the probe field. Each time the direction of current flow in the magnet coil is reversed the field between the probe jaws will be reversed and a signal proportional to $d\phi/dt$ will appear at the pre-amp input. The upper electrode, its split lead, and the potentiometer also form a single turn of wire within the magnetic field of the probe. The split lead wires are deliberately positioned on either side of the central plane of the probe to intercept a finite portion of the field. Therefore signal proportional to $d\phi/dt$ will also appear in the single turn secondary created by the use of a split lead from one electrode. By adjusting the potentiometer in the split lead circuit the undesired signal can be balanced out. Therefore the split lead potentiometer acts as an input balancer and is adjusted to minimize the undesired spike which occurs at the onset of each half-wave.

To permit the insertion of a vessel into the probe jaws the body of the probe is slotted near the split lead electrode. A slotted key is provided to close the slot after the vessel is in place.

The signal and magnet leads are twisted and brought out through individual shielded cables to minimize spurious signals induced in the electrode leads by the large magnet currents. The cables are carefully sealed to the probe to prevent fluid leakage. The probe and cables have exterior surfaces which exhibit minimum tissue reactivity. The functional elements of the probe are cast into a body of thoroughly catalyzed epoxy. The cable jackets are made of extruded polyurethane which provids high flexibility.

4. Preamplifier

The output of the probe and balancing network are connected to the input of a low noise differential AC amplifier. The unit used in this first model is a Telemedics (type MA) which provides a gain of over 20,000 with a common-mode rejection of 80 db. The high common-mode rejection not only helps eliminate spurious signals out prevents large signals such as EKG and streaming potentials from masking the small flow-induced signal by overloading the pre-amplifier. The total noise contributed by the amplifier in the pass band of the filter (±75 cps around the 200-cps carrier frequency) is approximately 0.25 microvolt when operating with a 1000-ohm source impedance.

The schematic diagram of the pre-amp is shown in Fig. 21. A five-position attenuator adjusts the gain of the pre-amplifier in fixed steps to provide a full scale output of 100, 300, 1000, 3000, or 10,000 cc per minute. The first attenuator position uses the full gain of the pre-amplifier. The second and third positions add a voltage divider at the pre-amplifier output, reducing the output to 30 per cent and 10 per cent of maximum, respectively.

To prevent overloading in the final amplifier stages the last two attenuator positions repeat positions two and three

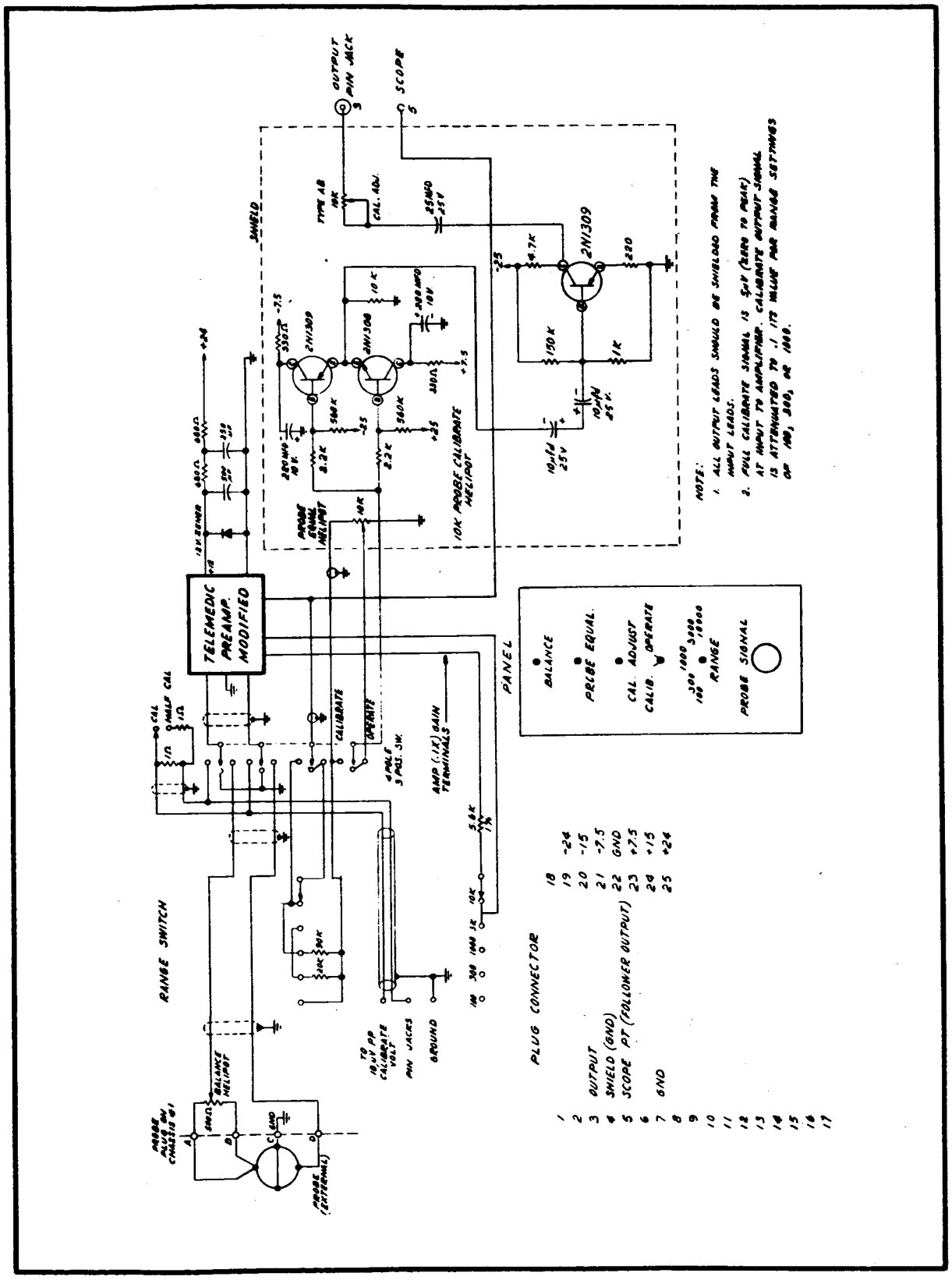

Fig. 21 Flowmeter Preamp Chassis 1

while shunting an internal feedback resistor with an external resistor chosen to reduce the amplifier gain by a factor of 10.

The pre-amplifier output is connected to a ten-turn 10 kilohm potentiometer (probe equalizer) which is adjusted to a value provided with each probe. This value is determined by measuring the individual probe flow sensitivity. The calibration setting then adjusts the overall gain of the pre-amp to a value which provides a fixed output signal for a standard flow rate from any probe. The variation in flow sensitivity from probe to probe is sufficiently small to be compensated for by a single potentiometer.

The output of the potentiometer is isolated by a complementary symmetry emitter follower using high beta NPN and PNP transitors, types 2N1308 and 2N1309, respectively.

The emitter follower output is amplified by a single stage amplifier using a 2N1309 transistor. The output of this amplifier is connected to an adjustable 10 k series resistor which, together with the input impedance of the following stage, acts as an adjustable voltage divider. This gain control (calibration adjustment) is used to set the overall gain of the system to a standard value and compensate for small changes in amplifier gain or probe drive which accumulate in time. A 10-microvolt calibration signal, derived from the probe drive circuit, is developed across a 1-ohm precision resistor and applied to the pre-amplifier input. The calibration adjustment is then set to provide full scale output on the 3000 cc/min range with the probe equalizer set to maximum.

A second 1-ohm precision resistor is available to parallel the first resistor reducing the calibration voltage to one half its normal value to check the linearity of the system.

The use of a calibration signal derived from the probe drive system provides automatic compensation for changes which may accumulate in the probe drive system. Thus if the probe drive should decrease 10 per cent, the calibration signal would also drop 10 per cent as would the flow signal for any given flow. The increase in gain required to achieve a normal output for the calibration signal would be the same as required to provide the proper flow indication from a probe. Therefore, the gain calibration will allow a fixed probe calibration to be used despite variations in either pre-amp gain or probe drive.

5. Timing Circuits and Magnet Drive

A schematic of the timing system is shown in Fig. 22. The timing circuits all derive their master time base from a single free running relaxation oscillator operating at 3200 cps using a 4E20 Shockley diode. The output of the oscillator is divided by three flip-flops to 400 cps. The flip-flops are built around 2N520 transistors and 1N658 diodes which are used for all logic functions. The 400-cps signal is delayed about 0.3 msec by a delay multivibrator used to fire a pulse generator which drives a pair of silicon controlled rectifiers(SCR), type TI-40. The S.C.R.'s act as a flip-flop and output driver amplifier. Each time the 400-cps pulse is applied to the gate inputs of both S.C.R.'s the unit which had been off fires and a small LC commutating network quenches the unit which had been conducting. The S.C.R.'s operate between ±24 vdc regulated lines and are coupled directly to the probe magnet through 100-ohm, 50-watt resistors. This provides a very low L/R ratio and insures rapid rise of the magnet drive current. A stable square current wave is produced in the probe magnet with a one-half amp magnitude.

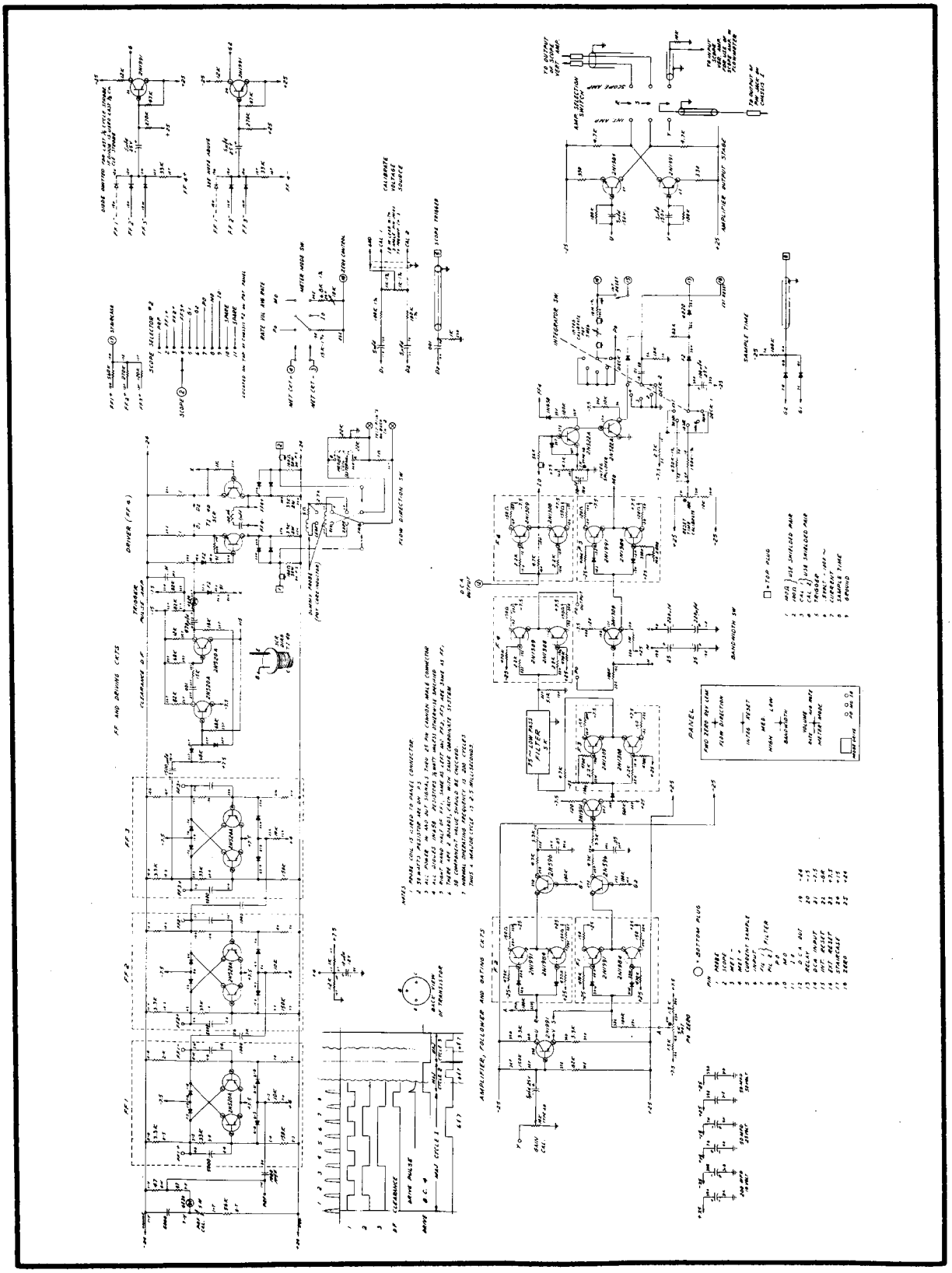

Fig. 22 General Purpose Laboratory Flowmeter, Model 1, Chassis 2: Timing, Drive and Signal Circuits

The probe may be replaced by a small internal inductor with similar L and R. This allows checking the zero of the unit with the gates in operation but with no drive signal applied to the probe magnet.

Since the 3200-cps master oscillator signal is divided to 200 cps there are eight oscillator pulses for each current reversal in the probe magnet. This provides eight distinct time intervals within each half cycle which may be selected by appropriate logic gates and used for auxiliary functions. In particular, a set of auxiliary gates selects the sixth and seventh time intervals for driving the sample gates. The gate drivers are 2N1991 PNP silicon transistors.

The output signal from the pre-amplifier section is connected to a 2N1991 transistor operating as a conventional "cathodyne" phase inverter. Each phase inverter output is connected to a single stage voltage amplifier consisting of a 2N1991 for the emitter output, and a 2N1984 NPN silicon transistor for the collector output. The 2N1984 and 2N1991 transistors are close complements and are used in identical circuits with considerable emitter degeneration. This provides very closely matched gains. The amplifier outputs are isolated by double emitter followers, consisting of PNP, NPN pairs capable of supplying current in either direction. 2N1984 and 2N1991 pairs were chosen to provide the necessary amplitude capability. The emitter followers are connected to 2N596 bilateral switching transistors capable of conducting in either direction when energized. These transistors act as sample gates and conduct during time intervals 6 and 7 on alternate half cycles. The outputs of the sample gates are filtered to remove the sampling frequency. The time constants at the outputs of the individual sample gates are of the same order

of magnitude as the time between successive pulses. Therefore, the sample gates act very much like conventional "box car" detectors. The combined output of the two separate sample gates are isolated by a NPN, PNP complementary emitter follower consisting of 2N1308, 2N1309 transistors. The output of the isolation amplifier is connected to the input of a 75-cps low pass filter which removes the residual carrier signal, and restricts the output to the frequencies of interest. Restricting the output bandwidth to only the 0 - 75 cps region also eliminates considerable noise. The maximum bandwidth of a sampling system extends to roughly one half the sampling frequency, which is 400 cps in this flowmeter. Therefore the output filter reduces the bandwidth from 200 cps to 75 cps which lowers the output noise by almost a factor of two. The filter output is isolated by another double emitter follower, again using a 2N1308, 2N1309 pair, and brought out on a front panel jack marked P.O. (pulse output). This signal contains the instantaneous flow rate information.

Two details of the system are unusual and warrant additional discussion: the gate configuration and the choice of gate interval. The use of an inverter plus two gates which operate on alternate half cycles is called "invert and add" logic. For the desired signal, the outputs from the inverter will be of the same magnitude and polarity on alternate half cycles. Therefore, when the gate outputs are added, two successive samples will add to produce a larger combined output. However, for a signal which varies slowly compared to the sampling rate, such as low frequency noise, the signal will fail to reverse synchronously with the sampling rate and successive samples will be of similar magnitude but opposite polarity. Therefore, they will subtract when combined, effectively removing the spurious signal from the output.

The choice of the sampling period is somewhat arbitrary and represents a compromise between a wide sample interval which provides maximum energy to the filters and therefore maximum signal-to-noise ratio, and a sample period located late in each half cycle to avoid, as far as possible, the inclusion of a portion of the spike which is generated each half cycle by the reversal of the magnetic field of the probe. Although the $d\phi/dt$ portion of the spike should be removable, investigation indicates that the origin of the spike is considerably more complex than expected from a simple model. The electrode-fluid interface plays a prominent role, as yet not completely defined. Eddy currents in the pole faces, and in the blood and surrounding tissues also contribute substantially. The entire phenomenon is under active investigation but is presently not well understood. The choice of intervals six and seven represents a good compromise since it is late enough to avoid most of the spike, wide enough to provide considerable energy to the filters and ends well before the onset of the next spike, insuring that the gate closes completely before the spike starts.

The pulse output signal is filtered through a single stage R.C. filter with a selectable time constant to convert it to a mean or average output. The filter output is isolated by a 2N1309 emitter follower followed by a 2N1984, 2N1991 complementary emitter follower and brought out on a front panel jack.

The flow signal is separately integrated by a Philbrick P-2 operational amplifier to yield a signal proportional to accumulated flow volume. A complementary emitter follower consisting of a 2N1308 and 2N1309 acts as an isolation amplifier between the integrator output and the front panel jack marked I.O. The full scale integrator output corresponds to a total flow equal to full scale on the flow rate range being used.

For example, if the 3000-cc/min range is being used, then maximum integrator output corresponds to 3000 cc.

When the integrator reaches full output a spillover circuit consisting of two 2N520's and a 4E20 detect this and reset the integrator through a relay. The reset is recorded on an electromechanical counter which acts as total flow accumulator for large total flows. The integrator may also be used to provide accumulated flow per unit time and may be reset manually or by means of an external signal at any time. An internal pulse generator will reset the integrator every 10 sec or every 30 sec if desired.

The voltage divider which provides the 10 microvolt P to P calibration signal to the pre-amp is also located on the timing chassis. Locating the divider on the pre-amp chassis produces undesirable pickup due to the large input signal to the divider.

6. Oscilloscope

A small oscilloscope is built into the flowmeter to permit viewing pertinent waveforms, such as the probe drive or the pre-amp output. The schematic is given in Fig. 23. Note that the flow integrator is actually mounted on the oscilloscope chassis.

7. Power Supply

A regulated power supply shown in Fig. 24 is built into the flowmeter. The output of the main supply is 50 VDC. A series of zener diodes provides intermediate voltages. The supply is grounded at the center of the zener diode series string providing output voltages of ± 7.5, ± 15 and ± 25 VDC with respect to ground. All outputs are regulated to ± 1 per cent and well filtered.

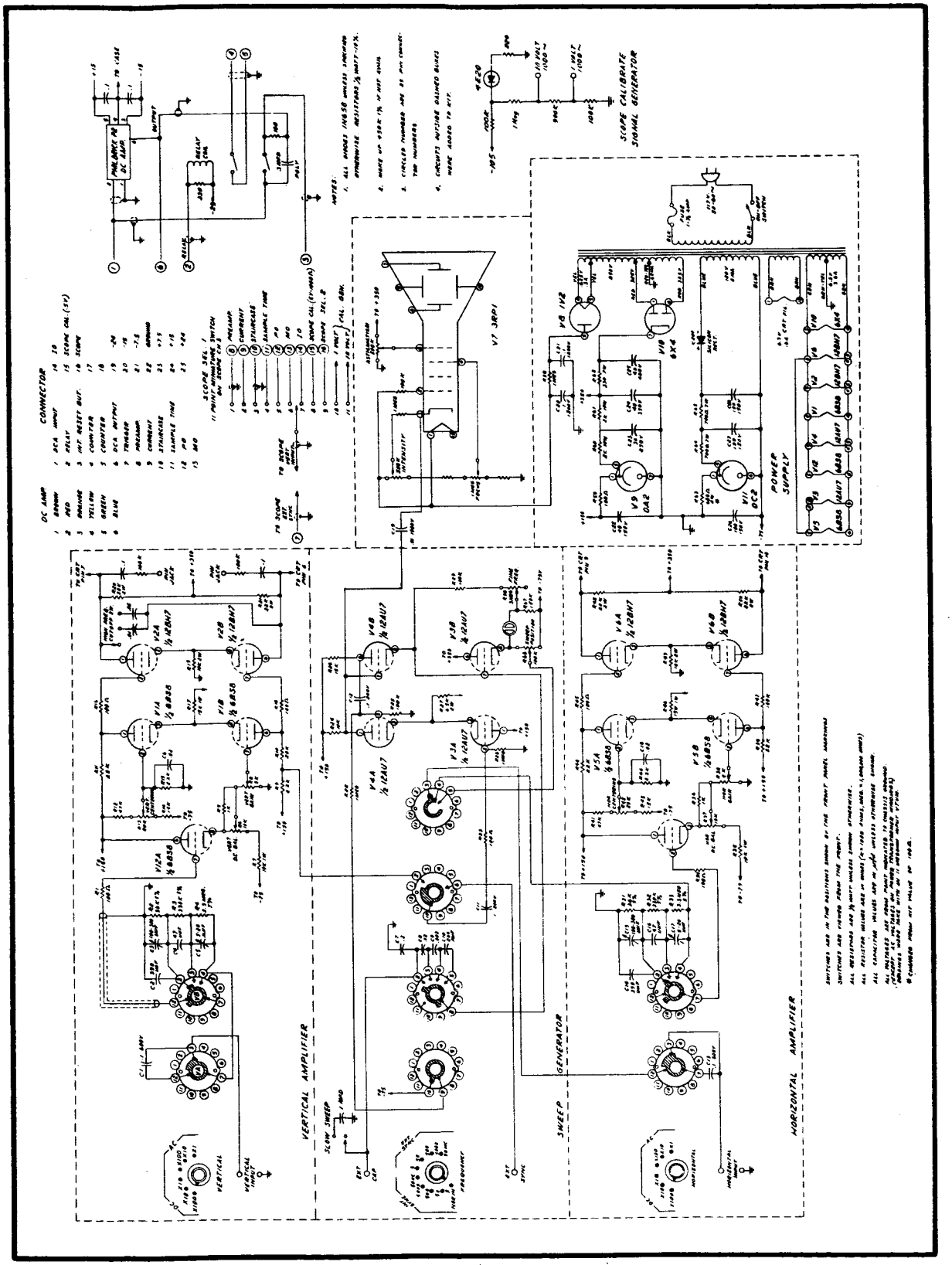

Fig. 23 General Purpose Laboratory Flowmeter, Model 1, Chassis 3: Oscilloscope

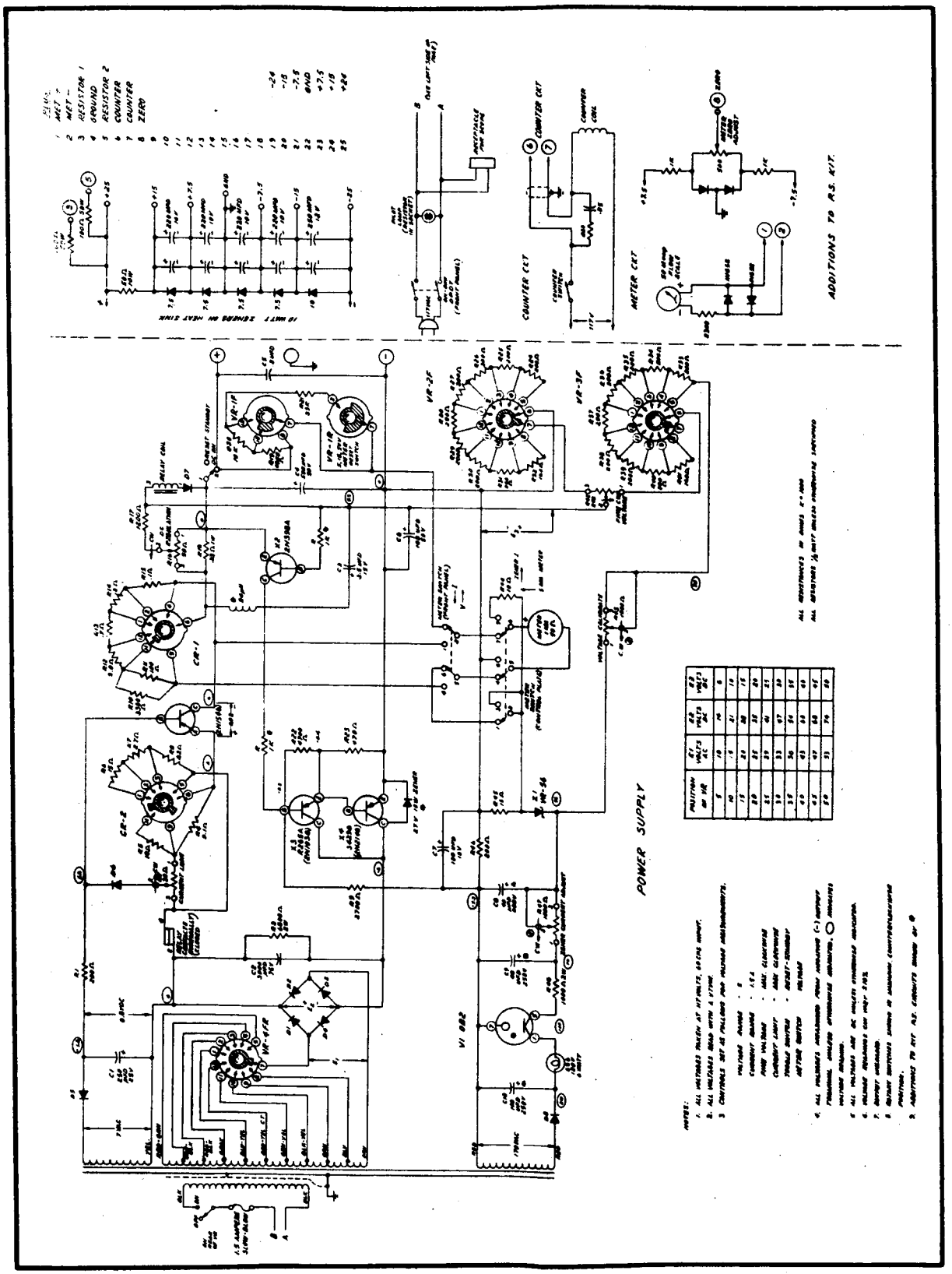

Fig. 24 General Purpose Laboratory Flowmeter, Model 1, Chassis 4: Power Supply

The power supply section also includes the mechanical counter for the integrator reset and a meter for displaying P.O., M.O. and I.O. A meter zero balance control is also provided.

8. Rear Chassis

A small chassis located at the rear of the equipment cabinet (Fig. 25) provides rear access to the P.O., M.O., and I.O. outputs plus an input for external resetting of the integrator. The 75-cps low pass filter is located on this chassis.

C. REMAINING PROBLEMS

Two closely related problems remain to be solved to complete flowmeter development. These are the routine and dependable attainment of an absolute electronic zero and the elimination of the "proximity effect." By "electronic zero" we refer to the establishment of an absolute zero baseline while the flowmeter probe is in place on a blood vessel and flow continues in an uninterrupted fashion. "Proximity effect" refers to a shift in zero baseline when the physical relationships of neighboring dielectric materials with respect to the probe are considerably altered.

These problems are related to the switching interval during which polarity of the magnetic field is reversed, as must frequently be done if polarization effects at the surface of the electrodes are to be cancelled out. During the switching interval a transformer voltage $d\phi/dt$ is induced in the loop consisting of the two electrodes, the conductive path between them and the electrode leads. The split lead arrangement described in Sec. IV-D operates so that an additional voltage spike might be induced to buck the $d\phi/dt$ spikes. The position of the potentiometer connecting the two split leads at which

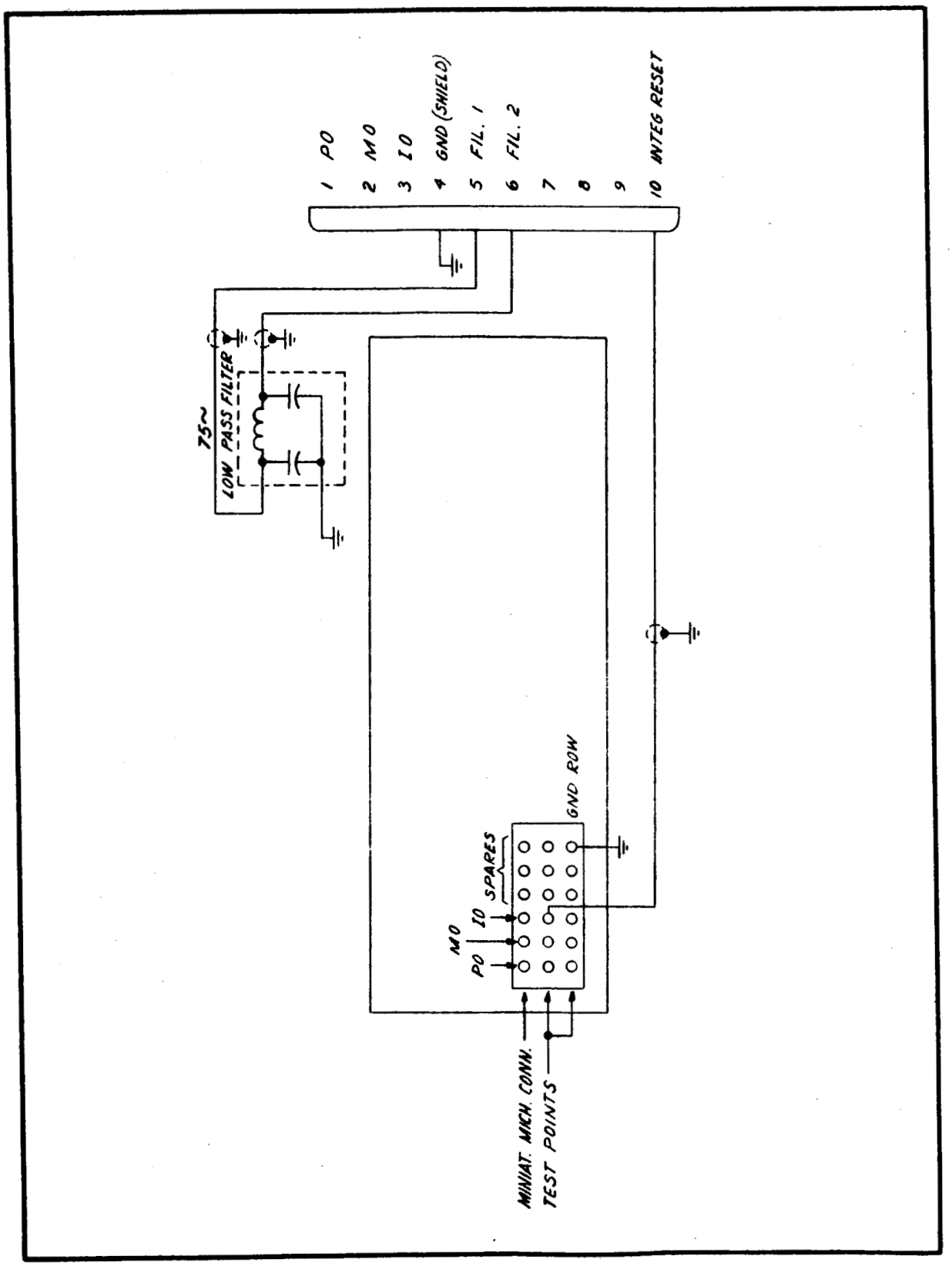

Fig. 25 General Purpose Laboratory Flowmeter, Model 1, Chassis 5: Back Panel

$d\phi/dt$ spikes are bucked to some small acceptable value is a "balanced condition" for the probe. In the "balanced condition" only flow-generated signals appear during the sampling interval and the zero baseline can be accurately obtained either by turning off the magnet driver by disconnecting the probe input. In the unbalanced condition, when the $d\phi/dt$ spikes are unduly large, the "tails" of the spikes are not at zero potential (due to AC coupling) and thereby introduce an error signal. This error signal is, in effect, a zero baseline offset for it would not be present if the magnet driver, or the probe input, were to be disconnected but would be present were flow simply to be interrupted.

During the switching interval, eddy currents are induced in the medium surrounding the flowmeter probe. The eddy currents both tend to alter the magnetic field and tend to introduce signals directly at the sensing electrodes. Since the eddy currents are dependent upon the shape and position of the medium surrounding the electrodes, they change with variations in the physical relationships of surrounding dielectrics to the probe. Thus a probe initially "balanced" can be put "out of balance" by changes in the "proximity" of dielectrics.

Extensive experimentation has demonstrated that a number of factors are of importance in accomplishing ease and maintainance of probe "balance." These include symmetry of magnetic fields and low impedance of the sensing electrodes. Thus probes fabricated with Helmholtz coils or with magnet cores wound with coils brought close to the magnet air gap are advantageous. Platinum or platinum/platinum chloride electrodes appear to be satisfactory.

High bulk resistivity in the materials of which the probe magnet cores are made diminish the eddy currents within the cores themselves.

Investigation in this general area will be intensified during the early part of the next grant period. An attempt will be made to design and implement a scheme to compensate for the adverse effects of the eddy currents.

V. IMPLANTABLE BLOOD OXYGEN SATURATION SENSOR AND HEMATOCRIT SENSOR

A. INTRODUCTION

A key transducer in the experimental assessment of the effects of sustained space flight on body physiology is the implantable transducer by means of which arterial oxygen saturation and venous oxygen saturation are monitored. (Items 1 and 2 Fig. 4.) Since suitable devices to accomplish this purpose do not otherwise exist (although they would be extremely useful tools in medical research), this Laboratory initiated a research program directed toward their development during the current report period.

After evaluation of a variety of approaches, a spectrophotometric method was chosen as most promising. Consistent with the general principle that implantable biological transducers should not come into contact with blood, specification of these devices called for their placement external to appropriate blood vessels. A mode of operation that senses the light within particular spectral bands scattered back (reflected) from the blood rather than transmitted through the blood was chosen. The reasons for this choice are two-fold. Analysis of the mathematics of the backscatter vs transmission mode of operation revealed a considerable simplification of implementation by the former; measurements by the backscatter mode require implementation of a linear relationship while measurements using the transmission mode demand implementation of a complex relationship, the ratio of two logarithms of two ratios. Further, the fraction of light available for measurement is considerably greater by backscatter than by

transmission. Since the power required to operate the devices and the propensity of the device to heat the blood vessel walls are directly related to the light levels required, the backscatter mode is of special advantage in a transducer coupled to blood vessel walls.

B. THE RELATIONSHIP BETWEEN BLOOD OXYGEN SATURATION AND OPTICAL BACKSCATTER

Figure 26 depicts the optical backscatter characteristics of oxyhemoglobin and reduced hemoglobin in the spectral region between 500 and 100 mμ. In this figure, the backscatter ratio (defined as the ratio of backscattered to incident light intensity) is plotted as a function of wavelength. The spectral distribution that is obtained for oxyhemoglobin (100 per cent oxygen saturation) is shown as a solid curve and that obtained for reduced hemoglobin (0 per cent oxygen saturation) is shown as a dashed curve. Basically, it is this marked difference in backscatter ratios of the pigments oxyhemoglobin and reduced hemoglobin, that permits the measurement of oxygen saturation by this technique.

It will be noted that oxyhemoglobin backscatters light at wavelengths greater than 600 mμ with a peak backscatter ratio occurring at 700 mμ. Reduced hemoglobin backscatters light strongest in the infrared (900 - 1200 mμ) region, poorest in the red region and its backscatter ratio essentially increases as a function of wavelength from 600 to 1000 mμ.

Both oxyhemoglobin and reduced hemoglobin have equal backscatter ratios at 805 mμ. This point is called the isosbestic point and at this point backscatter is independent of oxygen saturation.

The quantitative relationships between oxygen saturation and backscatter ratios are contained in Sec. V-C and Appen-

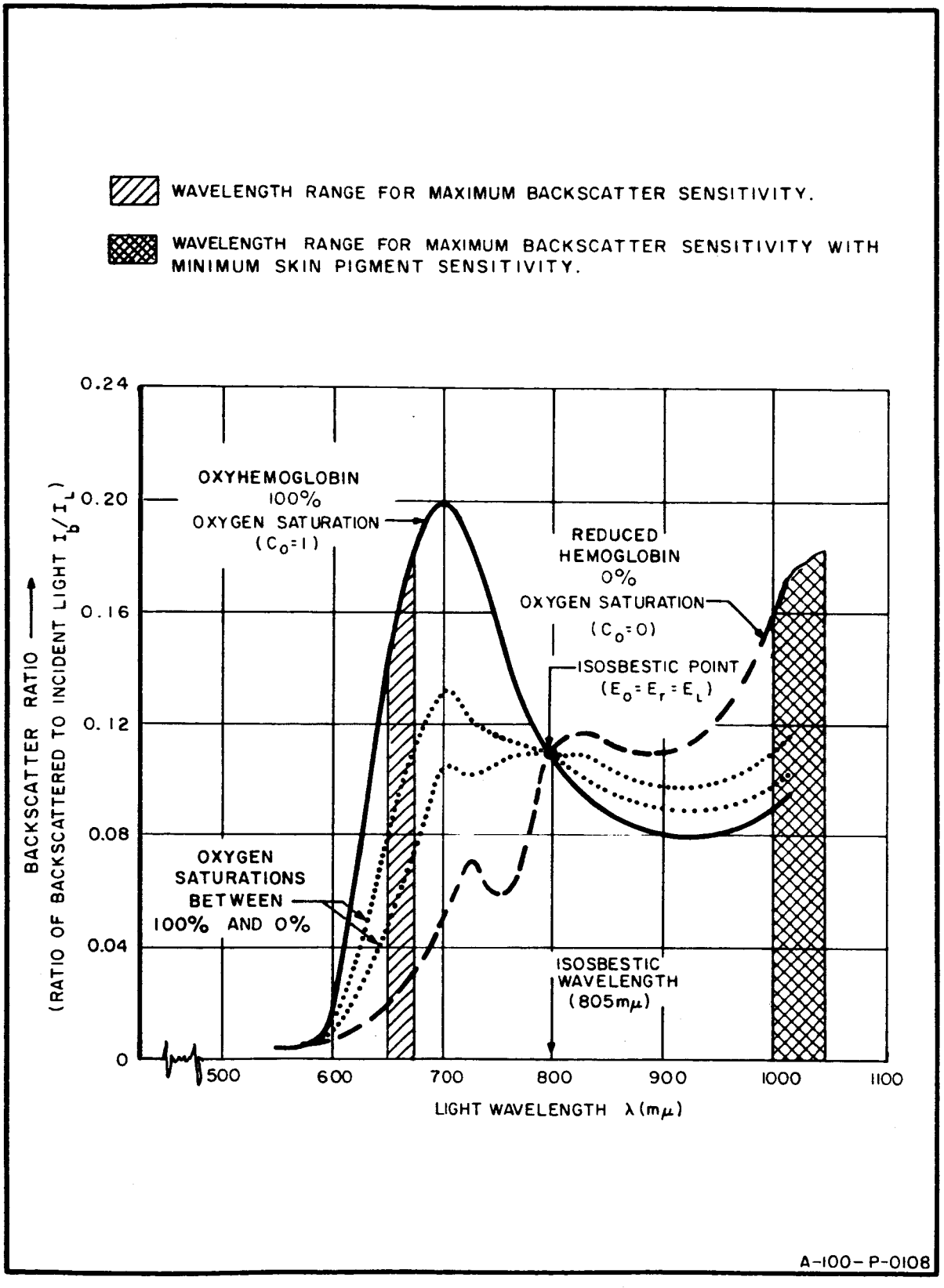

Fig. 26 Typical Spectral Distribution Obtained for Whole Blood Having a Fixed (Normal) Hemoglobin Concentration

dix V-A. These relationships have been confirmed experimentally and result in the following description for the optical properties of hemoglobin: If mixtures of reduced and oxygenated hemoglobin are present in whole blood (i.e., if oxygen saturation is between 0 per cent and 100 per cent), the spectral distribution curve for the mixture will fall between the solid and the dashed curves as illustrated in Fig. 26 by the dotted curves. Also, for light at a fixed wavelength within this spectral band the backscatter ratio changes monotonically with a monotonic change in oxygen saturation. For example, incident light having a narrow spectral width (i.e., essentially monochromatic light) centered at 660 mμ results in a backscatter ratio which changes monotonically from 0.16 to 0.02 as oxygen saturation is reduced monotonically from 100 per cent to 0 per cent. At 1000 mμ, backscatter ratio increases from 0.1 to 0.16 as the oxygen saturation is reduced from 100 per cent to 0 per cent. The only exception occurs at 805 mμ, the isosbestic point, where the backscatter ratio is independent of oxygen saturation.

The above holds true so long as the total hemoglobin concentration (reduced plus oxygenated) remains constant. As the hemoglobin concentration is increased, all of the curves in Fig. 26 shift up vertically by an amount which is linearly related to the increase in total hemoglobin concentration.

Since the backscatter ratio at the isosbestic wavelength is independent of oxygen saturation, measurements made at this wavelength essentially determine the average concentration of hemoglobin present (see Sec. VI). A simultaneous determination of the backscatter ratio at some other signal wavelength, and preferably one which is quite sensitive to oxygen saturation will, in combination with the isosbestic measurement, permit the quantitative determination of oxygen saturation.

C. QUANTITATIVE RELATIONSHIP BETWEEN BLOOD OXYGEN SATURATION AND OPTICAL BACKSCATTER

The approach to the problem of quantitatively relating blood oxygen saturation to the aforementioned backscatter ratios (ratios of light intensities) can be summarized as follows:

(1) Lambert's absorption law is applied to determine the absorption characteristics of the pigments present in skin and blood.

(2) Beer's absorption law for mixtures is then used to determine the combined optical characteristics of oxyhemoglobin and reduced hemoglobin.

(3) Fresnel's reflection law is then applied to determine the ratio of backscattered to incident light as a function of the aforementioned absorption characteristics, light wavelength, hemoglobin concentration and oxygen saturation.

(4) The resulting expressions are then used to solve for the oxygen saturation (ratio of oxyhemoglobin concentration to total hemoglobin concentration) as a function of measurable light intensity levels and known constants.

Such an analysis (see Appendix V-A) reveals the following relationship between oxygen saturation c_o and the measurable light intensities:

$$c_o = B + A \cdot \frac{I_{is}}{I_{ii}} \cdot \frac{I_{bi}}{I_{bs}} \qquad (1)$$

where

B = a known constant consisting of ratios of extinction coefficients for reduced hemoglobin and oxyhemoglobin at the signal wavelength λ_s . (See Eq. (11) in Appendix V-A)

A = a known constant consisting of ratios of extinction coefficients for reduced hemoglobin and oxyhemoglobin at the signal wavelength λ_s and at the isosbestic wavelength λ_i . (See Eq. (12) in Appendix V-A)

I_{is} = incident light intensity at the signal wavelength λ_s

I_{ii} = incident light intensity at the isosbestic wavelength λ_i

I_{bi} = backscattered light intensity at the isosbestic wavelength λ_i

I_{bs} = backscattered light intensity at the signal wavelength λ_s .

Equation (1) shows that oxygen saturation is quantitatively determined by forming the products of the ratios of light intensities at two particular wavelengths, multiplying this product by a known physical constant and then adding to the resulting product another known physical constant. Furthermore, the first ratio of light intensities (I_{is}/I_{ii}) appearing in Eq. (1) only contains incident light levels. This ratio is a measurable constant for a given light source so that it can be considered as being a controlled design constant for the biosensor.

Thus, oxygen saturation c_o is linearly related to the ratio of the backscattered light intensities at the isosbestic

and signal wavelengths. This linear relationship is valid independent of hematocrit (red blood cell concentration), blood flow velocity or species differences in hemoglobin.

D. BIOSENSOR IMPLEMENTATION

A block diagram of a biosensor system is shown in Fig.27. The required light intensities I_i at the isosbestic wavelength and I_s at the signal wavelength are generated by the light source and power supply. (At a further state of development this light source would consist of miniature injection laser diodes powered by a low voltage supply. Injection lasers are an efficient light source requiring a minimum excitation power. They are of small size and low weight and produce light over a narrow spectral region.) The light is transmitted by appropriate optics to the blood vessel to which the transducer is closely coupled. A fraction of the light generated by the light source (I_{ii} and I_{is}) is sensed by the "incident" photodetectors which are combined in a bridge circuit arrangement, to form the ratio of the incident light level at the signal wavelength to the incident light level at the isosbestic wavelength (I_{is}/I_{ii}). This electrical signal is fed back to the light source power supply in an appropriate manner to maintain the ratio (I_{is}/I_{ii}) equal to unity.

As a result Eq. (1) can be rewritten in the form

$$c_o = B + A \cdot \frac{I_{bi}}{I_{bs}} \quad . \tag{2}$$

A portion of the light transmitted through the blood vessel wall is backscattered by the blood and collected by the backscatter photo-detectors. These photo-detectors are

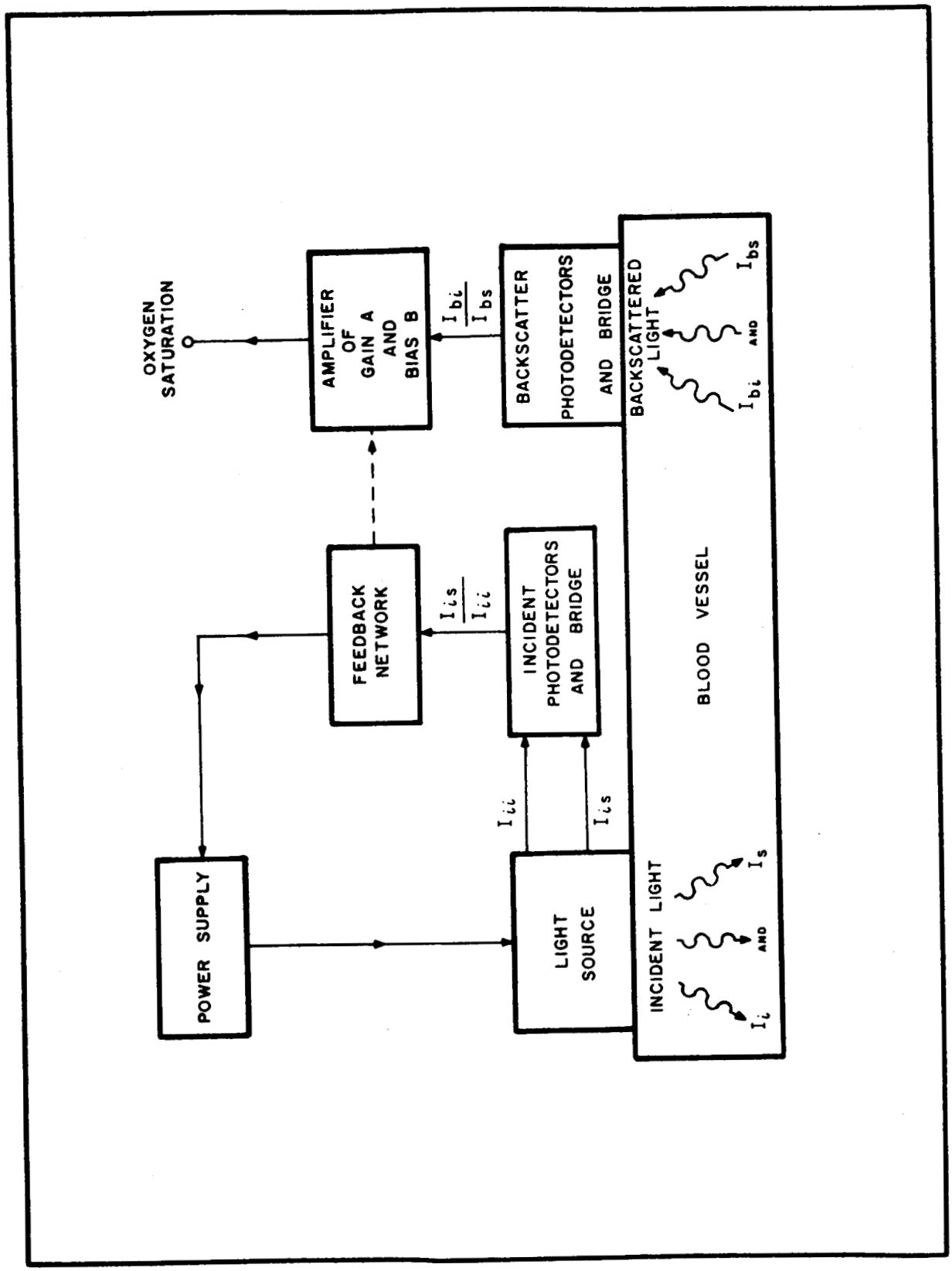

Fig. 27 System Block Diagram for Implantable Hemoglobin Oxygen Saturation Sensor

also combined in a bridge circuit arrangement to obtain the backscatter ratio I_{bi}/I_{bs}. This signal is then amplified by an amount A, and a bias network is employed to add the constant term B as required by Eq. (2) above. The output is, therefore, a direct measure of oxygen saturation, c_o.

E. PROTOTYPE CONSTRUCTION

Opto Electronic Devices, Incorporated (OED), a photocell manufacturing firm in Mountain View, California, fabricated two prototype devices to implement the above. Because of the modest budget available for prototype construction, these devices have not in any way been optimized with regard to individual components or to size. Rather, they were constructed to prove feasibility and to investigate any anomalous or unpredicted effects that might be observed.

A photograph of the OED prototype model is shown in Fig. 28. A drawing of the initial OED prototype design is shown in Fig. 29. Changes in configuration incorporated in the second OED prototype constructed are illustrated in Fig. 30. The basic configuration selected was the one that permitted coupling the light closely to the blood vessel and placing the photocell as close to the vessel as possible to maximize available signal energy.

Prototype Model 2 (Fig. 30) proved to be a more satisfactory construction. In this configuration, a thin aluminum structure acted as the lamp reflector, cell isolator and support. The incident light cells were enclosed by an outer reflective shield which also served to anchor the leads and the cable. These incident light cells were located on the back surface of the aluminum isolator and support so that thermal contact was maintained.

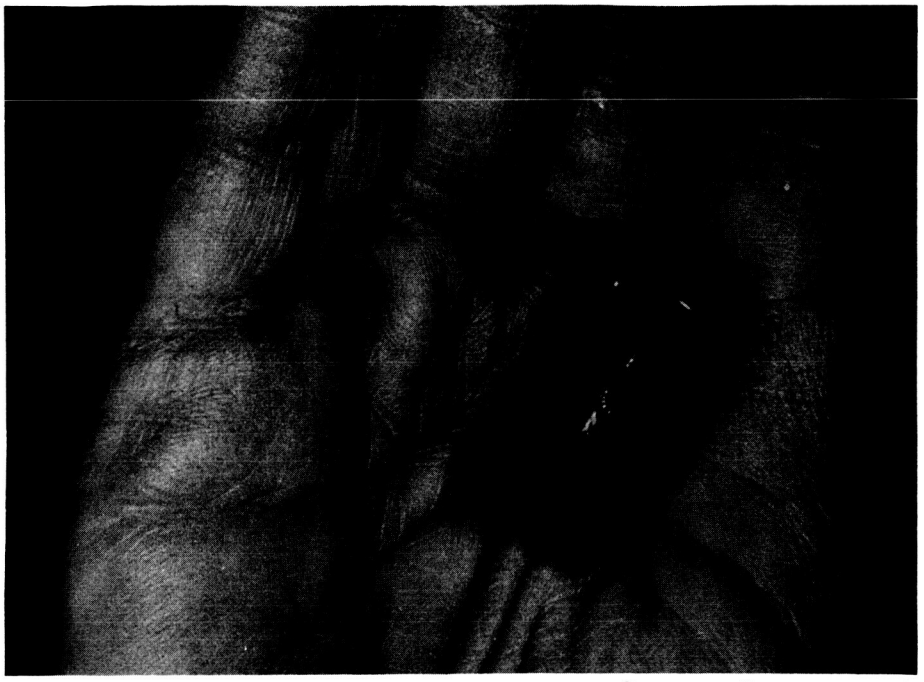

810H-169-A-0052

Fig. 28 OED Prototype Model, Vessel Oximeter

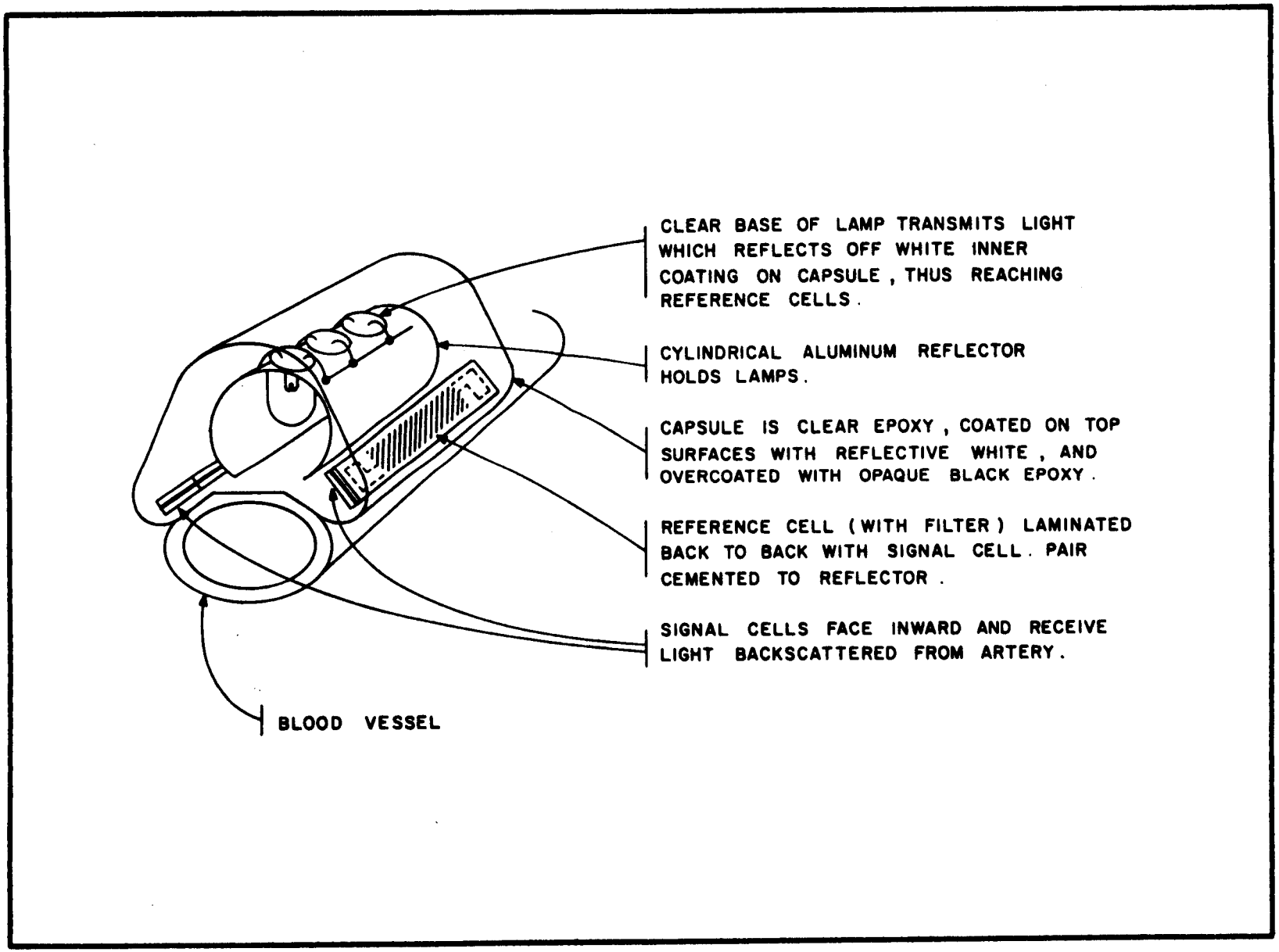

Fig. 29 Prototype Implantable Hemoglobin Oxygen Saturation Sensor Model 1
(This configuration was supplanted by Model 2,
shown in Fig. 30)

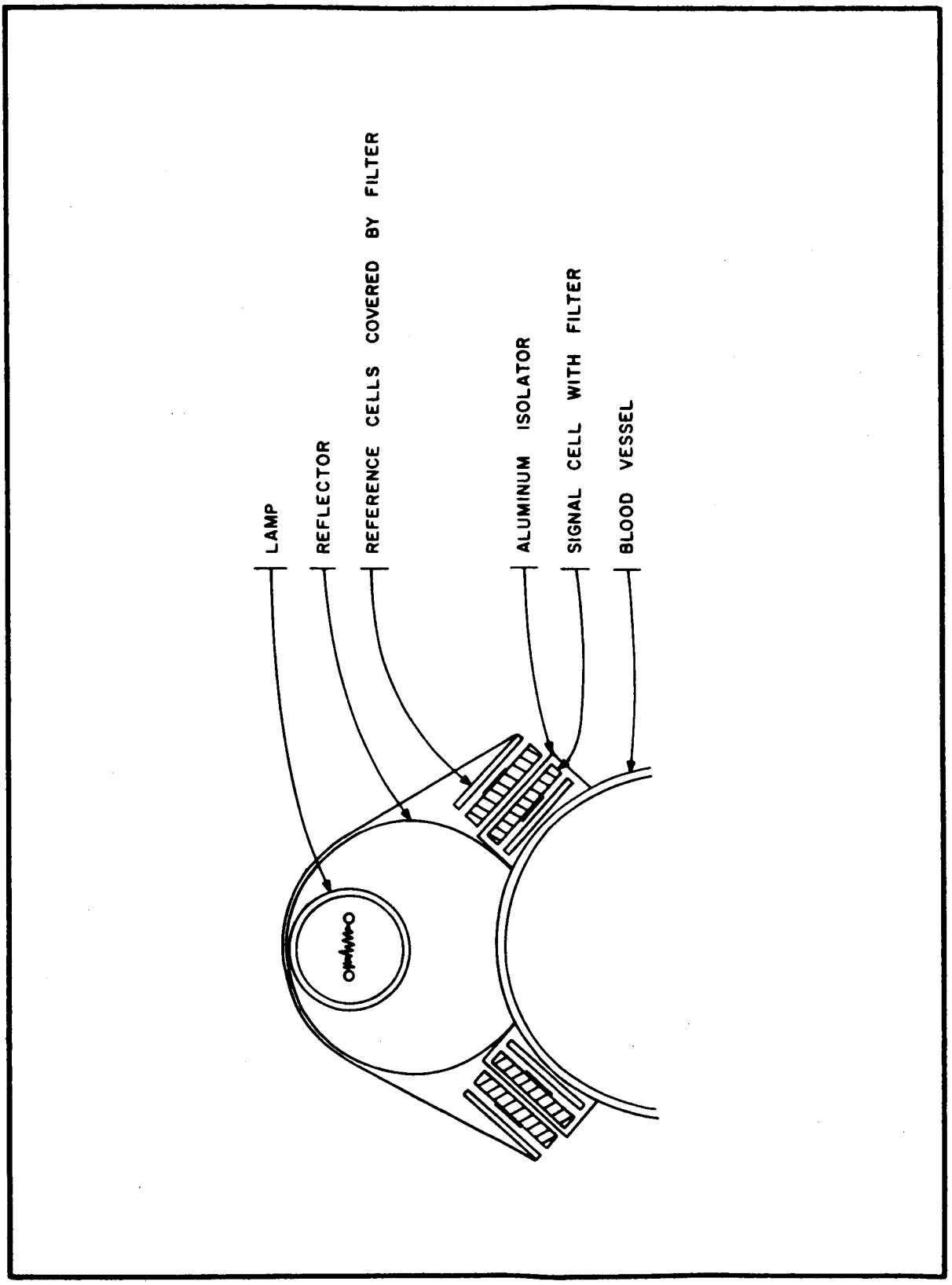

Fig. 30 Configuration of Prototype Implantable Hemoglobin Oxygen Sensor, Model 2

Leads from each cell were individually brought out to allow maximum flexibility in the measuring circuits in order that detailed performance could be studied. Future sensors would include internal bridge circuit connections and thus require fewer leads to external apparatus.

Epoxy resin was used to encapsulate the entire assembly. The same resin with carbon black filler was used to form a light tight coating over selected portions of the transducer structure.

The photocells were recognized as being major components of the system. The cells chosen were OED photoconductive cells of class II-VI compound which were of small size, high sensitivity, low noise or thermally stable. These cells utilized available manufacturing techniques and facilities. Techniques to furnish cells with higher resolution or of smaller size would be appropriate to a later stage of development. Such improvements would require advancing the art and hence are beyond the current scope of the initial phase of this program.

Numerous cells of several material compositions were made, tested and evaluated at OED. It was then decided that cells of one specific material could be used with appropriate light filters to provide both the 660 mμ and the 805 mμ responses. This minimizes effects of temperature variation and long term drift. Normalized response curves of the 660 mμ and 805 mμ cell filter combinations are shown in Fig. 31. While these spectral characteristics were not optimal, they were considered suitable for this preliminary feasibility study.

The spectral region of interest is one where tungsten filament lamps supply maximum radiant efficiency relative

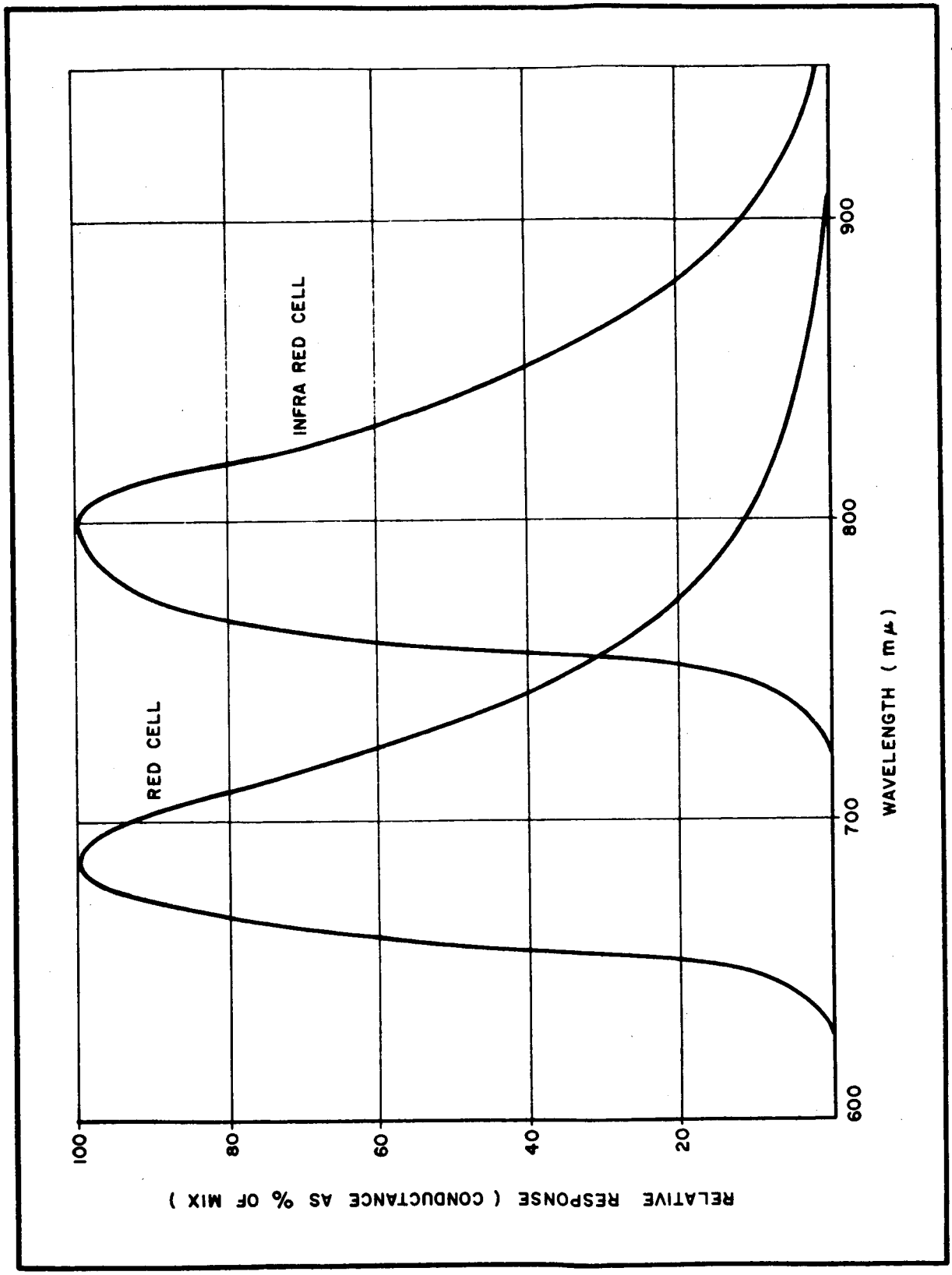

Fig. 31 Normalized Response of Cell Filter Combinations to Tungsten Lamp Excitation. Relative total current response of red cell with filters exposed to tungsten lamp is ten times as great as infra red cell due to drop-off of cell response at long wavelengths.

to other readily available sources. The lamp selected was a miniature incandescent lamp rated at 5 V and 0.060 A. To make maximum use of the light available, a reflector was used with an array of 2 lamps operating in parallel. Operation at reduced voltage was planned to reduce the transducer temperature rise to a minimum, and also to maximize component life. Multiple lamps also allow the transducer to be effective even if one lamp fails.

As illustrated in Fig. 26, the two wavelength regions used were in the deep red (about 660 mμ) and near infra-red (805 mμ) regions mainly for the sake of expediency; dyed gelatine filters were employed. These have the advantage of being readily available in a form which could be cut and cemented to the cell surface without adding bulk.

Testing of the transducer components was done at several stages of construction. The response of specific cell-filter combinations was measured with respect to a tungsten source. For this test a grating spectrometer was used at a spectral width of approximately 7 mμ. Results of this test are shown in Fig. 31.

F. PRELIMINARY EXPERIMENTAL STUDY OF PROTOTYPE SENSOR

The prototype sensor described in the previous sections has been examined by employing a blood flow circuit consisting of a roller pump, a bubble oxygenator and flow conduits of tygon tubing. The transducers were placed in the flowing stream of blood at a dilated portion of the flow network, and a 3-way stopcock was placed just beyond the prototype transducers to withdraw samples of blood for determination of oxygen saturation by standard spectrophotometric techniques. Oxygen and nitrogen, piped into the oxygenating

chamber, were mixed in varying ratios to vary blood oxygen saturation over a wide range of values. Current to the light source, hematocrit and pH were all monitored. As noted previously, in order to study the details of prototype performance, completion of the bridge configurations was not made within the transducer. Leads from each cell were brought out so that the resistance of each photocell could be separately measured.

The results obtained from these preliminary measurements on whole blood indicated that, as theoretically predicted in Sec. V-C and Appendix V-A for a constant hematocrit, (1) the 660 mμ signal photocell resistance monotonically decreased as blood oxygen saturation was increased and, (2) the 805 mμ photocell resistance remained essentially constant as blood oxygen saturation was increased. In addition, photocell resistance measurements with the same sensor were made for a constant oxygen saturation of 100 per cent and various hematocrit levels. Again, as theoretically predicted (see Eq. (8) in Appendix V-A) the 805 mμ photocell resistance increased monotonically as the hematocrit was increased.

These experimental results show that a sensor of this general design is inherently capable of producing output signals which can be used as a measure of both (1) the oxygen saturation of whole blood essentially independent of hematocrit and (2) the hematocrit of whole blood essentially independent of oxygen saturation. Additional experimental research is required to determine the operating characteristics of this sensor when it is employed on a blood vessel as a blood oxygen saturation sensor and/or an hematocrit sensor.

APPENDIX V-A

A SIMPLIFIED DERIVATION OF THE EQUATION RELATING BACKSCATTERED LIGHT TO OXYGEN SATURATION

Starting with Lambert's Absorption Law for a unidimensional model, we can write

$$I = I_i \epsilon^{-\alpha t} \qquad (1)$$

where I is the light intensity that emanates from a material which is illuminated with an incident light intensity I_i, t is the thickness of the material and α is the absorption coefficient of the material at the wavelength of incident light.

In general, due to absorption in a given material, the light intensity at a given depth x for an initial intensity at $x = 0^+$ of I_i is

$$I_x = I_i \epsilon^{-\alpha x} . \qquad (2)$$

When backscattering is present, the total light intensity backscattered by a layer of depth dx located at x is

$$I_i R \epsilon^{-\alpha x} dx \qquad (3)$$

where R is the backscattering (or reflection) coefficient for the medium. In traveling back to $x = 0$ (the surface), this backscattered light is attenuated further by an amount

$t^{-\alpha x}$. Thus, the total backscattered light is given by

$$I_b = \int_0^\infty I_i \, R \, \epsilon^{-2\alpha x} \, dx = \frac{I_i R}{2\alpha} \quad , \tag{4}$$

assuming that all backscattered light is collected.* Typically for blood, the penetration depth need not be large. In fact, Eq. (4) has been shown to be valid for penetration depths of 3mm and the ratio of backscattered to incident light level (the backscatter ratio) is

$$\frac{I_b}{I_i} = \frac{R}{2\alpha} \cong 0.1$$

i.e., 10 per cent of the incident light is backscattered.

Now, from Beer's Law, the absorption coefficient is actually composed of the sum of the absorption coefficients for oxyhemoglobin and reduced hemoglobin. Thus, from Beer's Law,

$$\alpha = \alpha_o + \alpha_r \tag{5}$$

where

$\alpha_o \equiv$ absorption coefficient for oxyhemoglobin

$\alpha_r \equiv$ absorption coefficient for reduced hemoglobin.

We note, however, that the absorption coefficient α is dependent also upon the hemoglobin concentration. In order to show this dependency explicitly, we define the following parameters

* These same results are obtained for a three-dimensional model.

$$\alpha_o \equiv w\, E_o C_o$$

$$\alpha_r \equiv w\, E_r C_r \qquad (6)$$

where

$w \equiv$ the average weight of hemoglobin per unit volume in the illuminated region,

$E_o \equiv$ the specific extinction coefficient of oxyhemoglobin

$E_r \equiv$ the specific extinction coefficient of reduced hemoglobin

$C_o \equiv$ relative concentration of oxyhemoglobin,

$C_o \equiv$ oxygen saturation (as a fraction),

$C_r \equiv$ relative concentration of reduced hemoglobin.

With these definitions, the specific extinction coefficients are independent of hemoglobin concentration, $C_o + C_r = 1$, and $100 \times C_o$ is the percent of oxygen saturation in the sample of blood that is illuminated. Thus, combining Eqs. (4) (Lambert's Law), (5) (Beer's Law) and (6) (definition of specific extinction coefficient) we obtain the result

$$\frac{I_b}{I_i} = \frac{R}{2w[E_o C_o + E_r C_r]}$$

and since $C_r = 1 - C_o$ we can write

$$\frac{I_b}{I_i} = \frac{R}{2w[(E_o - E_r)C_o + E_r]}. \qquad (7)$$

In general, the specific extinction coefficients E_o and E_r for blood are functions of light wavelength. For oxyhemoglobin and reduced hemoglobin this is a light wavelength (800 mμ) such that $E_o = E_r$. This wavelength is usually referred to as the isosbestic wavelength for a two element mixture and we shall refer to this wavelength by employing the subscript "i". Thus, we write

$$E_o = E_r \equiv E_i$$

at this isosbestic wavelength (800 mμ). Also, we can now write Eq. (7) in the form

$$\frac{I_{bi}}{I_{ii}} = \frac{R_i}{2w\,E_i} \tag{8}$$

where

$I_{bi} \equiv$ backscattered light at the isosbestic wavelength

$I_{ii} =$ incident light at the isosbestic wavelength

$R_i =$ Reflection coefficient at the isosbestic wavelength

$E_i =$ extinction coefficient for blood (both oxyhemoglobin and reduced hemoglobin) at the isosbestic wavelength

$w =$ average weight of hemoglobin per unit volume in the illuminated region.

Since both R_i and E_i are known constants for blood, we see that by measuring the ratio of backscattered to incident light intensities at the isosbestic wavelength, we obtain a direct measure of the total weight of hemoglobin per unit volume, independent of the oxygen saturation present.

Now, if a (simultaneous) second measurement is made at a second (signal) wavelength denoted by the subscript "s", we obtain

$$\frac{I_{bs}}{I_{is}} = \frac{R_s}{2w[(E_{os} - E_{rs})C_o + E_{rs}]} \cdot \tag{9}$$

Combining Eqs. (8) and (9) and solving C_o we obtain

$$C_o = B + A \frac{I_{bi} I_{is}}{I_{ii} I_{bs}} \tag{10}$$

where

$$B \equiv E_{rs}/(E_{rs} - E_{os}) \tag{11}$$

$$A \equiv [E_i/(E_{os} - E_{rs})][R_s/R_i] \tag{12}$$

Also, for the light wavelengths of interest, it has been shown that $R_s = R_i$.

Thus, since the specific extinction coefficients for oxyhemoglobin and reduced hemoglobin are known, oxygen saturation C_o is obtained by measuring the ratios of incident to backscattered light levels at two different wavelength as shown in Eq. (10).

VI. EVALUATION OF IMPLANTABLE TRANSDUCERS FOR BLOOD PRESSURE MEASUREMENT

A. TRANSDUCERS

In the experimental assessment of the effects of sustained space flight on cardiovascular-respiratory physiology, the measurement of left ventricular or arterial blood pressure would be most useful (Fig. 3). While chronic measurement of vascular or arterial pressure has been performed by means of small plastic cannulae left in a heart chamber or peripheral artery, this method is not suitable for orbital experiments. The possibility during the lengthy periods demanded by such an experiment, of a cannula becoming plugged with a blood thrombus or being pulled out by the experimental animal with consequent hemorrhage, is almost a certainty. Consequently, during this report period as part of the general program, this Laboratory has evaluated a number of commercially available pressure transducers that might be suitable for chronic implantation in experimental animals.

Of the commercially available pressure transducers surveyed, only two appeared suitable for evaluation. One of these was a cuff-type device fabricated by the Bio-Metrics Instrument Corporation of Plano, Texas and the other a miniaturized silicon diaphragm device manufactured by Micro Systems, Inc., San Gabriel, California.

The transducer manufactured by Bio-Metrics Instrument Corporation is a slotted, stainless steel cuff (Fig. 32). Two semi-conductor strain gauges oriented at right angles to

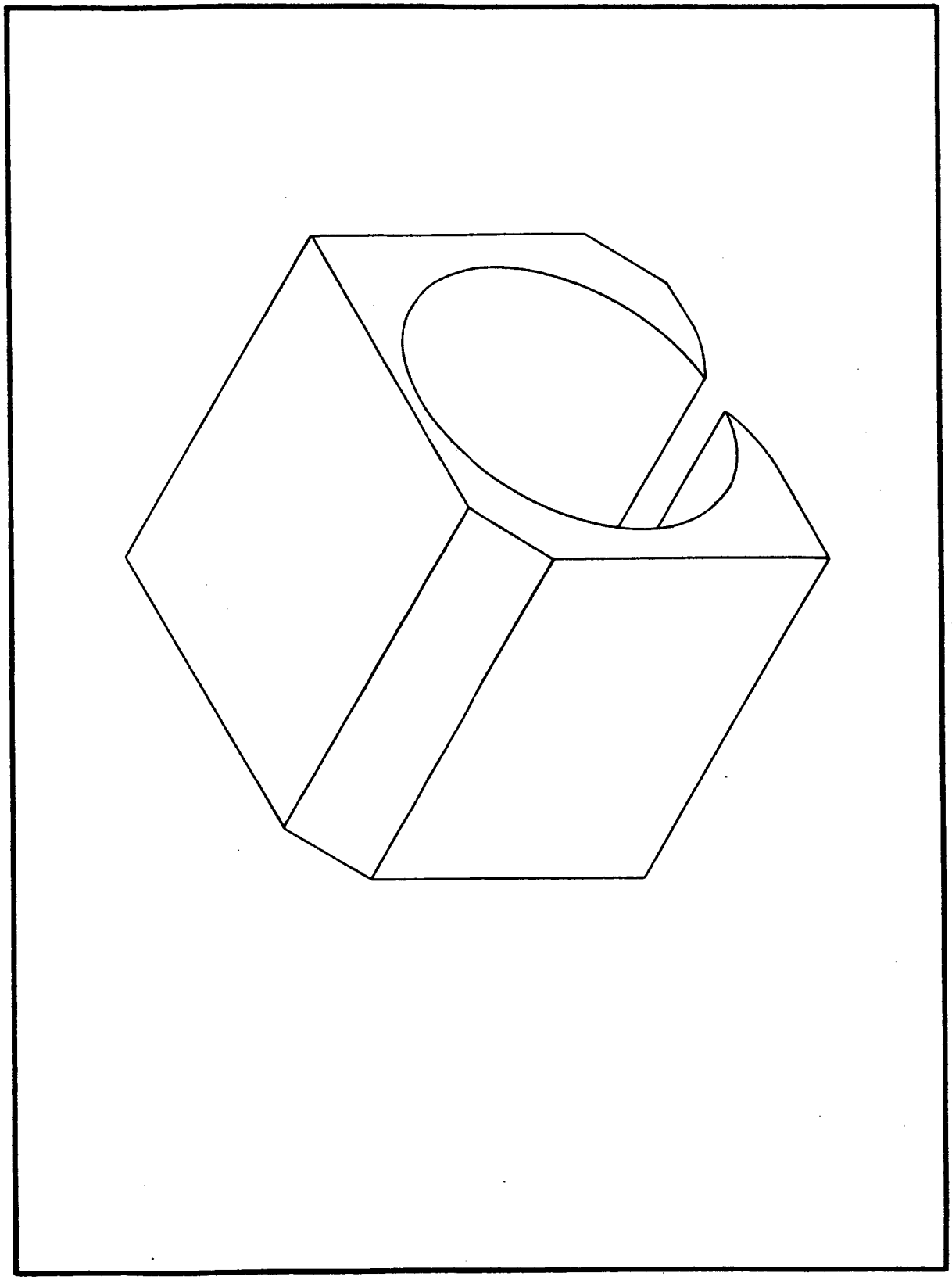

Fig. 32 Diagramatic Drawing of Cuff-Type Blood Pressure Transducer

each other are bonded to one cuff wall that has been ground down to a very thin cross section. When the cuff is implanted around an arterial vessel the pressure changes within the artery are transmitted to the extra-vascular cuff and distort one of the strain gauge elements. The second element, at right angles to the first, serves as a temperature compensating element when used in a bridge configuration. A thin film of resilient protective coating covers the entire cuff. In application, a cuff such as this could be implanted around any convenient small, medium, or large artery to continuously monitor arterial pressure.

The pressure transducer fabricated by Micro Systems, Inc. (Fig. 33) directly measures pressure by means of a miniature silicon diaphragm with four active elements formed by solid state diffusion. The entire sensing element is only 0.090 in. in diameter and is hermetically sealed in a small cylindrical metal housing which is gold plated. A small pocket of trapped air behind the diaphragm allows the disk to flex with variations in blood pressure. The four strain elements are internally connected in a bridge configuration and leads are brought out for excitation, signal output and for connection of an external balancing resistor.

In application, this device would probably be implanted in the muscle of the heart chamber wall with the silicon sensing element situated beneath the endocardium. Because of the anti-clotting characteristics of silicon, it could probably also be quite satisfactorily inserted into a small branch of a major artery with the silicon tip positioned flush with the major arterial channel. Even if a thin layer of blood clot did form in this latter arrangement, there should be no appreciable deterioration of the pressure signal. Such a device would also be suitable for measurement of intrapleural pressure (Item No. 7, Fig. 4).

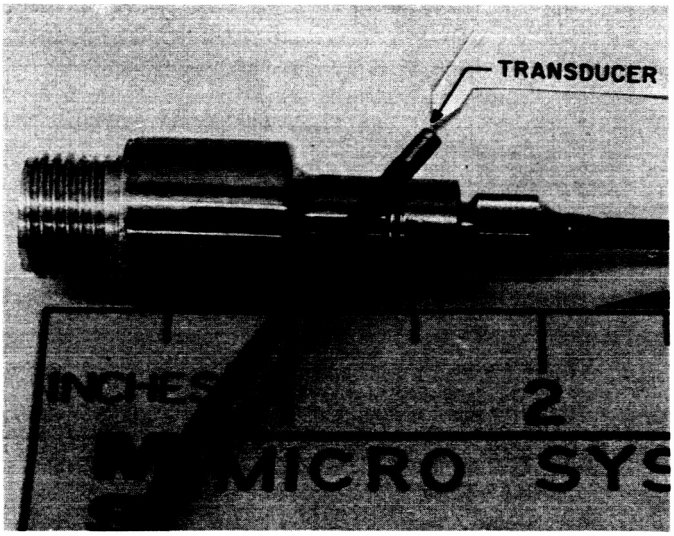

810H-169-A-0055

Fig. 33 A Micro System Pressure Transducer

B. EVALUATION

In evaluation of these transducers the following test program was followed;

1. Long term stability, loaded and unloaded, in air;
2. Linearity and hysteresis;
3. Temperature stability;
4. Stability, loaded and unloaded, in distilled water;
5. Stability, loaded and unloaded, in physiological saline;
6. In-vivo testing.

C. RESULTS

Two units of each type were thoroghly tested. The cuff type transducer was mechanically stressed (Fig. 34), while the diaphragm type transducer was stressed with compressed air (Fig. 35).

When tested in air, both transducers exhibited satisfactory characteristics with regard to stability, repeatability, linearity, and hysteresis. However, during static tests while immersed in distilled water, the diaphragm type transducers suffered electrical breakdown. Breakdown typically occurred within one to two days after immersion. The cuff type transducers performed satisfactorily in distilled water but suffered electrical breakdown in isotonic saline.

All units were returned to their manufacturers with a report of the test results. The manufacturers are currently investigating better methods for protective coating. Each of these transducers may prove satisfactory if they can be adequately protected from tissue fluids.

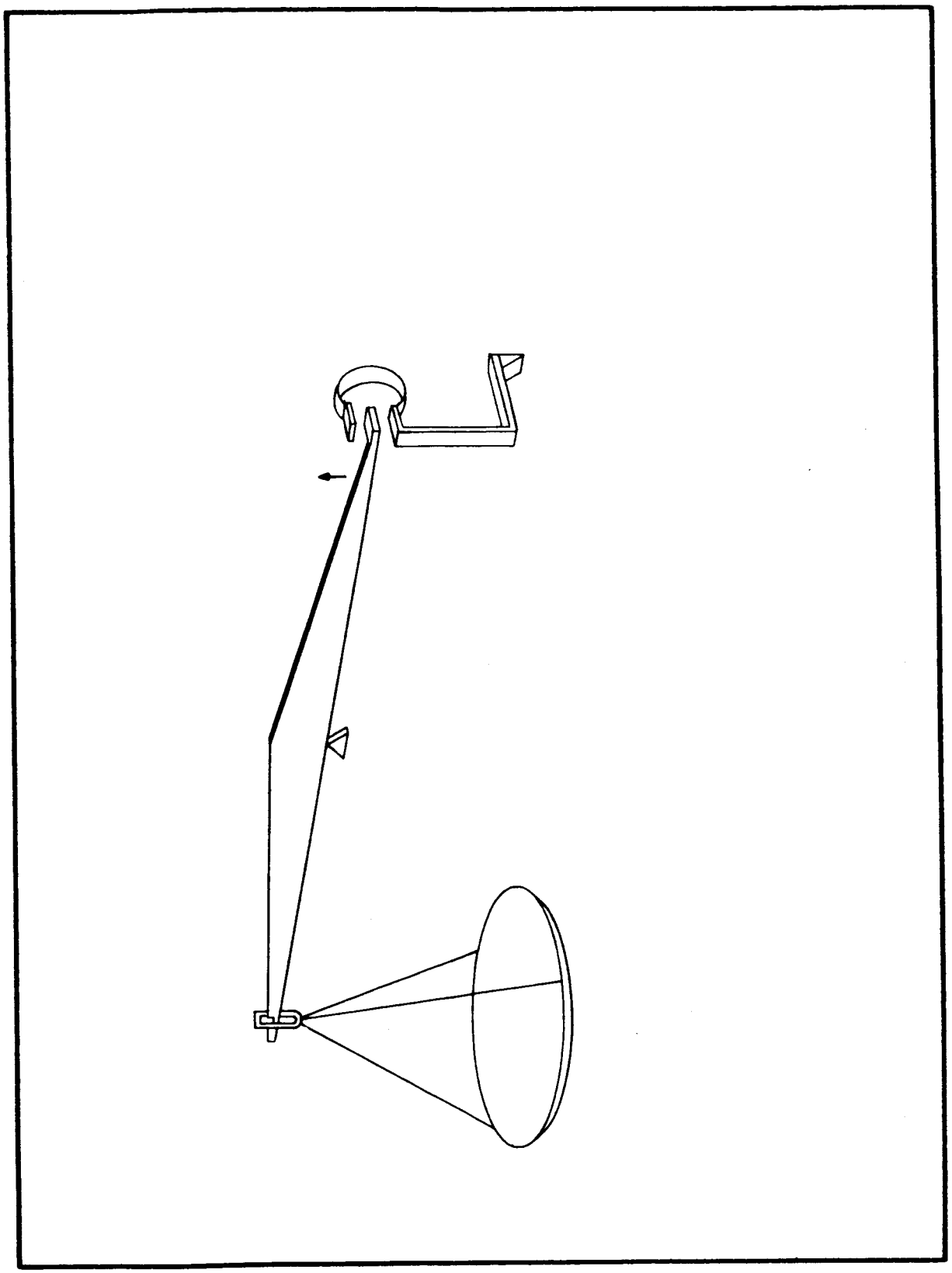

Fig. 34 Arrangement for Mechanical Stressing of Cuff-Type Blood Pressure Transducer

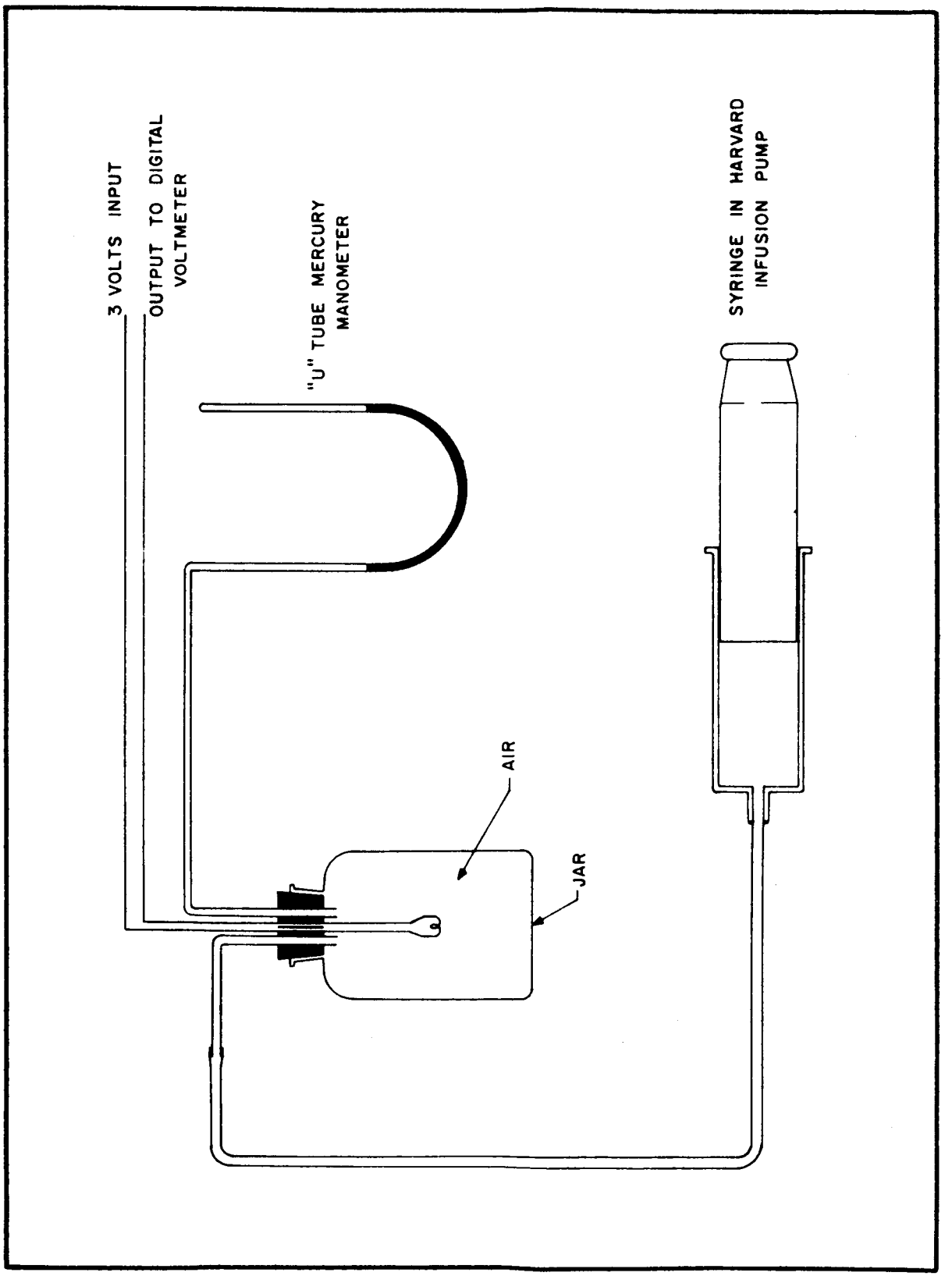

Fig. 35 Diagram of Pressure System for Calibration of Diaphragm Type Blood Pressure Transducer